NORTHWESTERN UNIVERSITY

North American Mantle Processes during the Mesoproterozoic through Cenozoic Eras from Seismic Field Experiments and Visualizations

A DISSERTATION

SUBMITTED TO THE GRADUATE SCHOOL
IN PARTIAL FULFILLMENT OF THE REQUIREMENTS

for the degree

DOCTOR OF PHILOSOPHY

Field of Earth and Planetary Sciences

By

Trevor Alan Bollmann

EVANSTON, ILLINOIS

September 2019

ABSTRACT

North American Mantle Processes during the Mesoproterozoic through Cenozoic Eras from Seismic Field Experiments and Visualizations

Trevor Alan Bollmann

The structure of the North American crust and mantle was investigated using P wave teleseismic tomography and the links between seismic tomographic models, locations of volcanism, sediment isopachs, and continental scale crustal structures via plate reconstruction modeling. Nearly 50,000 teleseismic P wave delay times were measured from seismograms recorded by the USArray Transportable Array (TA), Superior Province Rifting EarthScope Experiment (SPREE), and permanent seismic stations; then combined with measurements from previous studies in a tomographic inversion for the mantle beneath the North American Midcontinent. High-velocity anomalies are prevalent in the study area but there are also prominent relatively low velocity anomalies. Two are coincident with rift-related Bouguer gravity anomaly highs and could be related to underplating of the Midcontinent Rift. Another two are located at the syntaxes of crustal terranes, amalgamated during the formation of Laurentia. In the mid-mantle we image high-velocity anomalies, interpreted as fragments of the subducted Farallon and Kula plates.

Next, the anomalous morphology of the Western Interior Basin (WIB) was investigated through the use of sediment isopachs, surface expressions of volcanism, crustal structures, and subducted slab locations through time. By correlating these diverse datasets, two hypotheses for the formation of the WIB were tested. Although no hypothesis was conclusively proven or disproven, it was determined that a fragment of the subducted Farallon slab was in the correct location to interact with the overriding crust at the time of basin expansion.

To facilitate the aforementioned studies, a seismic experiment was conducted. Best practices in seismic field work, a project overview, possible issues, and methods to overcome them were compiled. An assessment of the Canadian SPREE stations was completed to determine if noise sources identified during the siting phase of the project correlated with station quality. During this assessment, a number of noise characteristics were identified. Namely, a diurnal change in noise levels between day and night due to changes in cultural activity and prevailing wind changes throughout the day, summer/winter changes in long period noise attributed to atmospheric circulation, and the observation of microseisms that originated from Lake Superior.

Acknowledgements

0.0.1. Personal Acknowlegements

I would like to thank Dr. Suzan van der Lee for being a very understanding advisor. She is a very caring individual and without her allowing me to continue the work for my Ph.D. remotely, I never would have been able to finish it. She also realized very quickly that I work best when I have minimal supervision and I applaud her for giving me the independence I needed to be successful. That being said, when I did reach out for assistance, she always made time for me in her hectic schedule. Her intense knowledge of all things tomography was irreplaceable and was an amazing person to have in my corner.

Dr. Bradley Sageman was my secondary advisor and I definitely picked a good one. We initially started working together as a requirement for my qualifying exam but after being in the field for a month as the field portion of Brad's depositional systems course, I realized that our personalities worked well together and I was going to keep the relationship going. Just like Suzan, Brad understood my situation and allowed me to continue working remotely. As a part of my project with him, he allowed me to steer the work as I wanted and more importantly let me go down a number of different paths. Many of which were not successful. This was definitely a learning experience for me and it was much appreciated.

While he was not one of my advisors, I did a considerable amount of work with Dr. Andrew Frederiksen of the University of Manitoba. We collaborated on numerous papers

and conference presentations. His expertise definitely made me a better tomographer. He was also a great help in getting the vanDecar code to run on my Mac and even brought me up to Winnipeg for a week to work on it.

I would like to thank my committee, Drs. van der Lee, Sageman, and Jurdy, for helping me put together my thesis and the time it takes to critique a document of this size. Writing is not my strong suit so I appreciate the numerous revisions that helped shape this final document. The staff of the Department of Earth and Planetary Sciences have always been there to support my scholastic endeavors and I am grateful for that.

The graduate students in Earth and Planetary Sciences Department were a great group of people to spend 6 years of my life with. I would especially like to thank Emily Wolin and Mike Witek for being there to bounce ideas off of or to simply look at a piece of code to help me debug it. I would also like to thank Laurel Childress and Jeremy Gouldey for their friendship. You two were always available to go out for a beer when I needed to relax.

To my family, you always believed in me no matter what I have decided to do, even if you didn't completely understand what I was doing. Everyone in my family has always been supportive but most of all was my wife, Morgan. When I decided to attend Northwestern, we had been dating for just over 3 years and that decision guaranteed that we would be in a long distance relationship for a minimum of 5 years. Even though you weren't thrilled with the prospect of being apart for that long, you were very understanding. Fast forward 10 years and you continue to support me on a daily basis and understand that having a full time job with two children, on top of trying to complete a Ph.D. in what spare time I have is not an easy task. You even volunteered to take

the kids and go up to your parent's so I can finish everything with no distractions. I am eternally grateful to you and I love you.

0.0.2. Research and Data Acknowledgements

The relative P-wave velocity model with respect to *iasp91* and the travel time pick files used to derive the model we present in this paper are available for download at http://geophysics.earth.northwestern.edu/seismology/SPREE18/. Data from the USArray Transportable Array and SPREE were obtained from the IRIS Data Management Center (http://www.iris.edu; last accessed April 2014). Network Codes and years of operation: SPREE - XI(2011-2013), USArray TA - TA(2003-present), USNSN - US(1990-present), CNSN- CN(1980-present), GSN- II(1980-present), FedNor - WU(1991-present), POLARIS - PO(2000-present), FLED - XR(2001-2002), APT-89 - 91-003-APT(1989), TW ST - XK (1997). All picking of traveltimes were completed using the AIMBAT traveltime picking tool (*Lou et al.*, 2013) This research was supported by NSF grant EAR-0952345. The Superior Province Rifting Earthscope Experiment (SPREE) was supported by the Earthscope program through NSF grant EAR-0952154. This project would not have been possible without the support of the landowners that allowed for the installation of TA and SPREE seismic stations. Please see https://www.earth.northwestern.edu/spree/People.html for full acknowledgements. In addition, we thank Basil Tikoff for discussion about our velocity anomalies with respect to the structural and tectonic history of the Mid-continent.

I would like to thank Craig Jones for discussions on Western Interior Basin formation and answering other questions pertaining to his hypotheses. Shannon Peters for walking

me through the current capabilities of the Macrostrat database and how it could be used in the future. Christopher Scotese for discussions about using plate reconstruction models to "move" plates over previously subducted slabs.

All maps and figures were created with the Generic Mapping Tools (GMT) (*Wessel et al.*, 2013). Seismic Analysis Code (SAC) was used to QC data in the field as well as creating the record sections for landowners. The data used in the noise analysis is from the SPREE network (*van der Lee et al.*, 2011, 2013; *Wolin et al.*, 2015) and is available online from the Iris Data Management Center (http://www.iris.edu).

Table of Contents

List of Figures

CHAPTER 1

Introduction and Overview

1.1. Introduction

Mantle processes are an integral part of plate tectonics and have been for billions of years, leaving evidence in the crust above. For the last 10 years, I have been investigating different facets of these processes using a multitude of datasets. This has allowed me a glimpse into how interconnected the processes of the earth are. This dissertation consists of three parts: 1. An overview of best practices for operating seismic field experiments, 2. Using teleseismic P wave delay times in a tomographic inversion to gain insight into the formation of the Midcontinent Rift, and 3. Using diverse datasets to investigate the anomalous morphology of the Western Interior Basin.

1.2. Chapter 2: *P* Wave Teleseismic Traveltime Tomography of the North American Midcontinent

The Midcontinent Rift lies in a tectonically stable portion of North America and has done so for 1.1 Ga. It was initially discovered due to its large Bouguer gravity signature and its formation processes have remained uncertain. Using delay times measured from from seismograms recorded by the USArray Transportable Array (TA), Superior Province Rifting EarthScope Experiment (SPREE), and permanent seismic stations; a tomographic model to investigate the rift was created. This model revealed many prominent relatively low velocity anomalies within the predominantly high velocity upper mantle. Namely, patchy low velocity anomalies coincident with the Midcontinent Rift, two anomalies at the syntaxes of Proterozoic terranes amalgamated during the formation of Laurentia. In the mid-mantle high velocity anomalies were interpreted as the subducted fragments of the Farallon slab. This work was published in the Journal of Geophysical Research: Solid

Earth as Bollmann et al. [2019]. Preparatory work for this study was published in the Journal of Geophysical Research: Solid Earth as Frederiksen et al. [2013a].

1.3. Chapter 3: Possible causes of the Anomalously Large Western Interior Basin

The Western Interior Basin has an anomalous morphology in that it is much wider and deeper than a textbook example of a foreland basin. Sediment isopachs, surface expressions of volcanism, crustal structures, and subducted slab locations through time were used in conjunction with tomographic models to test two hypotheses for the formation of the WIB. While unequivocally proving or disproving these hypotheses was not an outcome of this work, I was able to determine that Farallon slab fragments were in the correct location at the correct time to influence WIB formation.

1.4. Chapter 4: Aspects of operating a broadband seismic field experiment: SPREE

It is easy to take for granted the quality of seismic networks but in reality it takes a great deal of planning, knowledge, and work to generate research-grade data. Stations are sited, installed, and serviced according to a set of guidelines but there are many issues in the field that can challenge the quality of individual stations and the network as a whole. Within the SPREE array the challenges varied over the field area. Challenges lead to compromises and some of these are reflected the data quality. To assess this quality, I share probability density function plots of PSDs for the stations that were my responsibility within SPREE, namely the Canadian stations located in Northern Ontario. An analysis of the SPREE network revealed a number of features in the noise spectrum, including

diurnal noise fluctuations in due to changes in cultural activity and wind speed changes throughout the day and night, summer/winter changes in long period noise attributed to atmospheric circulation, and the identification of microseisms originating in Lake Superior.

CHAPTER 2

P Wave Teleseismic Traveltime Tomography of the North American Midcontinent

2.1. Introduction

The remnants of the Midcontinent Rift (MCR), including both igneous material emplaced during rifting and associated rift basins that were filled in and covered by Mesoproterozoic and younger sediments (*Van Schmus*, 1992; *Miller et al.*, 2013), lie in a tectonically inactive portion of the North American continent. When the rift initiated at 1.1 Ga, the core of Laurentia had already been formed ∼900 My earlier through a series of Paleoproterozoic collisions between Archean cratons (*Bleeker*, 2003). The rift system was active for over 20 My, during which time a large amount of volcanic material was episodically emplaced into the crust from the Nipigon Embayment, north of Lake Superior to Kansas in the south (*Ojakangas et al.*, 2001). The most prominent positive Bouguer gravity anomaly in North America is due to the high density of the volcanic material and its current shallow depth of burial (Figure 2.1) in the midcontinent.

The amalgamation of North America left many sutures and shear zones as a reminder of the turbulent history of the continent's formation. These sutures are more easily reactivated during rifting than the creation of new rift margins, especially through cratonic material. This has been seen in the opening and closing of repeatedly rifted ocean basins such as the Atlantic (*Buiter and Torsvik*, 2014). A discriminating feature of the MCR is that it does not consistently follow these weakened zones as expected for a passive rift but also cross-cuts them in a seemingly random manner (*Van Schmus and Hinze*, 1985; *Ojakangas et al.*, 2001). Since the formation of the MCR, no major tectonic events have affected the mid-continent of North America. The crustal portion of the failed rift has since been covered by Mesoproterozoic sediments (*Van Schmus and Hinze*, 1985; *Ojakangas et al.*, 2001; *Ojakangas and Dickas*, 2002).

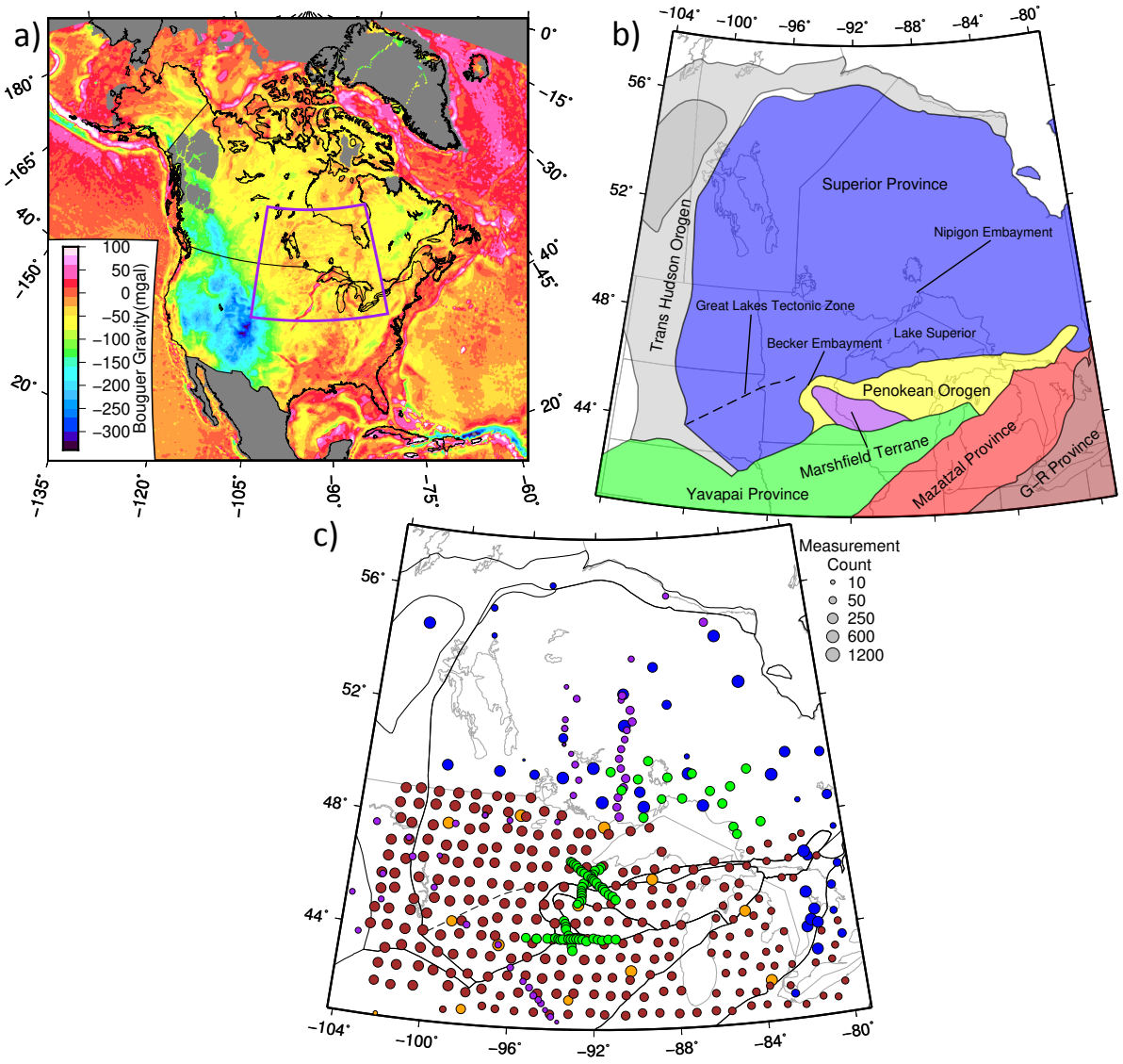

Figure 2.1. a) The Bouguer gravity anomaly of North America from the Decade of North American Geology 6 km spacing gravity grid (*Tanner et al.*, 1988). The study region is shown by the box. b) Map of the terranes/provinces of the region from *Whitmeyer and Karlstrom* (2007). c) Seismic stations used in this study. Green circles are stations from the SPREE network, red are USArray Transportable Array stations, orange are permanent stations in the GSN or USNSN, blue are CNSN, University of Manitoba, Polaris Ontario or Fednor stations, and purple are stations from the pre-EarthScope TW∼ST, FLED, or APT-89 experiments. Station symbols are sized by the number of measurements at each station.

Previous continental-scale tomographic studies that include this region image a fairly homogeneous upper mantle structure beneath the MCR (*Grand*, 1994; *van der Lee and Nolet*, 1997; *van der Lee and Frederiksen*, 2005; *Bedle and van der Lee*, 2009). This could be due to 1.1 Gy of mantle cooling, plate movement and a limited role of the lithosphere during rifting, or due to limits in resolving power, controlled by the distribution and operational periods of the seismic stations used. *Frederiksen et al.* (2013a) used teleseismic P-wave tomography to investigate the lithosphere beneath the southwestern edge of the Superior Province. However, like the larger-scale tomographic studies (*van der Lee and Nolet*, 1997; *van der Lee and Frederiksen*, 2005; *Bedle and van der Lee*, 2009; *Simmons et al.*, 2010; *Sigloch and Mihalynuk*, 2013; *Schmandt and Lin*, 2014), the data used had little resolving power for structures at the scale of the MCR. Other recent tomographic studies of seismic surface waves and seismic noise recorded by the 75-km spaced Transportable Array do show crustal structures in the shape of the MCR (*Shen et al.*, 2013; *Pollitz and Mooney*, 2014), but have insufficient depth resolution to say whether the mantle retains evidence of the rifting. Here we define our study area so that the MCR, overlain by the more densely-spaced stations of the SPREE project (*Wolin et al.*, 2015), is at the center of the model. We show that this addition of stations increases the resolving power of our model to the level of being able to image rift structures within the MCR.

2.2. Geologic Background

The Superior region consists of numerous terranes that were accreted to the margins of the Superior Province (Figure 2.1) during its formation in the Proterozoic (*Hoffman*,

1988; *Bleeker*, 2003; *Whitmeyer and Karlstrom*, 2007). The Superior Province, which formed at 2.7 Ga (*Bleeker*, 2003), is the largest and oldest province in this region, and forms the core of the eastern Canadian Shield. On the western and northern border of the Superior is the Trans-Hudson Orogen, which affixed the Superior Province to other Archean crustal blocks during the assembly of Laurentia beginning at around 1.9 Ga (*Hoffman*, 1988).

Directly to the south of the Superior Province are the Penokean Orogen and the Marshfield Terrane (Figure 2.1b). The former is an oceanic arc terrane, while the latter is a small piece of Archean crust that collided with the southern margin of the Penokean Orogen in a northwesterly direction (*Schneider et al.*, 2002). Their emplacement may have been guided by offsets, from a prior rifting event, in the southern margin of the Superior Province (*Schulz and Cannon*, 2007; *Chandler et al.*, 2007), at least partially resulting in the arcuate shape of the province at its western syntaxis. South of here, the Yavapai and Mazatzal Provinces were accreted on a NE-SW margin. These terranes are a combination of juvenile crust from the Yavapai and Mazatzal orogenic events and are only differentiated by their Nd model ages, being 1.8-1.7 Ga and 1.7-1.6 Ga respectively (*Karlstrom and Humphreys*, 1998; *Bowring and Karlstrom*, 1990; *Shaw and Karlstrom*, 1999). After a roughly 50 My tectonic lull, the Granite-Rhyolite Province was added to the southern margin during the following 150 My (*Bowring and Karlstrom*, 1990). During the accretion of the Granite-Rhyolite Province, extensive granitoid bodies were emplaced within the Granite-Rhyolite Province and, to a lesser extent, the older terranes to the northwest (*Van Schmus et al.*, 1996; *Karlstrom and Humphreys*, 1998).

The cause of initial rifting is unclear but associated with the MCR are ∼2 million km^3 (*Cannon*, 1992) of 1.1 Ga basalts distributed over a 1000 km long linear feature (*Van Schmus and Hinze*, 1985; *Ojakangas et al.*, 2001). These iron-rich basalts are the source of the largest positive gravity anomaly in North America due to their volume, density, and proximity to the surface (*Hinze et al.*, 1992). In the United States portion of the rift, the associated volcanics follow a linear path along the axis of the rift although in Canada the volcanics cover a wider area in the form of sills and flood basalts in the Nipigon Embayment and other locales along the north shore of Lake Superior (*Hollings et al.*, 2007). The MCR's volcanic rocks show a strong iron enrichment over time (*Ojakangas et al.*, 2001). Some of the later, most iron rich magma may have remained in the previously depleted lithosphere. This could have been related to an underplated layer as observed by *Zhang et al.* (2016).

The MCR crosscuts all of the above mentioned terranes, from the Superior Province southwards, with the exception of the Granite-Rhyolite Province, which is too far to the south and east. Another aspect of the MCR is the path it took cutting through these provinces without following the known shear or collision zones along which the provinces were accreted (*Klasner et al.*, 1982). Instead, as rifting of Laurentia began, it cleaved through these provinces in a fairly linear fashion. Some basaltic lava flows were deposited sub-aqueously along with siltstones and shales of the Nonesuch formation, likely deposited in a series of lakes or a shallow sea (*Anderson and McKay*, 1997; *Ojakangas et al.*, 2001). After rifting ceased, south of Lake Superior the two sides of the rift were thrust back towards each other during 1060 - 1045 Ma (*Cannon et al.*, 1989; *Cannon*, 1994; *Zhang et al.*, 2016).

2.3. Data and Methods

2.3.1. Instrumentation

The ∼3.2 million km^2 study area of this paper was covered by a number of different seismic networks. The greatest number of stations belong to the TA (*Meltzer et al.*, 1999), which covered the southern half of the study area with stations spaced approximately 75 km apart. The United States National Seismic Network (USNSN) (*Masse et al.*, 1989), Global Seismic Network (GSN) (*Butler et al.*, 2004), and FLED (*French et al.*, 2009) added 42 stations to the station coverage that the TA provided. The Canadian portion of the study area was covered by a combination of the digital Canadian National Seismograph Network (CNSN) (*North and Basham*, 1993), POLARIS (*Eaton et al.*, 2005), University of Manitoba, and the temporary deployments FedNor (*Darbyshire et al.*, 2007), TW∼ST (*Kay et al.*, 1999), and APT89 (*Silver and Kaneshima*, 1993).

With the movement of the TA through the Midwest, there was complete coverage of the US portion of the study area and the southernmost portion of Ontario for the first time. This was a vast improvement over *Frederiksen et al.* (2013a), in which the TA had only reached the Minnesota-Wisconsin border. Another major improvement in our ability to image structures on the scale of the MCR was the station coverage provided by the SPREE array. SPREE was an 82 station deployment of the EarthScope Flexible Array instrumentation in the United States and Canada (*Wolin et al.*, 2015). Its 16 Canadian stations extended the ambient coverage that the TA provided northward, while the US portion of SPREE constitutes 66 closely spaced stations (∼13 km spacing on average) along and across the MCR (Figure 2.1c) (*Wolin et al.*, 2015). Positioning the US stations

in these lines, two crossing at relatively strong and weak gravity highs, respectively and one following the rift axis of the MCR in Wisconsin and Minnesota, allows us to resolve small structures in the lithosphere and upper mantle related to the rift. Together these make up 206 new stations for which we measured teleseismic delay times for 255 earthquakes spanning a 30.5-month period from April 16, 2011 to October 31, 2013. We also include the delay measurements used by *Frederiksen et al.* (2013a) and delay times from FLED stations (*French et al.*, 2009; *Lou and van der Lee*, 2014) within the study region. With this inclusion, we invert all available delay times for the study area from June 8, 1989 to October 31, 2013. This results in nearly double the number of delay times used in all previous studies and much improved station coverage.

2.3.2. Traveltimes

Delay times of P-wave first arrivals were measured in vertical-component seismograms of teleseismic events at all stations within the study area recording the event. Data were downloaded and preprocessed using the Standing Order for Data (SOD) (*Owens et al.*, 2004). SOD used the instrument response to convert seismograms to ground velocity records and applied a band pass filter from 0.01 to 6 Hz.

The traveltimes were measured using the multichannel cross-correlation method of *VanDecar and Crosson* (1990) as implemented in the AIMBAT travel time picking tool (*Lou et al.*, 2013). This method yields absolute and relative traveltimes. The observed relative traveltime for event i and station j is

$$t_{ij} = T_{ij} - \bar{T}_i \tag{2.1}$$

where T_{ij} is the true absolute traveltime and $\bar{T}_i$ is the average of all traveltimes for the ith event. The observed relative delay times were then compared to the predictions from the model *iasp91* (*Kennett and Engdahl*, 1991) by subtracting the *iasp91* predicted travel times, T_{ij}^{IASP91}, from the observed times as shown in Equation (2).

$$\delta t_{ij} = t_{ij} - T_{ij}^{IASP91} + \bar{T}_i^{IASP91} \tag{2.2}$$

The residuals δt_{ij} have a zero event mean and are easily compared from event to event.

Relative delay times from a total of 255 earthquakes between April 16, 2011 and October 31, 2013 (of magnitude 5.5 and greater, 30° - 93° from the center of the study area) were picked at 364 stations for a total of 45,006 new travel time picks. These were added to relative delay time picks for events from the previously mentioned studies for a total of 101,233 traveltime picks (Figure 2.1c) for 1,720 events (Figure 2.2) and 460 stations. At 1205 measurements, the CNSN station ULM, in Lac du Bonnet, Manitoba, yields the most traveltimes. All delay times were corrected for topography and the ellipticity of the Earth.

2.3.3. Rift-related Delay Times

We grouped delay times from stations on the rift (as identified by the Bouguer gravity high) and compared them to delay times from stations away from the rift (Figure 2.3).

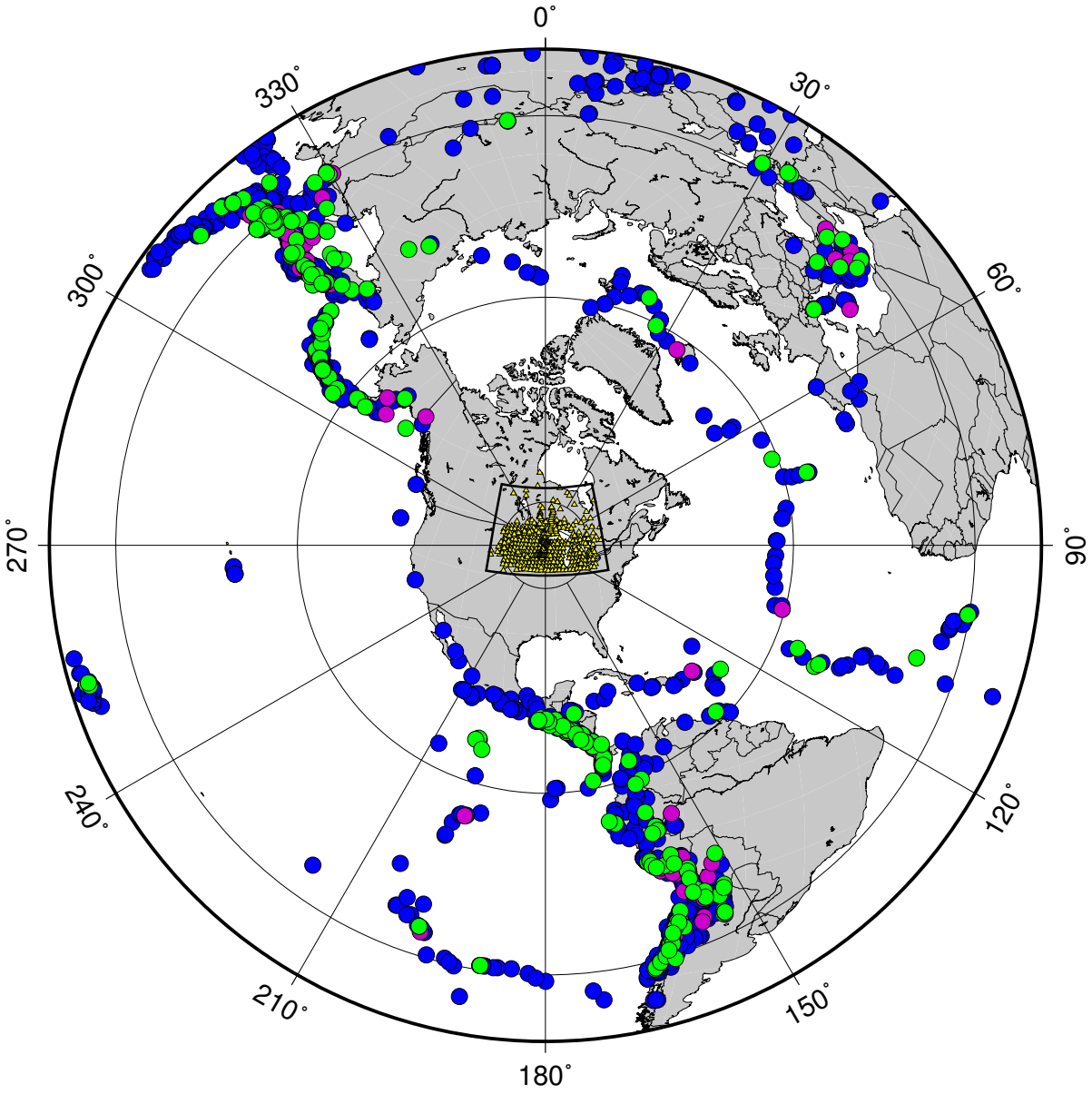

Figure 2.2. The 1,721 events used in this study. Green circles are new events, blue circles are events also used in *Frederiksen et al.* (2013a, 2007), and purple circles are events recorded by the FLED array (*French et al.*, 2009). Yellow triangles indicate locations of seismic stations used in this study. The box around the stations is the study region.

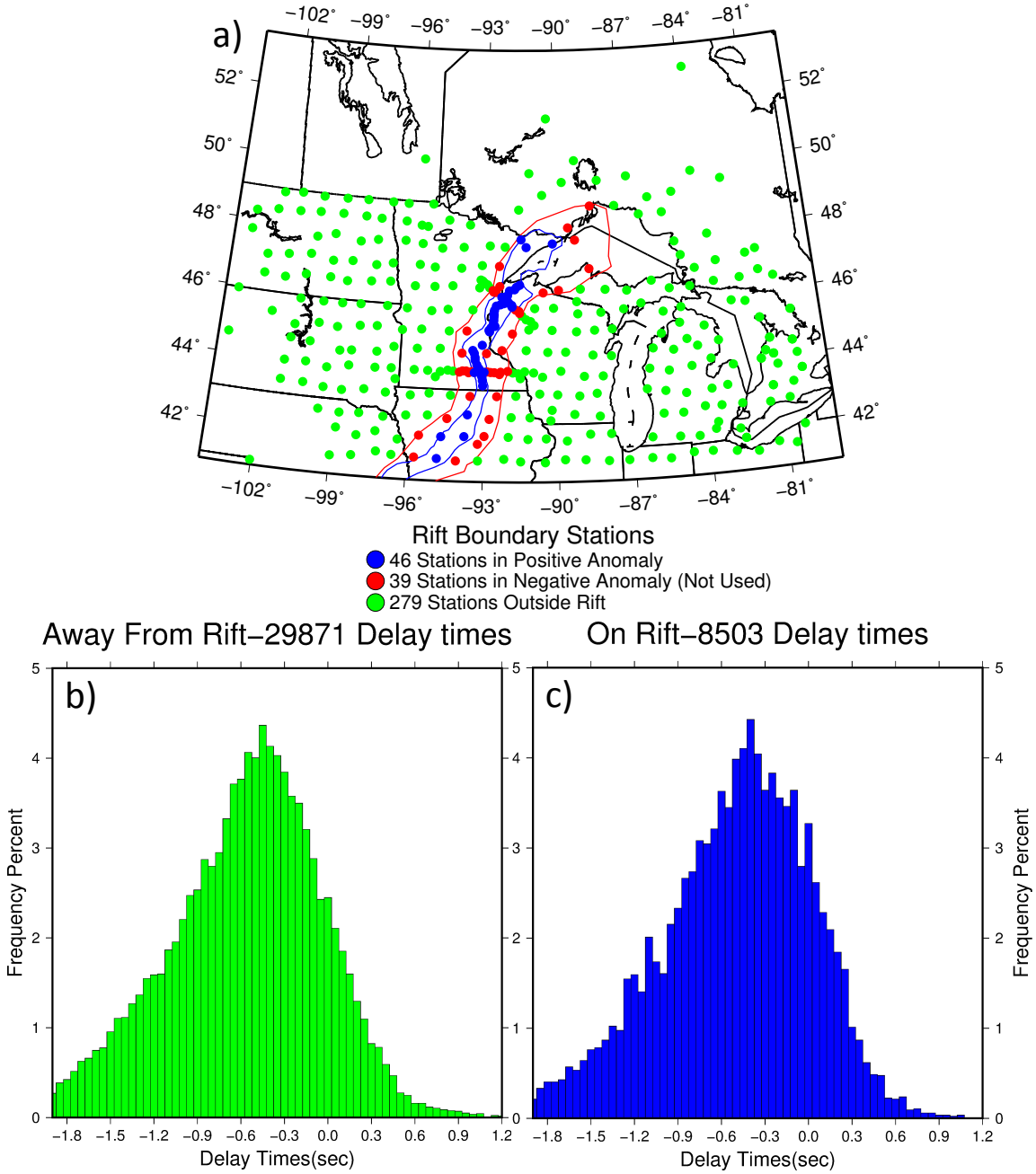

Figure 2.3. a) Map of stations with new delay times separated by whether they are within the positive Bouguer anomaly, the negative Bouguer anomaly, or outside the rift completely. b) Frequency-percent histogram of delay-time measurements away from the rift. c) Frequency-percent histogram of delay-time measurements from on the rift.

Stations in between these two domains, on the sedimentary flanks (and Bouguer gravity lows), were not included in either group in order to enhance their contrast. The standard deviations of both groups of relative delay times are similar to the standard deviation of all relative delays of 0.4 s. The mean delay time of the on-rift group is roughly 0.05 s later than that of the away-from-rift group (with a mean relative delay around 0 s) and the difference between the mean delay times of the two groups is approximately an order of magnitude smaller than the groups' standard deviations, which are similar to the standard deviation of the distribution of all relative delays in this study. This 0.05 s difference in magnitude is consistent with what one would expect from an underplated layer found along the rift by *Zhang et al.* (2016). The standard deviation of our relative delay times from Equation (2) is 0.4 s. This is less than the standard deviation of relative delay times of 0.5 s measured for the Kenya rift (*Park and Nyblade*, 2006) and the Ethiopian hotspot (*Bastow et al.*, 2008), which are active segments of the East African rift. Both these studies have similar post-imaging residual-delay distributions as our study does, but started from a wider distribution, suggesting that 1 billion years of post-rift stability experienced by the MCR, likely reduced heterogeneity.

2.4. Tomographic Model

2.4.1. Basis

In our inversion, the traveltime (t_{ij})consists of components for the event term (e_i), station term (s_j), and path component (p_{ij}) (*VanDecar*, 1991):

$$t_{ij} = e_i + s_j + p_{ij} \tag{2.3}$$

The event term consists of four components and corrects for structure on the source side as well as source mislocations and origin time errors, the station term corrects for station side structure including crustal structure and site response, and the path component represents the contribution of 3-D structure along the ray path. Since we use teleseismic events, the incidence angles of the paths in the crust vary between 48° and 24° from vertical, and primary crustal structure is absorbed by the station term s_j. Similarly, source-side structure is considered to be the same for all measurements t_{ij} for event i because the ray paths near the source are similar due to the source-receiver distance being much greater than the aperture of the array.

A number of ray crossings in the upper and mid-mantle are expected (Supplemental Figures A.1 and A.2 available in Appendix A), with the densest regions being beneath the US portion of the SPREE network. The model base is at a depth of 1500 km. Laterally, the model grid extends roughly 1.5 degrees on all sides outside the footprint of the array.

2.4.2. Inversion Parameters

We use the method of *VanDecar* (1991) to perform a tomographic inversion for P velocity. The model is parameterized in terms of deviations from *iasp91* P-wave velocities on a set of splines under tension. This allows for smooth interpolation between the nodes of the grid, shown in Figure 2.4, which also illustrates that our model extent is identical to that of *Frederiksen et al.* (2013a). Due to the dense spacing and therefore greater resolving

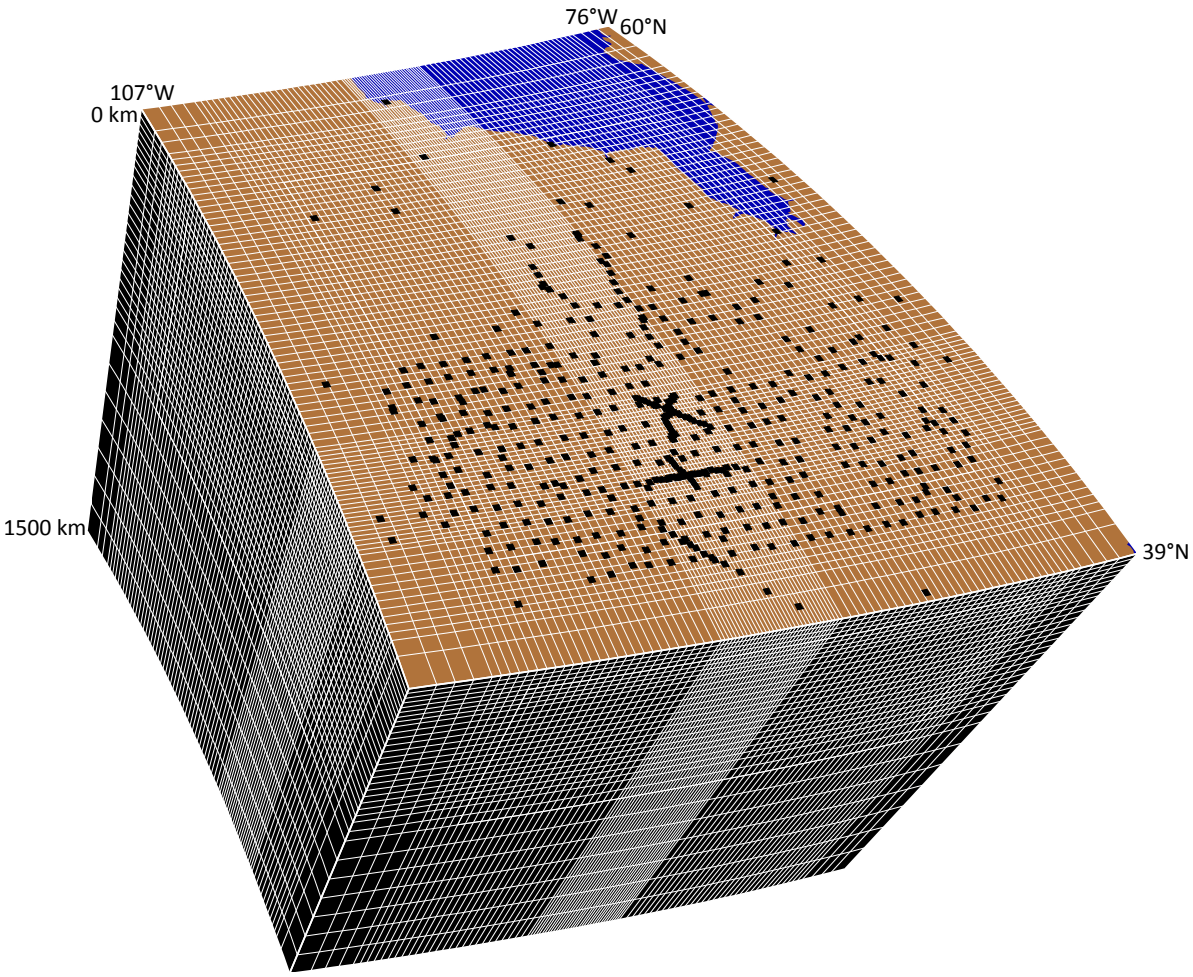

Figure 2.4. The model grid used in the inversion. Grid knots are located at the intersections of the white lines. Between the knots, the model is interpolated according to *VanDecar* (1991). The center of the model is densified to take advantage of the increased density of stations, which are shown by black squares.

power of the SPREE stations in the center of the model, the horizontal knot spacing was decreased to 0.15 degrees in latitude and longitude (∼17 km and ∼12 km at 45°N, respectively) in the central portion of the model space, whereas the surrounding knots have a spacing of 0.25 degrees (∼28 km) in latitude and 0.33 degrees (∼29 km at 45°N) in longitude. At the edges of the model the knot spacing was widened to 0.66 degrees then 1.0 degrees in longitude and 0.5 then 1.0 degrees in latitude. Vertical knot spacing is 25 km in the uppermost 200 km, increasing to 33 km from 200 to 700 km depth, 50 km from 700 to 800 km, and 100 km from 800 km to the base of the model at 1500 km. This brings the total grid knots in the model to 286,638.

Additional unknowns in the inversion are 460 station terms and 6,884 event terms. Combining these terms with the grid nodes, results in an inverse problem with 293,982 unknowns that is therefore mixed determined, meaning some nodes are overdetermined while under-sampled nodes are strongly underdetermined.

2.4.3. Regularization

Since the inverse problem has a strongly underdetermined portion, the recovered model will be very dependent upon the nature and strength of the regularization used. We applied a smoothing regularization (minimizing model curvature) to the model in order to favor long-wavelength structure in the final model. Small amounts of flattening (slope minimization) and damping (minimization of deviation from *iasp91*) were also included. We also damped the event location perturbations and station time corrections, while event time corrections were left undamped to compensate for the relative nature of the time picks.

The level of smoothing was chosen using the"L-curve" method, in which the model roughness is plotted against data misfit for a number of different smoothing levels (*Parker*, 1994). The appropriate level of smoothing is determined by selecting a level at which a reasonable misfit is found and features in the output model are deemed geologically feasible. Below this point represents a level of regularization where noise instead of data is being fit. The smoothing level we selected reduced the RMS misfit from 0.40 to 0.03 s, which is comparable to the remaining misfit found for tomographic studies of the East African rift (*Park and Nyblade*, 2006; *Bastow et al.*, 2008). Our data are thus fit to similar noise levels.

One of the most striking features of Figure 2.5 and Figure 2.6 is that the station terms of the pre-EarthScope temporary networks (APT-89, TW∼ST, and FLED) do not match the sign or magnitude of the stations nearest to them. This phenomenon is most likely due to those experiments being conducted at a time that did not overlap with other stations used in this study. Therefore the travel times for those stations were measured with respect to a different effective baseline. This difference in baseline is visible in Figure 2.5 and not in the tomographic anomalies in Figure 2.6, so it thus has been absorbed by the station term calculation. Other noticeable features in the station terms are that the largest negative terms of ∼-0.8 s occur in the Canadian Shield stations to the north, whereas the largest positive station terms of ∼0.75 s occur in the central portion of the Williston Basin in the western Dakotas (∼47 °N, ∼103 °W) These features align with the regions of the least and most sediment or rock younger than Precambrian, respectively. The large negative signature is due to the Canadian Shield having a higher velocity than the crust to the south and the large positive signature is due to the thick stack of sediments

in the Williston Basin having a lower velocity than the surrounding regions, which are not deep sedimentary basins.

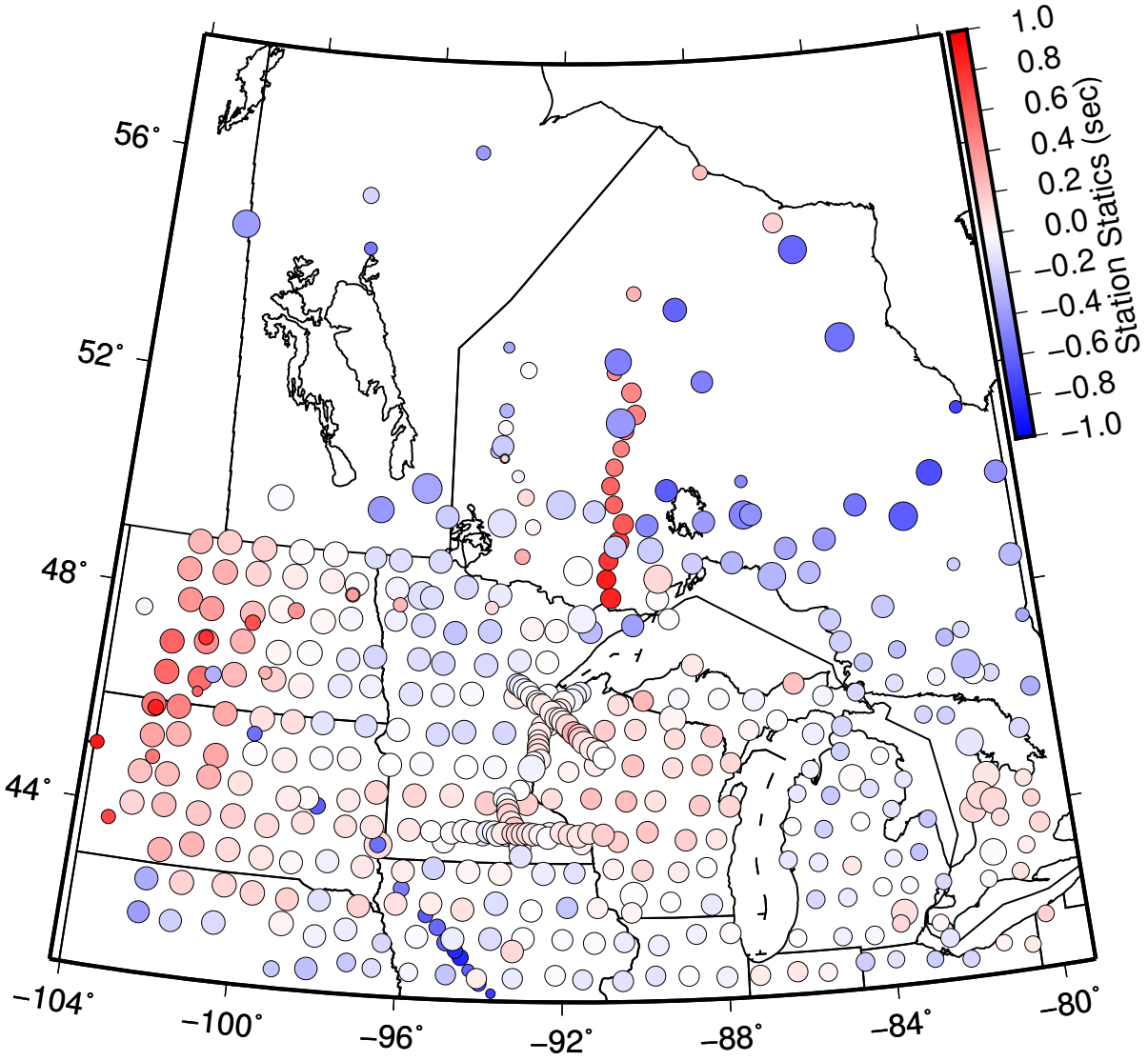

Figure 2.5. Station statics calculated during the inversion. Station symbols are sized by the number of measurements taken at each station.

2.4.4. Model Features

A series of plan sections taken through the final model are shown in Figure 2.6. The largest lithospheric anomaly in our model is a high-velocity region labeled Western Superior (WS) in Figure 2.6c. The eastern border of WS is well resolved, running roughly parallel to the 90° W meridian and the WS velocity anomaly is at least 300 km thick (Figure 2.7). Its northwestern border is poorly resolved due to a lack of stations in that region. To the east of WS, a low-velocity region labeled Eastern Superior Low-Velocity Anomaly (ESLVA) is located in the lithosphere and continues throughout the upper mantle. On the western edge of ESLVA there is a portion of the anomaly that underlies the Lake Nipigon Embayment.

Another striking feature is a pair of low-velocity anomalies labeled Mid-continent Rift (MCR). They are located between 50 and 150 km in depth and follow the rift at the locations of the highest gravity anomalies. Other features include a a high-velocity region located around 400 km deep, labeled Transition Zone (TZ), two deep linear features labeled Farallon Slab (FS) and Kula Slab (KS) at depths of 1000 and 1200 km, respectively, a high-velocity zone at a depth of 200 km to the northwest of TZ, labeled Minnesota River Valley (MRV), and two low-velocity zones located at different syntaxes of the Penokean Orogen that extend from 100 to 250 km in depth, labeled Syntaxis 1 and 2 (S1 and S2).

2.4.5. Resolution Tests

To assess the resolving power of our dataset, we computed synthetic data from theoretical models. These synthetic data were then inverted to reveal what sizes of structures could be resolved in different regions of the model, and the manner in which the input structures

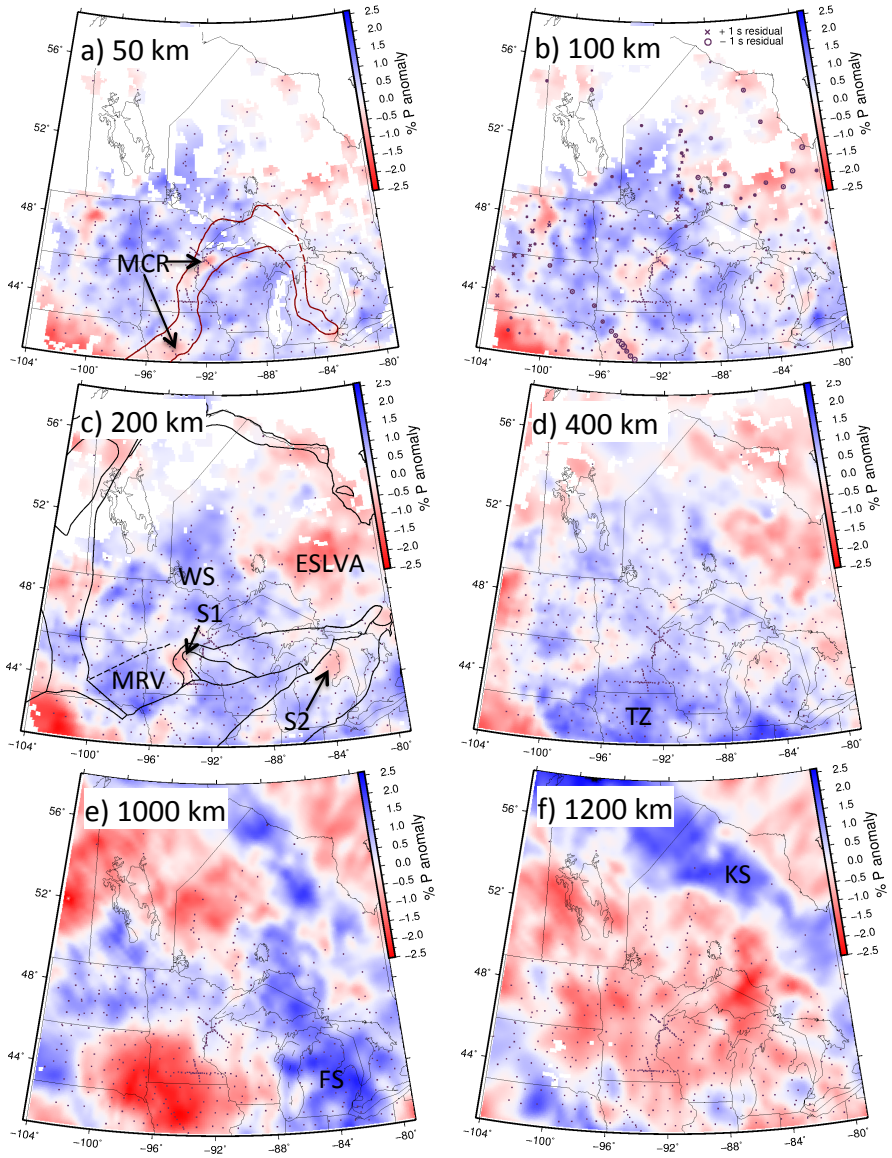

Figure 2.6. Plan sections through the final model. MCR-Midcontinent Rift, WS-Western Superior, ESLVA-Eastern Superior Low Velocity Anomaly, MRV-Minnesota River Valley, S1/S2-Syntaxis Anomalies, TZ-Transition Zone, FS-Farallon Slab, KS-Kula Slab: (a) includes the outline of the MCR gravity anomaly (dark red line), (b) includes station residuals calculated during the inversion, and (c) includes terrane boundaries from *Whitmeyer and Karlstrom* (2007) (solid black lines) and the surface expression of the Great Lakes Tectonic Zone, modeled after *Holm et al.* (2007) (dashed line). Small black dots in sections are seismic stations.

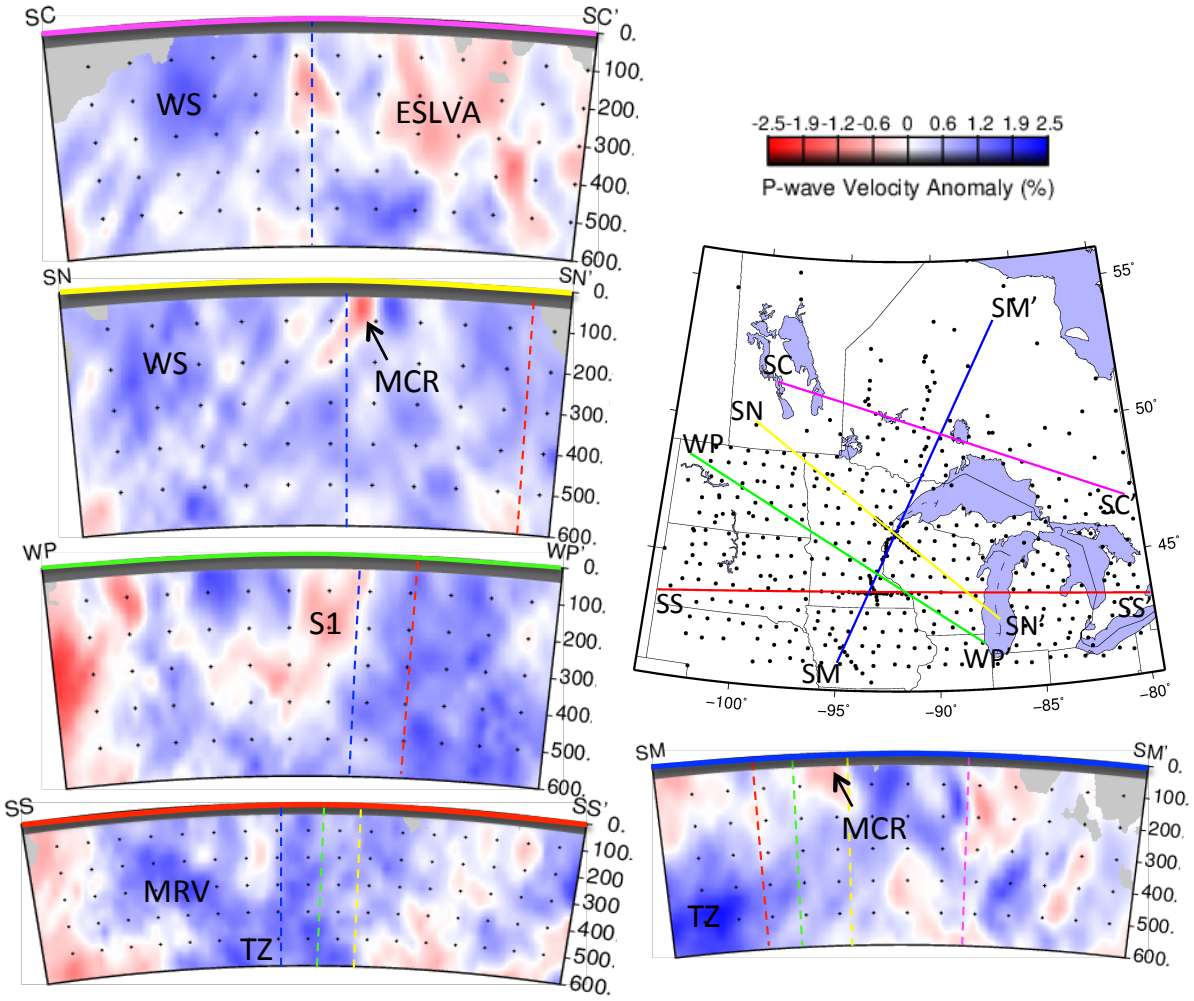

Figure 2.7. Cross-sections through the final model to a depth of 600 km. Dashed lines on the cross-sections are intersection points of cross-sections and match the color of the section lines on the map view. Labeled features in cross-sections are the same as in Figure 2.6.

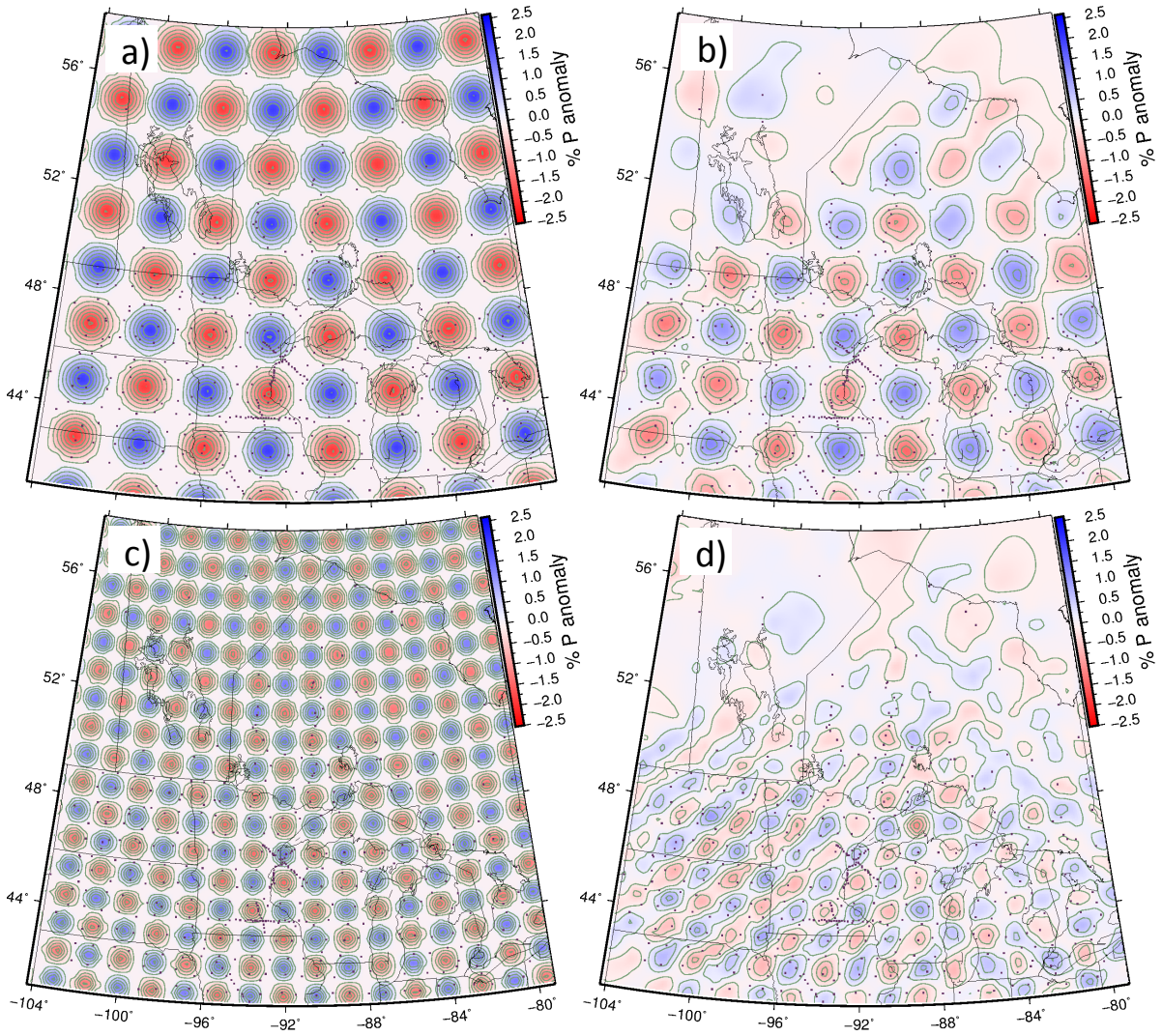

Figure 2.8. Selected checkerboard resolution tests. (a) Coarse input at 200 km depth. (b) Coarse output at 200 km depth. (c) Fine input at 266 km depth. (d) Fine output at 266 km depth.

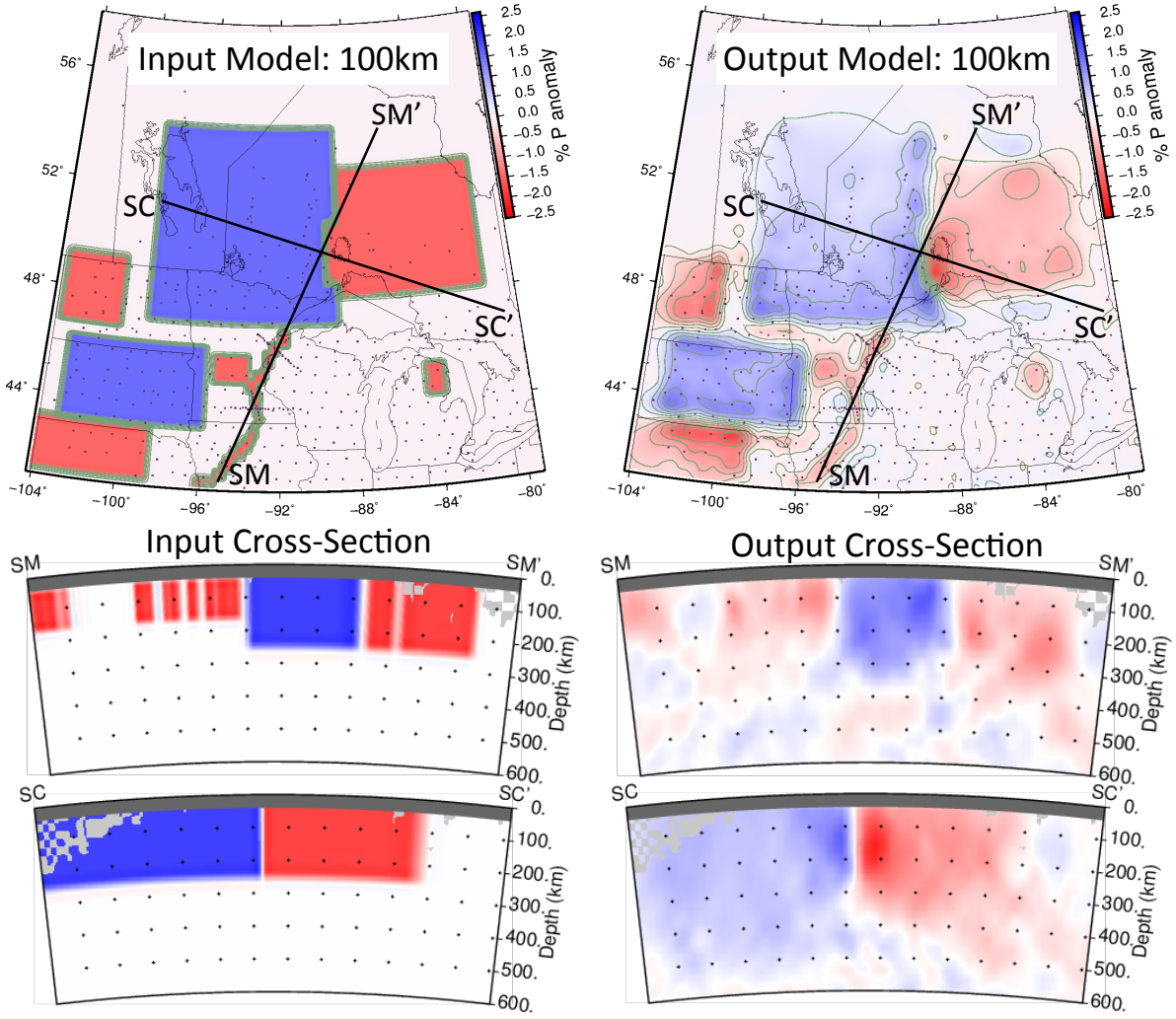

Figure 2.9. Structural resolution test to quantify the amount of lateral and downward smearing of features similar to those seen in the final model. Cross-section locations are the same as in Figure 2.7.

are smeared along the teleseismic ray paths. One set of hypothetical models consists of a number of three-dimensional "checkerboards" (Figure 2.8). These consist of alternating polarity Gaussian anomalies whose amplitudes reach ±2% of the background velocity. We created these tests for two different 3-D spacings, 100 km and 200 km. Random noise

with a standard deviation of 60 ms was also added to the computed data for all forward models to mimic the noise that occurs in real measurements.

Figure 2.8b shows that 200-km-scale structures in the study region are easily resolved, although 100 km structures in the western portion of the model become somewhat smeared in the southwest-northeast direction (Figure 2.8d). Reduced resolving power is also found for smaller structures beneath the eastern half of Lake Superior, which has fewer crossing ray paths than the west side of the lake.

Checkerboard resolution tests determine if small features can be detected by the model but can also mask the effects of smearing. Resolution tests with synthetic structures similar to features seen in the model were carried out to address this problem (Figure 2.9). Synthetic structural resolution tests illustrate which features can be resolved, assess the role of smearing, and evaluate the tendency of our smoothing-dominated inverse process to evenly distribute structural anomalies even when delays can be caused by isolated anomalies. Features were assigned velocity anomalies of $\pm 1.5\%$ and thicknesses of 250 km. Features S1, S2, and the MCR were assigned a thickness of 100 km and are situated in the lower lithosphere from 100 km to 200 km in depth to mimic the structure seen in the final model. The plan section in Figure 2.9 shows that the data are capable of resolving sharp lateral boundaries of the input structures and can even discern the shape of the narrow feature modeled after the MCR gravity anomaly. There is minimal lateral smearing with the exception of regions that have little-to-no station coverage. Because relative travel times are inverted, the centers of large anomalies appear weaker in the output model than in the input model. This is because the relative delay between two stations that pass through nearly identical anomalies would be very small or zero, whereas

stations that cross a boundary between anomalies have a large relative delay. Absolute delay times would better preserve the amplitude in the features' centers due to being independent of relative changes between adjacent arrivals, but are not used in this study. Another reason for the lessened amplitude of the output model is due to the damping regularization that is necessary for the numerical stability of the inversion in combination with the relative delay times used. These factors combine to create a model relatively insensitive to large wavelength features and more sensitive to abrupt changes in velocity and therefore Earth structure.

The structural test is especially effective in showing the degree of vertical smearing to expect in the final model caused by the nearly vertical nature of the teleseismic rays. The cross-sections in Figure 2.9 show that vertical smearing is a major feature of the output model and the depths to which features are smeared depend on ray path coverage. In cross-section SC-SC' the large features are consistently smeared down to a depth of 400-450 km with some regions smearing farther, whereas in cross-section SM-SM' the features are smeared to a depth of 350-400 km. The difference in station coverage and raypath density in the areas of cross-section SM-SM' and SC-SC' corroborate this theory, with the majority of SM-SM' having a higher station density than SC-SC' (Supplemental Figure A.1 available in Appendix A). When comparing the depth that features in the final model reach with those same features in the synthetic model, it is apparent that the features are most likely confined to the lithosphere which has a thickness of approximately 200-250 km (*van der Lee and Nolet*, 1997; *Goes and van der Lee*, 2002; *Darbyshire et al.*, 2007). The large amplitudes of the anomalies are also not being smeared down to the location of feature TZ, so it is unlikely that it is a smearing artifact.

2.5. Discussion

2.5.1. Depth Controls on the MCR Low-Velocity Anomaly

Near the southern tip of Lake Superior and in Central Iowa we see two low-velocity anomalies (labeled MCR in Figures 2.6 and 2.7) that coincide with the highest Bouguer gravity anomalies associated with the rift in those areas (Figure 2.10). Resolution tests show that the shapes of the features are reasonably well resolved, especially under the footprint of SPREE where the amplitude of the anomaly is also better preserved (Figure 2.9).

Since teleseismic tomography tends to smear anomalies vertically along lithospheric segments of ray paths, it is necessary to conduct more than one resolution test of geologically feasible scenarios in order to assess the resolving power for depth and depth extent of the anomalies. One test scenario was modeled after the discoveries of MCR underplating by *Behrendt et al.* (1990) and *Zhang et al.* (2016). The receiver function analysis by *Zhang et al.* (2016) of all SPREE receiver functions revealed a complex crustal structure beneath the MCR that is remarkably consistent along the axial gravity high of the MCR. Together with the results and interpretation of *Behrendt et al.* (1990), these SPREE findings on crustal structure provide a strong interpretation framework for inconclusive results from receiver function studies for a handful of individual stations on the MCR's gravity high (*French et al.*, 2009; *Moidaki et al.*, 2013; *Shen et al.*, 2013). At first glance, receiver functions produce sharp peaks for Moho conversions away from the gravity high, but these peaks are weaker, broader, and less consistent for Moho conversions beneath the gravity

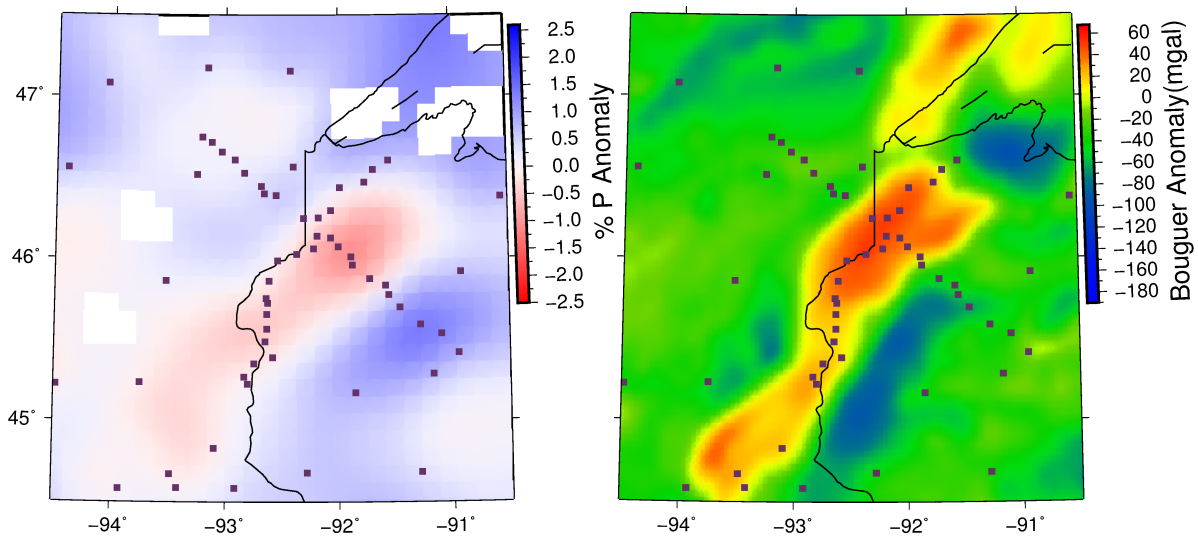

Figure 2.10. Zoomed in map of the northern MCR velocity anomaly at 50 km (left) and Bouguer gravity anomaly (right) to show similarity in anomaly shape. Black squares are seismic stations.

high. A closer inspection of the individual receiver functions showed that seismic waves from different azimuths produce weak positive conversions from two different discontinuities, one above and one below the regional Moho depth (*Zhang et al.*, 2016). The distance between these weaker discontinuities decreases with increasing distance from the rift axis, and the intermediate-impedance material between the two discontinuities is interpreted as "underplated", following *Behrendt et al.* (1990) and dozens additional publications of crustal structure of the MCR beneath Lake Superior. (*Zhang et al.*, 2016) infer that the underplated "layer" is located at 30-50 km in depth and extends axially along the segment of the MCR between Lake Superior and Iowa, and likely beyond (Figure 2.12). A second test scenario is an identically shaped low-velocity anomaly, but residing in the upper mantle lithosphere at depths of 100-120 km (Figure 2.13). These scenarios were then compared to the MCR resolution test with a low-velocity anomaly of 100 km thickness

(Figure 2.11). A side by side comparison of the final tomographic model and the three scenarios (Figure 2.14) shows subtle differences between these resolution tests. Figure 2.14 shows that if there is a substantial mantle signature of the rift, our data would "see" it. However, our model shows weak intermittent structures, similar in character to the tests shown in Figures 2.12 and 2.13, suggesting that rift-related anomalies are relatively thin but that their depths cannot be uniquely established. We thus conclude that the MCR anomaly seen in our tomographic model could either be caused by smearing of a crustal underplating associated with the rift or from a structure in the upper mantle lithosphere. We know from *Zhang et al.* (2016) that a slowing underplated "layer" exists along the entire rift segment covered by SPREE stations and its modeled effects on P velocity delay times is of the same order of magnitude as the difference between mean delay times measured on and away from the rift (Figure 2.3).

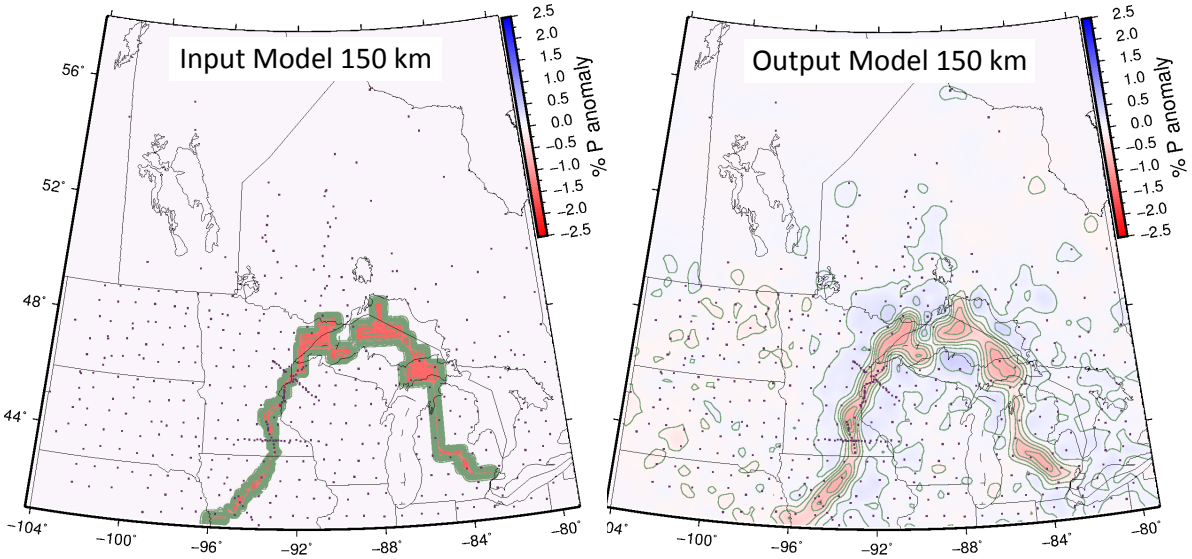

Figure 2.11. Resolution test mimicking the spatial extent of the MCR Bouguer gravity anomaly between 100 and 200 km depth and a velocity anomaly of 2 percent.

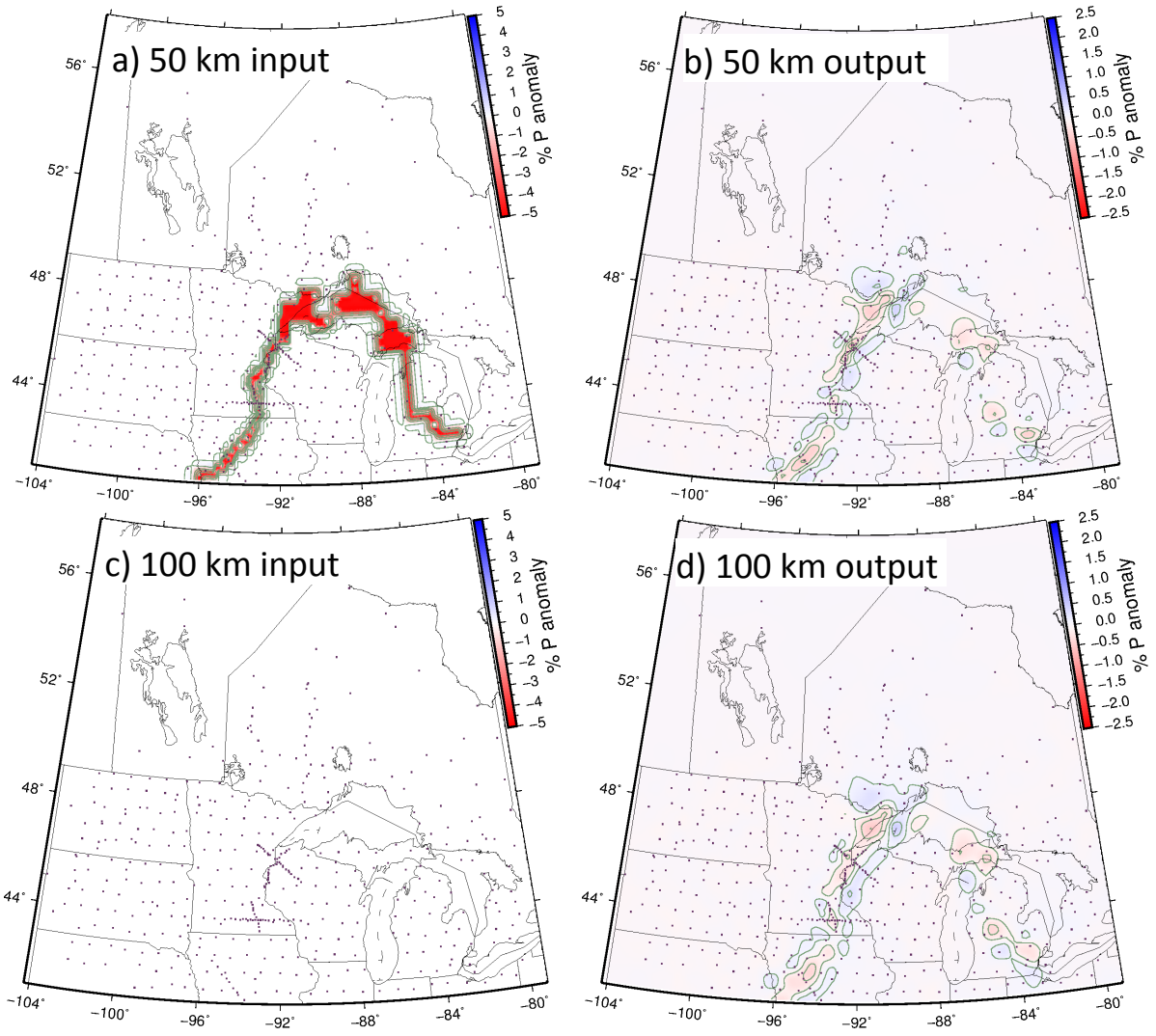

Figure 2.12. Input and output models of a resolution test mimicking the spatial extent of the MCR Bouguer gravity anomaly with a depth of 30-50 km and a velocity anomaly of 5 percent. All anomalies present in the 100 km output are due to vertical smearing along the ray paths. This resolution test was completed to test the theory that the rift is underplated in the crust and upper mantle.

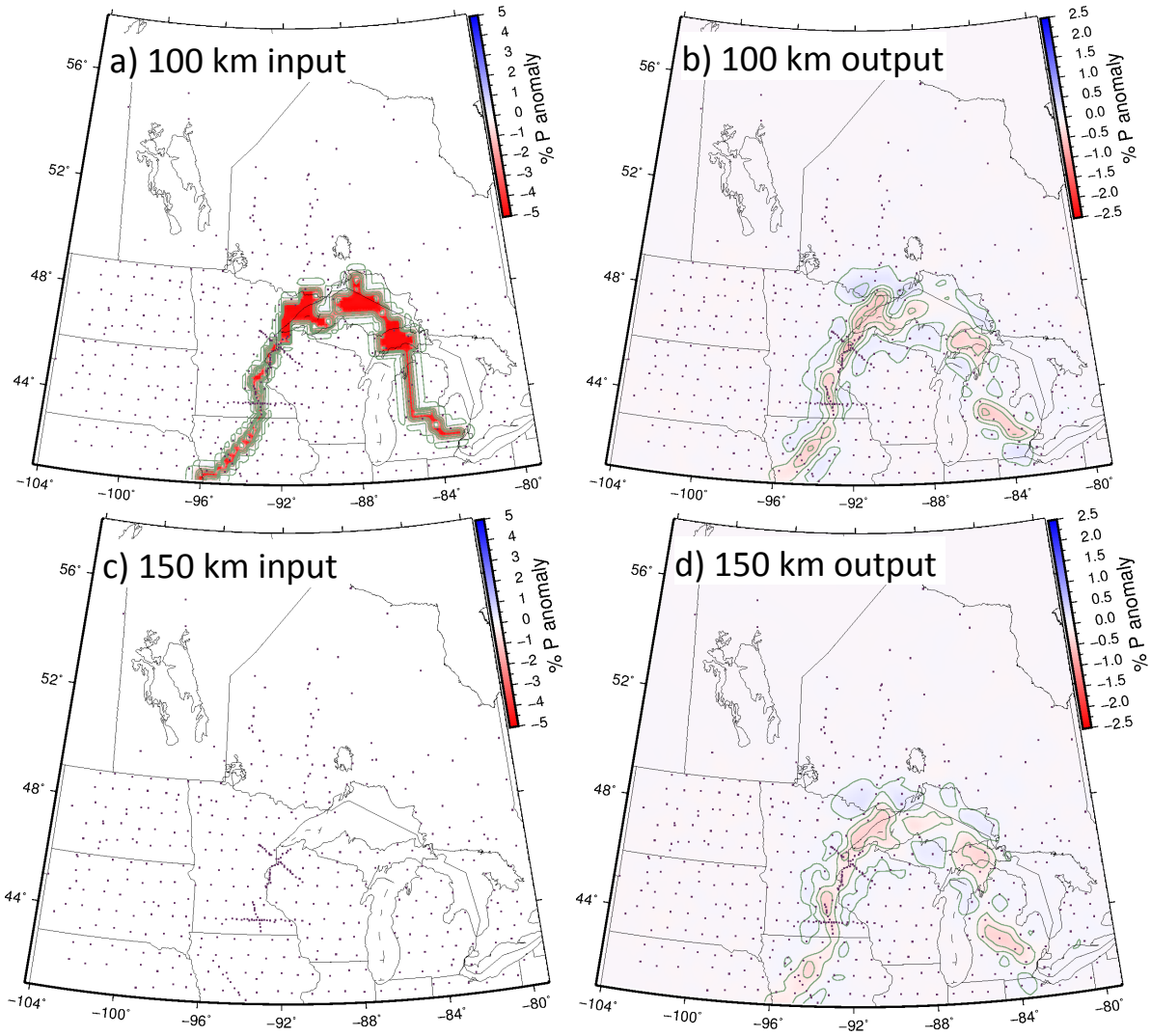

Figure 2.13. Input and output models of a resolution test mimicking the spatial extent of the MCR Bouguer gravity anomaly with a depth of 100-120 km and a velocity anomaly of 5 percent. All anomalies present in the 150 km output are due to vertical smearing along the ray paths.

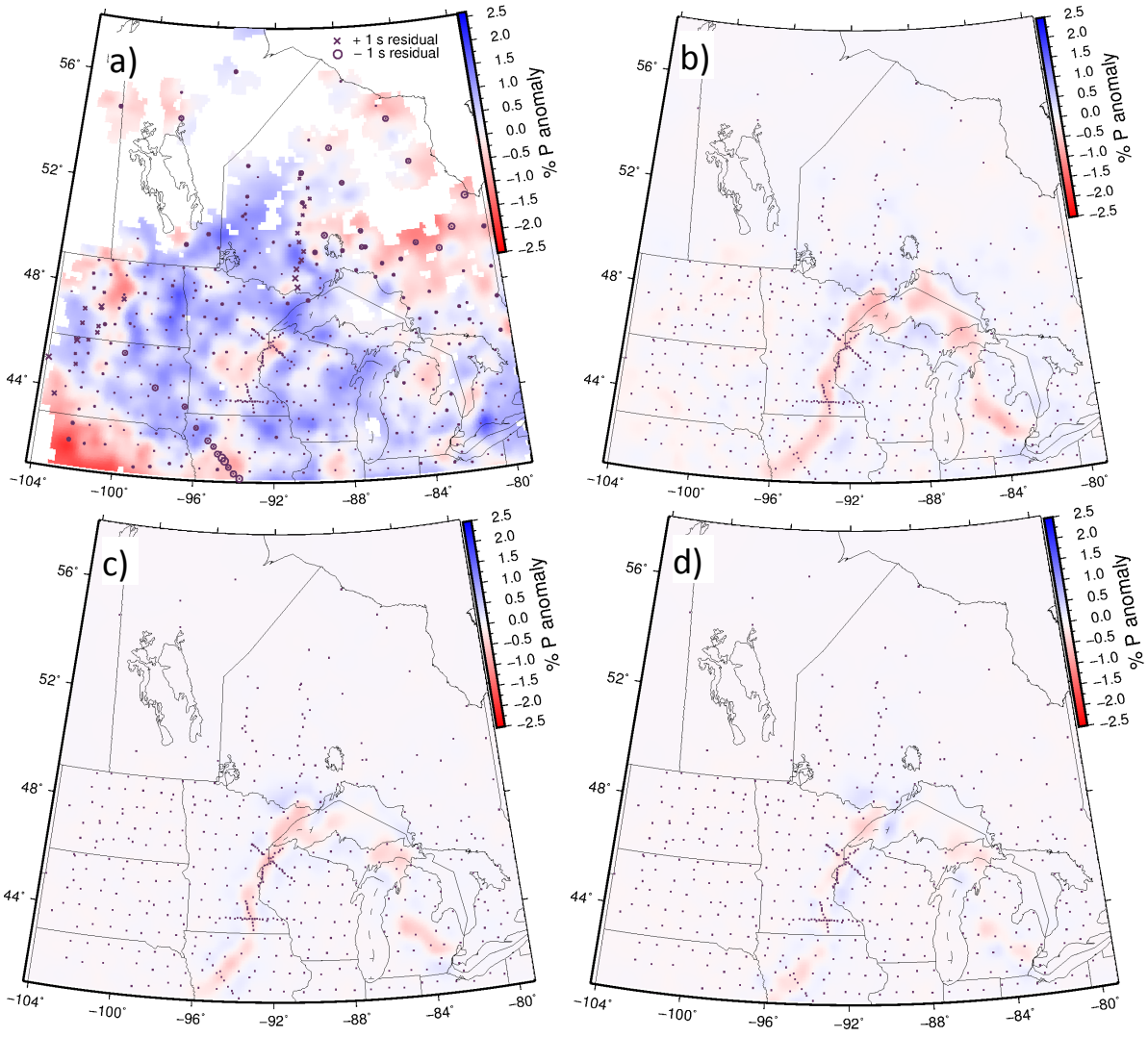

Figure 2.14. Comparison at 100 km depth of our tomographic model against multiple resolution tests with low velocity anomalies mimicking the spatial extent of the MCR Bouguer gravity anomaly with differing depths and thicknesses. a) Tomographic model b) Depth of 100-200 km c) Depth of 100-120 km d) Depth of 30-50 km.

2.5.2. Mid-continent Rift

With the MCR forming at 1.1 Ga, the large thermal signature that comes with magmatic intrusion has long since faded (*Turcotte and Schubert*, 2014). However, the basalts of the MCR are enriched in iron, with later basalts richer than earlier ones (*Ojakangas et al.*, 2001). Moreover, these basalts were not devoid of volatiles (*Hollings et al.*, 2007, 2010, 2012). If these volatiles and iron were extracted from the deeper lithosphere, it would have increased the seismic velocity of the cooled lithosphere rather than decreased it. If the extraction depth was sub-lithospheric, the depletion and an associated stiffening would have thickened the high-velocity lithosphere (*Goes and van der Lee*, 2002; *van der Lee and Wiens*, 2006). Contrary to these expectations, we observe low-velocity anomalies beneath the MCR. To explain the absence of high-velocity, depleted mantle beneath the rift, we propose that the source of the deposited basalts was located deep beneath the lithosphere and is no longer geographically connected or the surrounding lithosphere is equally depleted from prior melting events.

Wave paths through the mantle lithosphere beneath the Lake Superior portion of the MCR do not need to cross through the rift- and lake-centered underplated layer before being recorded at stations surrounding the Lake and underlying rift structure. In agreement with this geometry and with inferences made by *Yang et al.* (2015) of electrical conductivity of the lithosphere in the SPREE study region, our seismic-tomographic model's velocities beneath the western portion of the lake indeed look similar to those of the western Superior high-velocity anomaly, away from the MCR. According to resolution tests (Figures 2.8 and 2.9) there is no significant lateral smearing in the western half and

vertical smearing is similar to other places within the model. However, if there were a lithospheric anomaly, it would be resolved (Figure 2.11).

The previous study (*Frederiksen et al.*, 2013a) had limited ray paths beneath Lake Superior, but the Canadian SPREE stations add crossing rays that address this issue. Data associated with these ray paths confirm that the low-velocity anomaly beneath Lake Nipigon is not connected to the low-velocity anomaly associated with the main arm of the MCR but that it is actually connected to the Eastern Superior Low Velocity Anomaly to the east (Figures 2.6a and c). This is in contrast with the MCR aged volcanics in place around Lake Nipigon. It is likely that the original velocity signature beneath Nipigon was similar to the Western Superior until the process that caused the Eastern Superior Low Velocity Anomaly overprinted this signature, as it did further to the east.

Mapping of the MCR from gravity (*Chase and Gilmer*, 1973) and interpretation of COCORP seismic lines (*Brown et al.*, 1982) show that there is also an arm of the rift in Michigan. However, our model shows no low-velocity lithospheric feature beneath Michigan as it does beneath some parts of the main arm of the MCR. Resolution tests (Figure 2.11) show that if there were a significant low-velocity structure in the mantle, it would be resolvable. However, subcrustal underplating or intra-crustal anomalies would be too shallow to be resolved by our data due to the lack of densely organized stations over the Michigan arm of the rift.

Lastly, we reduced our residuals to the same level as those used to image portions of the East African Rift System (*Park and Nyblade*, 2006; *Bastow et al.*, 2008), where strong heat-related, low-velocity anomalies are observed in the mantle beneath the EARS, corresponding to a larger spread in pre-imaging delay times. Our less variable pre-imaging

delay time distribution confirms that our data support the absence of rift-related heterogeneity in the mantle lithosphere beneath the MCR.

2.5.3. Deeper Anomalies

In and below the transition zone, there are a number of prominent anomalies. The shallowest is the anomaly labeled TZ in Figure 2.6d. This anomaly has a strong high velocity indicative of the mantle in the tectonically quiet portion of the North American continent. There is an anomaly of similar extent and velocity in the tomographic model of *Burdick et al.* (2014). Two linear high-velocity anomalies, labeled FS and KS, occur at 1000 and 1200 km in depth, respectively. These anomalies are interpreted as fragments of the Farallon and Kula Plates due to their linear nature and the fact that they are in the correct location both laterally and vertically to be slab fragments of the previously subducted plates (*Grand*, 1994; *Bunge and Grand*, 2000; *Liu*, 2015). Alternatively these fragments could belong to westward subducted oceanic lithosphere from the Mezcalera and Angayucham slabs, Mesozoic predecessors of the Farallon Plate (*Sigloch and Mihalynuk*, 2013), but it would extend both slabs slightly more westwards than projected by (*Sigloch and Mihalynuk*, 2013). Further comparison with global tomographic models shows a general continuity throughout the different models in terms of size and shape of the anomalies, as predicted by both subduction models.

2.5.4. Syntaxis Anomalies

To the southwest of the northern MCR anomaly lies the semicircular low-velocity anomaly S1 (Figure 2.6c). This feature does not correlate with the gravity anomaly and continues

to a greater depth than the imaged MCR anomalies. The location of this low-velocity anomaly coincides with 1) the surface expression of the rift as it turns to the southeast and is offset by the Belle Plaine fault (*Chandler et al.*, 2007), 2) the western syntaxis of the Penokean Province, which is, the suture zone where the Penokean Province and the Marshfield Terrane collided with the Superior Province (*Whitmeyer and Karlstrom*, 2007), 3) the East Central Minnesota Batholith, a 1.78-1.76 Ga post-Penokean granitic magmatic event (*Holm et al.*, 2005), 4) the location of a high electrical-conductivity anomaly imaged by (*Yang et al.*, 2015).

A low-velocity anomaly of similar size and shape to S1, named S2, is located in the lower peninsula of Michigan near the eastern syntaxis of the Penokean Province, where it abuts the Yavapai and Mazatzal provinces (*Whitmeyer and Karlstrom*, 2007). The anomaly is also near a 1.472 Ga anorogenic volcanic intrusion (*Windley*, 1993; *Goodge and Vervoort*, 2006), and also has a counterpart in *Yang et al.* (2015)'s electrical-conductivity model. With S1 and S2 having nearly identical velocities and sizes it is possible that they may have similar causes, making a relationship with the Penokean Orogeny likely.

These anomalies are beneath the syntaxes of the Penokean Province. This correspondence may indicate that the Penokean Orogeny created weak zones in the lithosphere, which may have attracted some of the MCR volcanics to become entrained. A second possibility for these low-velocity anomalies is that they represent the fossil remnants of slab crust or subduction-induced metasomatism, trapped by the Penokean or Mazatzal collisions in the continental lithosphere. Using a GLIMPCE seismic profile (*Green et al.*, 1989) in Lake Michigan between S1 and S2, *Cannon et al.* (1991) suggests that young ocean basin lithosphere subducted during the final stages of the Penokean orogeny in a northerly

direction. This created the possibility for portions of the young slab's low-velocity crust, or its transformation products, to be trapped by the collision. The suture between this orogeny and the Superior Craton is known for its sulfide deposits and ophiolites (*Sims et al.*, 1989; *Schulz and Cannon*, 2007). *Yang et al.* (2015) imaged high-conductivities along this suture, including in the lower crust at the western syntaxis, where we image low velocities, which they attribute to graphitic carbon or sulfides, both associated with subducted seafloor sediments.

A third possibility pertains to the previously stated volcanic intrusions near the anomalies. These could have caused the low-velocity anomalies at different times, both well pre-dating the MCR, depending on the composition of the emplaced magma and alteration of the lower crust by the migrating magma. It seems that the conductivity images of *Yang et al.* (2015) would favor the 2nd explanation, which is the entrapment of subducted crust within the orogeny.

2.5.5. Western Superior High-Velocity Anomaly

We interpret the large high-velocity anomaly (WS) as the cratonic lithospheric root of the Superior Province, in agreement with prior studies (*van der Lee and Frederiksen*, 2005; *Bedle and van der Lee*, 2009; *Frederiksen et al.*, 2013a). With improved resolution provided by the SPREE stations, we find that lithospheric velocities in this region are on average at least 1.5% higher than the *iasp91* velocities for the model. However, this is most likely an underestimate due to the weaknesses of using relative delay times, as discussed in Section 5.4. Our model shows that this high-velocity region extends through

the western portion of Lake Superior and northern Wisconsin. In Figure 2.7, cross-section WP-WP' shows that above 200 km in depth the lithosphere between feature S1 and the low-velocity at the northwestern edge of the model is similar in velocity to that of the lithosphere beneath the western Superior Province (cross-section SC-SC', Figure 2.7). Below that (200-400 km in cross-section WP-WP', Figure 2.7) there is a weak low-velocity zone that extends from feature S1 to the northwest. This low-velocity zone is the same as the low-velocity "channel" noted in the *Frederiksen et al.* (2013a) tomography and it separates features WS and MRV, which roughly correlate to the locations of two sub-provinces of the Superior Province, the Wawa and Minnesota River Valley (MRV) (*Chandler et al.*, 2007).

Chandler et al. (2007) indicate that the southern portion of the Superior Province, the MRV sub-province, was accreted to the southern margin of the Superior Province at 2.6 Ga. It also has a vastly different geology, both in age and composition, than the Wawa sub-province to the north. The crustal boundary between the Wawa and MRV sub-provinces is the Great Lakes Tectonic Zone (GLTZ) (Figure 2.1b), which runs west-southwest to east-northeast between the two sub-provinces (*Sims et al.*, 1980). This does not seem to be the case in the lithosphere as the previously mentioned low-velocity zone in central/western Minnesota departs from the Becker Embayment to the northwest instead of following the GLTZ to the southwest. This low-velocity zone also seems to be a line of demarcation where the shear wave splitting of *Frederiksen et al.* (2013b) and *Ola et al.* (2016) decreases in split time moving to the southwest and crossing the previously mentioned low-velocity zone. Either the GLTZ is too small to image with the resolution of the model or it does not have a lithospheric signature. The rifting and

material associated with the MCR could have possibly further modified this portion of the lithosphere due to its already weakened nature from the northwest directed collision of the Marshfield Terrane with the Penokean Orogen and Superior Province (*Holm et al.*, 2007; *Foster et al.*, 2017).

2.6. Conclusions

Inversion of teleseismic P delays from permanent, TA, SPREE, and other short term seismic station deployments shows a number of low-velocity zones in the North American mid-continent that agree with the tectonic history of the area. Some of the low-velocity patches appear associated with the Mid-continent Rift, but cannot be uniquely ascribed to mantle structure. It is more likely that the observed anomalies are associated with P-wave delay times caused by an along-rift sub-crustal layer of igneous origin, as found by *Zhang et al.* (2016). In other words, and despite our data having sufficient resolving power to image anomalies in the mantle lithosphere, our results show no convincing evidence of one billion-year-old rift-related structures remaining as anomalies in the mantle lithosphere. The resolving power of our analysis was enabled by the combined data coverage of the midwestern portion of the Transportable Array and densely spaced SPREE stations along and across the rift. Other interesting features include anomalies that occur at two different syntaxes of Proterozoic crustal terranes, the Western Superior Craton, and the presence of the subducted Farallon and Kula plates. These syntaxis anomalies had not been previously imaged seismically, but they do align very well with the provincial boundaries shown in Figure 2.1b, and coincide with electrical conductivity anomalies images by *Yang et al.* (2015). The locations of the Western Superior Craton and Farallon

and Kula plates match very well with previous studies, albeit with a clearer image due to our increased resolution, especially in the case of the Western Superior Craton.

CHAPTER 3

Possible causes of the Anomalously Large Western Interior Basin

3.1. Introduction

During the Late Cretaceous, the Sevier Orogeny was occurring along a large portion of the western edge of the North American continent. This was due to the oceanic Farallon plate being subducted under the continental North American Plate. The subduction created compressional forces and heated the lithosphere of the region through subduction volcanism. Due to the extra heat, the lithospheric strength of rock in the region decreased (*Brace and Kohlstedt*, 1980) allowing for easier folding and thickening of the crust during the orogeny. This extra mass of rock from the orogeny caused the lithosphere surrounding it to flex and subside, creating a basin adjacent and parallel to the orogenic belt. Initially the basin formed as expected, with the deepest part of the basin remaining adjacent to the Sevier front, but as time progressed, the basin widened. In opposition to the textbook style of foreland basin, the basin width more than doubled and the deepest part of the basin moved away from the orogenic belt. This large foreland basin, named the Western Interior Basin (WIB), along with rising sea level, allowed for the ocean to flood into the interior of the continent to form the Cretaceous Western Interior Seaway (WIS). Large volumes of sediment were deposited from the erosion of the Sevier Orogeny and deposited in the WIB due to the increased accommodation space it afforded.

When orogenies such as the Sevier form, the crust is thickened, causing the surrounding crust around the orogeny to depress in order to retain isostatic equilibrium. This creates a basin landwards of the orogen that deepens towards the source of the lithospheric flexure, called a foreland basin (*Allen and Allen*, 1990). Under normal conditions, loading of the lithosphere causes flexural subsidence in the lithosphere directly adjacent to the loaded region and forms a foreland basin. In the case of this study, the Sevier Orogen is the source

of lithospheric flexure, and its foreland basin extends from the location of the Sevier Front in Utah (Figure 3.1), eastward to the plains states of Kansas and Nebraska. The area in and around the Wyoming Craton contains this foreland basin, but the extent and depth of the basin is larger than could be formed purely from lithospheric loading (*Bird*, 1984). There are two hypotheses on the cause of this abnormality that we will discuss here. Both attribute the large basin size to the interaction of the subducted Farallon plate with the overriding lithosphere, but with small discrepancies.

Jones et al. (2011), asserts that a small portion of the shallowly subducting Farallon plate was viscously coupled to the keel of the Wyoming craton, both pulling down on the crust and pulling up on the shallowly subducting slab. This coupling in the upper mantle causes localized subsidence at the southern edge of the craton by pulling down on the crust while at the same time the Farallon plate is pulled up (*Jones et al.*, 2011). There was also a suggestion for a connection to the relative motion of the Farallon plate with respect to the North American Plate, using data from *Engebretson et al.* (1985). The Farallon plate was moving in a northeasterly direction relative to the North American Plate as it was being subducted, and thus the basins extended in generally the same direction.

Another hypothesis by *Liu et al.* (2010) poses a similar hypothesis to *Jones et al.* (2011) for the creation of the anomalous Cretaceous foreland basin present in Wyoming and Colorado. The overriding plate still interacted with the subducting Farallon plate, but rather than flat slab subduction causing slab-craton coupling, it was instead the Shatsky Rise conjugate within the Farallon slab that interacted with the keel of the craton. The Shatsky rise is an oceanic plateau hypothesized to have been created by a mantle plume that was located under a triple junction Pacific spreading center

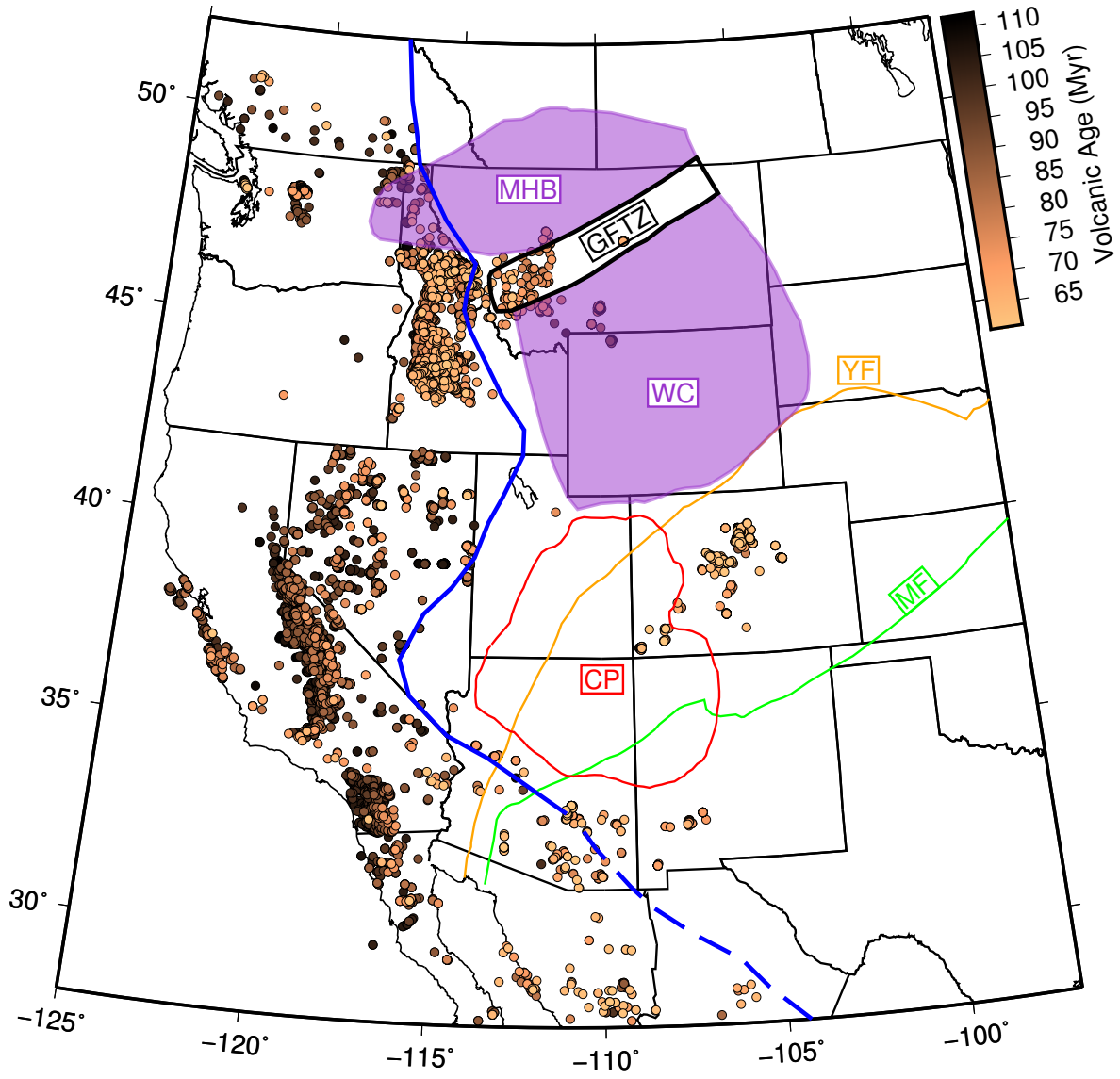

Figure 3.1. Regional map of major geologic structures and volcanics from the timeframe of the study. Purple areas denote cratonic fragments (WC-Wyoming Craton, MHB-Medicine Hat Block), orange line is the Yavapai Front (YF), green line is the Mazatzal Front (MF), and black lines are tectonic zones (GFTZ-Great Falls Tectonic Zone). All were from *Whitmeyer and Karlstrom* (2007). The thick blue line is the leading edge of the Sevier Orogenic Belt, modeled after *DeCelles* (2004). Where the line becomes dashed interpreted locations vary. Red lines bound the Colorado Plateau (*Spencer and Patchett*, 1997). Colored points are dated instances of erupted or emplaced volcanic material (*Walker et al.*, 2006).

(*Nakanishi et al.*, 1999). As it formed directly over a spreading center it is reasonable to assume that only half of the original structure is visible today. The other half would have moved away from the spreading center and was subducted with the rest of the Farallon Plate. In Liu's hypothesis, this subduction allowed for the slab-crust interaction and caused the lithosphere to be pulled down and the basin to be created. It is not clear which of the hypotheses are correct, but the work that follows will attempt to shed light on which might be more likely.

3.2. Data and Methods

To investigate the cause of the WIB's unusual foreland morphology, we compiled many different data types that are not normally used together in an effort to investigate relationships occurring between them and obtain insight on the cause of the previously mentioned anomalous WIB. To do this we first separated data into two major types, geologic and non-geologic data. For the geologic data types, we were able to acquire age dated volcanic locations from NAVDAT (*Walker et al.*, 2006), isopachs of sediment thickness for major stages of the Late Cretaceous from *Roberts and Kirschbaum* (1995), and the locations of major crustal structures in the region (*Whitmeyer and Karlstrom*, 2007; *DeCelles*, 2004; *Spencer and Patchett*, 1997). These data were used in investigating spatial relationships occurring solely in the crust. The non-geologic data types were tomographic models and plate reconstruction models. The tomographic models were used to locate possible subducted Farallon slab fragments beneath the North American Plate and the plate reconstruction models were used to estimate where current features would have been located in the past and where past features are located in the present.

A combination of the geologic and geophysical data was used to investigate possible correlations of activity in the mantle to crustal features and vice versa.

The first and most basic method used in our investigation was to jointly map the major structural features of the North American crust with the locations of volcanism that were occurring during the formation of the WIB (Figure 3.1). This was done to reveal possible patterns that could direct our investigation further. Only large scale structures were used given that only continental scale structures could influence the creation of a structure as large as the WIB. These structures included features of various ages but the oldest are the Wyoming Craton and the Medicine Hat Block, which are Archean cratonic fragments (3.6-3.0 and 3.3 Ga respectively) and have a significantly larger crustal root than the other features used (*Houston et al.*, 1993). Those cratonic fragments are separated by the Great Falls Tectonic Zone (GFTZ), a 2.0-1.8 Ga juvenile arc formed by the collision of the Archean blocks (*Mueller et al.*, 1996, 2002). To the south of the Wyoming Craton are the Yavapai and Mazatzal Fronts which are the northern boundaries for zones of juvenile crust (1.80-1.70 and 1.70-1.60 Ga respectively) formed during separate orogenic events as juvenile crust was accreted to the southern edge of Laurentia (*Roberts and Kirschbaum*, 1995). The last two crustal features plotted are relatively young compared to the others, but are still a major part of the WIB formation. First is the Sevier Front. This is the easternmost extent of the Sevier Orogeny, the precursor to the present day Rocky Mountains (*DeCelles*, 1994) with the earliest thrust of the orogeny occurring in 140-110 Ma (*Yonkee et al.*, 1992). Last is the Colorado Plateau, a hotly debated feature that may have, at least in part, uplifted contemporaneously with the formation of portions of the WIB (*Nations*, 1989). While these structures have vastly different ages, compositions, and

sizes, this was done purposefully in order to encapsulate as many influential structures as possible.

The next step was to plot the same crustal structures and locations of volcanism with the sediment isopachs from the Late Cretaceous (Figures 3.2 and 3.3). This was done to determine if compositional differences in the crust caused differential deformation when put under sediment load and to observe temporal changes in the pattern of volcanism with respect to sedimentation. A detail of interest is determining if the portion of the WIB deposited on portions of the crust made up of Archean fragments have different characteristics than the younger portions of crust. How the pattern of volcanism changes also has an element of time involved, as an abrupt change in pattern from linear to dispersed volcanism at the same time as increasing sedimentation due to an increase in the accommodation space, would support the hypothesis that flat slab subduction played a part in the formation of the WIB.

The sediment thickness from each isopach map was also combined to show total sediment accumulation in time steps over the period of interest (Figure 3.4). This allows us to determine if, when, and where the depocenter migrated over time and if that migration correlates with any of our other data. This was completed by digitizing the isopach contours for each time step, creating a surface from them, then superimposing each time step's sedimentation onto the next. Since our isopachs were limited to discrete time steps in the Late Cretaceous the number of sedimentation steps we were able to show was limited. Even though this was the case, it did not adversely affect the robustness of the isopach data.

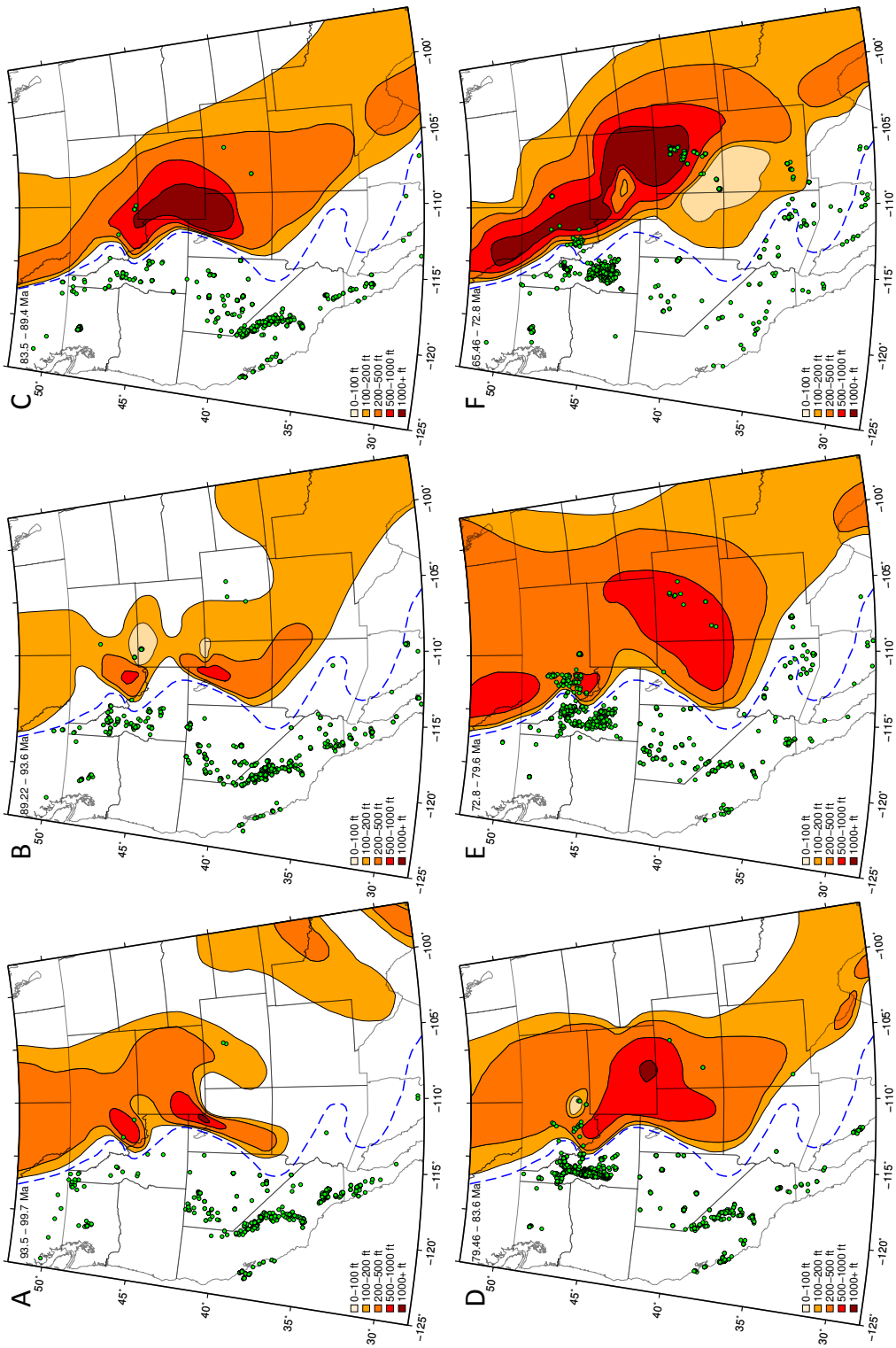

Figure 3.2. Isopachs from *Roberts and Kirschbaum* (1995) overlain with volcanics (*Walker et al.*, 2006) also seen in Figure 3.1.

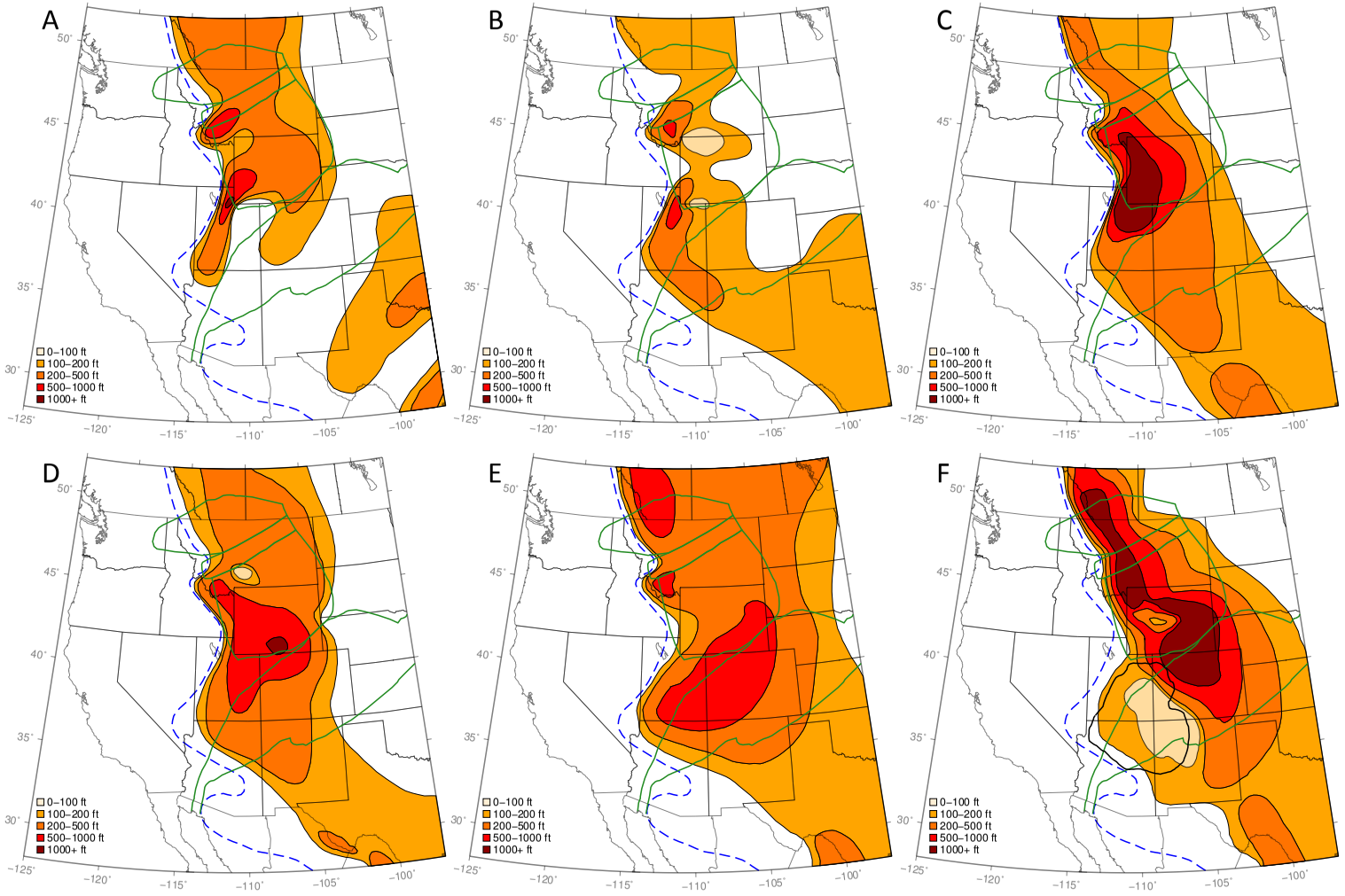

Figure 3.3. Sediment isopachs from *Roberts and Kirschbaum* (1995) overlain with crustal structures also seen in Figure 3.1.

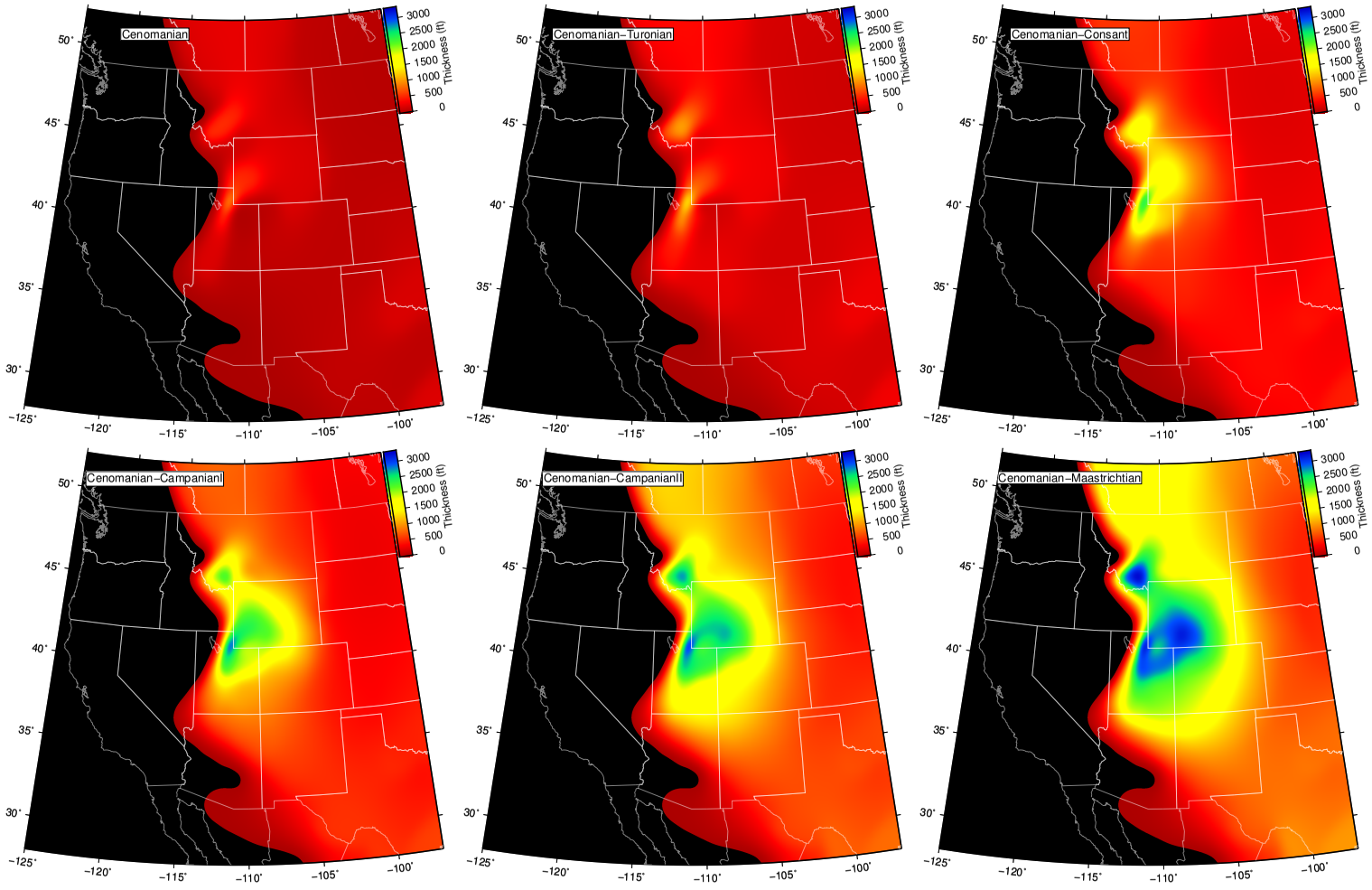

Figure 3.4. Cumulative sedimentation created using isopachs from *Roberts and Kirschbaum* (1995), used to track the depo-center over time.

With respect to the mantle structures, we used the tomographic model of *Sigloch and Mihalynuk* (2013) to find the current locations of subducted fragments of the Farallon Plate as this feature is most prominently mentioned as a cause of the anomalous WIB. The fragments we were most interested in are mentioned in the literature as the Shatsky Rise Conjugate (SRC) and the Hess Rise Conjugate (HRC). Both are the hypothesized subducted conjugates of oceanic plateaus that were originally formed at or near the Pacific-Izanagi-Farallon triple junction spreading center (*Livaccari et al.*, 1981; *Nakanishi et al.*, 1999) . Once these fragments were located in the tomographic model, we used the plate reconstruction software, GPlates (*Boyden et al.*, 2011) and ODSN (*DeConto et al.*, 1999), to model how the North American plate moved over the subducted Farallon Slab fragments from the Cenomanian age to present day, using the plate reconstruction models of *Dietmar Müller et al.* (1993), *Schettino and Scotese* (2005), *Seton et al.* (2012), and *Doubrovine et al.* (2012). This modeling included where the slab fragments would have been located during the formation of the WIB. It is important to note that the resulting slab motion tracks are actually the movement of the North American plate with respect to the Farallon slab. As a part of this process we assumed only minor lateral movement of the slabs as they equilibrated and descended deeper into the mantle, essentially keeping them fixed in x-y space. We realize that this assumption may not be completely accurate, but due to the preliminary manner of this work, it is acceptable. With this assumption, the slabs location only moves in a downward vertical direction with respect to the rest of the mantle as the slab is subducted and equilibrates, while the North American plate moves laterally above it due to plate tectonics.

While having the locations of the subducted slabs through time is useful, it only shows single points at each time step with no information on the slab extent. Therefore, using the two hypotheses for WIB formation mentioned in the Introduction, we created two end members for the size of the body interacting with the overriding continental crust: an oceanic plateau and a flat slab. *Saleeby* (2003) states that the width of the Laramide slab segment is 500 km along the plate edge so we use this as the width of the flat slab and a slab length of 700km, which is the length suggested by *English and Johnston* (2004). For the size of the oceanic plateau end member we look to the size of the Tamu massif portion of the Shatsky rise, whose conjugate is suggested by *Liu et al.* (2010) to be the interaction point causing the drawdown of the continental crust. The Tamu massif is an extremely large extinct underwater volcano that rivals the size of Olympus Mons on Mars and has a size of 450 x 650 km (*Sager et al.*, 2013). Since this size is similar to the flat slab end member and only half of the massif has significant topography, we will use half the size of the total massif (225x325 km) as the oceanic plateau end member. These end members were then centered on the current slab fragment locations identified in the *Sigloch and Mihalynuk* (2013) tomographic model, and using the plate reconstruction models of *Seton et al.* (2012) and *Dietmar Müller et al.* (1993), the movement of the North American Plate relative to the slab location through time was modeled. The plate reconstruction models of *Schettino and Scotese* (2005) and *Doubrovine et al.* (2012) were not used due to earlier modeling showing that at the time the slab was being subducted, the slab location according to these models would not be coincident with the edge of the North American plate were the Farallon Plate was actually subducted.

With the previous modeling completed, we were able to make a number of different comparisons. First was taking the tracks of the SRC and HRC from the *Seton et al.* (2012) and *Dietmar Müller et al.* (1993) plate reconstruction models and placing the flat slab and oceanic plateau end members at each time step location to show the extent of the slab fragment end members through time (Figures 3.6 and 3.7). We also made comparisons of sediment isopachs with slab end member locations and volcanism locations with the slab end member locations at each of the isopach time steps. These maps can be seen in Figures 3.8 and 3.9. Plotting the locations and extents of these features at each time step helps determine if the Farallon slab fragments were in the correct location to influence WIB formation, if either end member seems a more likely cause for the WIB's anomalous features, and if the pattern of volcanism correlates with either of the slab end members.

By modeling the depocenter locations in the Late Cretaceous forward in time to the present and compared with the current location of Farallon Slab fragments from tomographic models, we were able to investigate the hypotheses by viewing data from the past forward into the present. For this method we used the depocenter locations for the Campanian I and Campanian II time periods due to these ages having a large portion of the sedimentation during the Late Cretaceous (Figure 3.10). The Maastrichtian age also had a large amount of sedimentation, but the depocenter location did not change significantly from the Campanian II so it was not used. They were forward modeled using the plate reconstruction software, GPlates (*Boyden et al.*, 2011) and ODSN (*DeConto et al.*, 1999), with the plate models of *Dietmar Müller et al.* (1993), *Schettino and Scotese* (2005), *Seton et al.* (2012), and *Doubrovine et al.* (2012). These forward modeled tracks and present

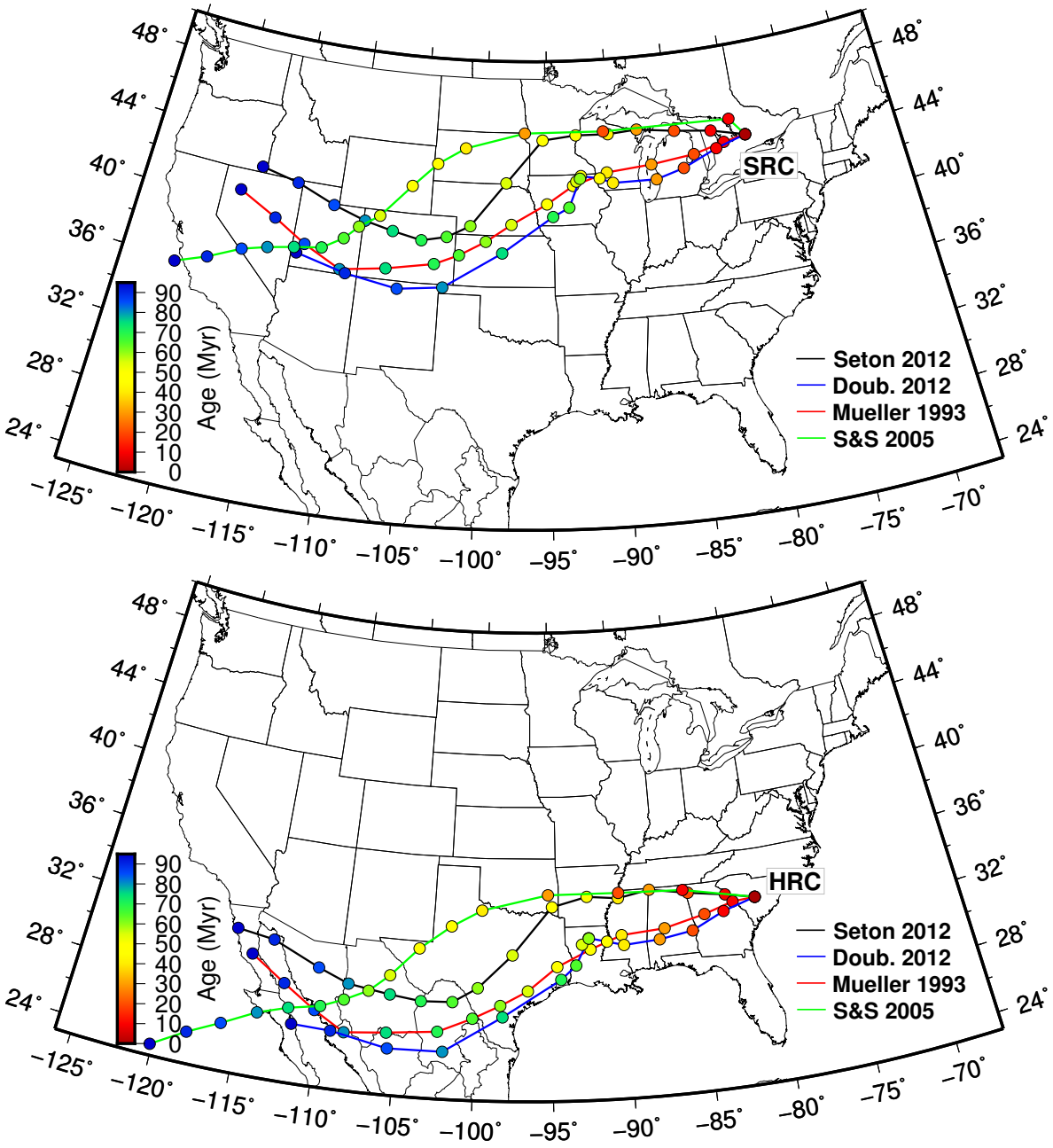

Figure 3.5. Plate motion tracks used to find the location of the Shatsky Rise Congujate(SRC) and the Hess Rise Conjugate(HRC) in the late Cretaceous

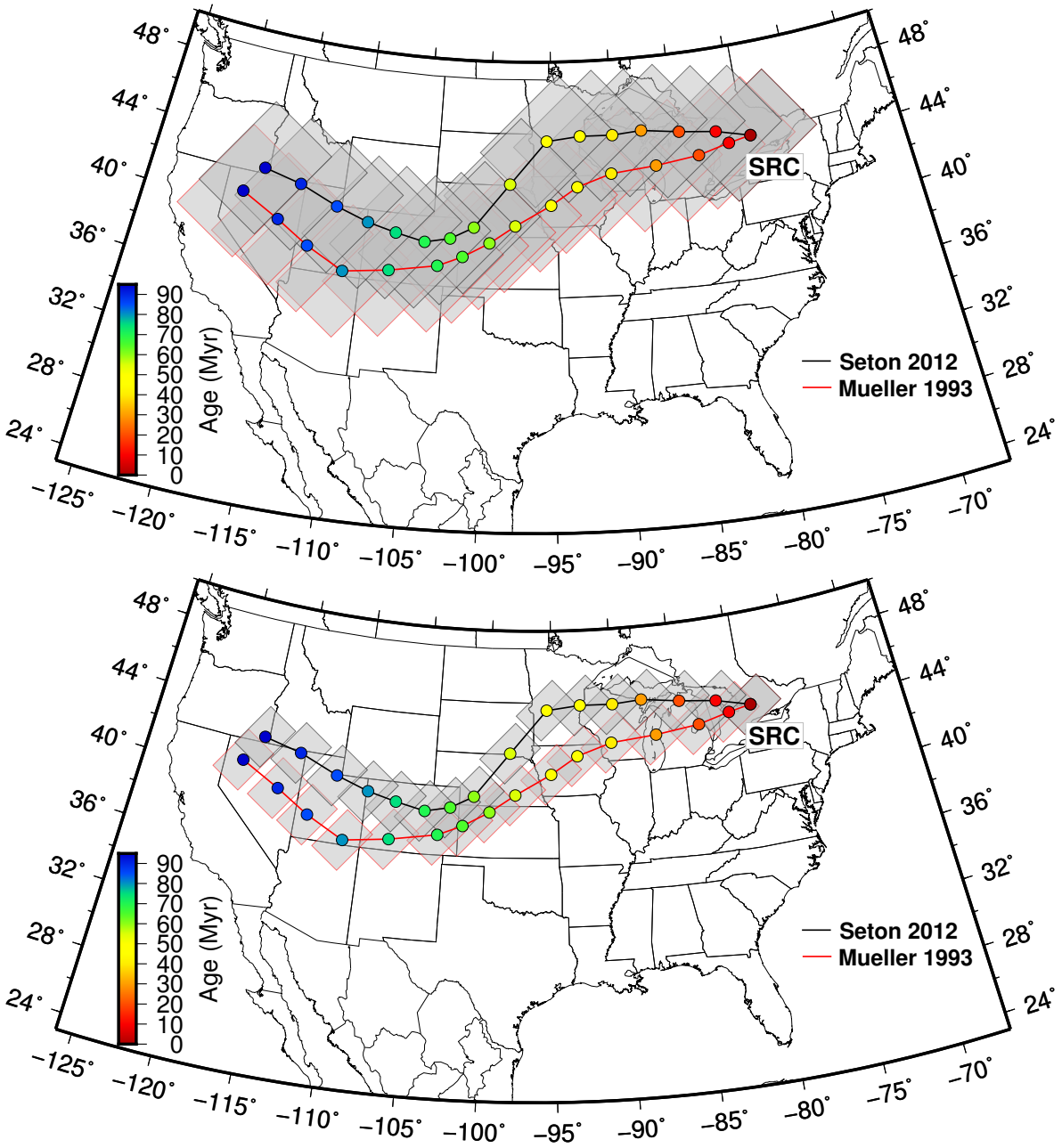

Figure 3.6. Two plate motion tracks of the Shatsky Rise Conjugate(SRC) with the flat slab and oceanic plateau end members sized boxes on each point to illustrate the possible areal extent of the subducted structure and the portions of the crust it may have influenced as the North American plate moved over it.

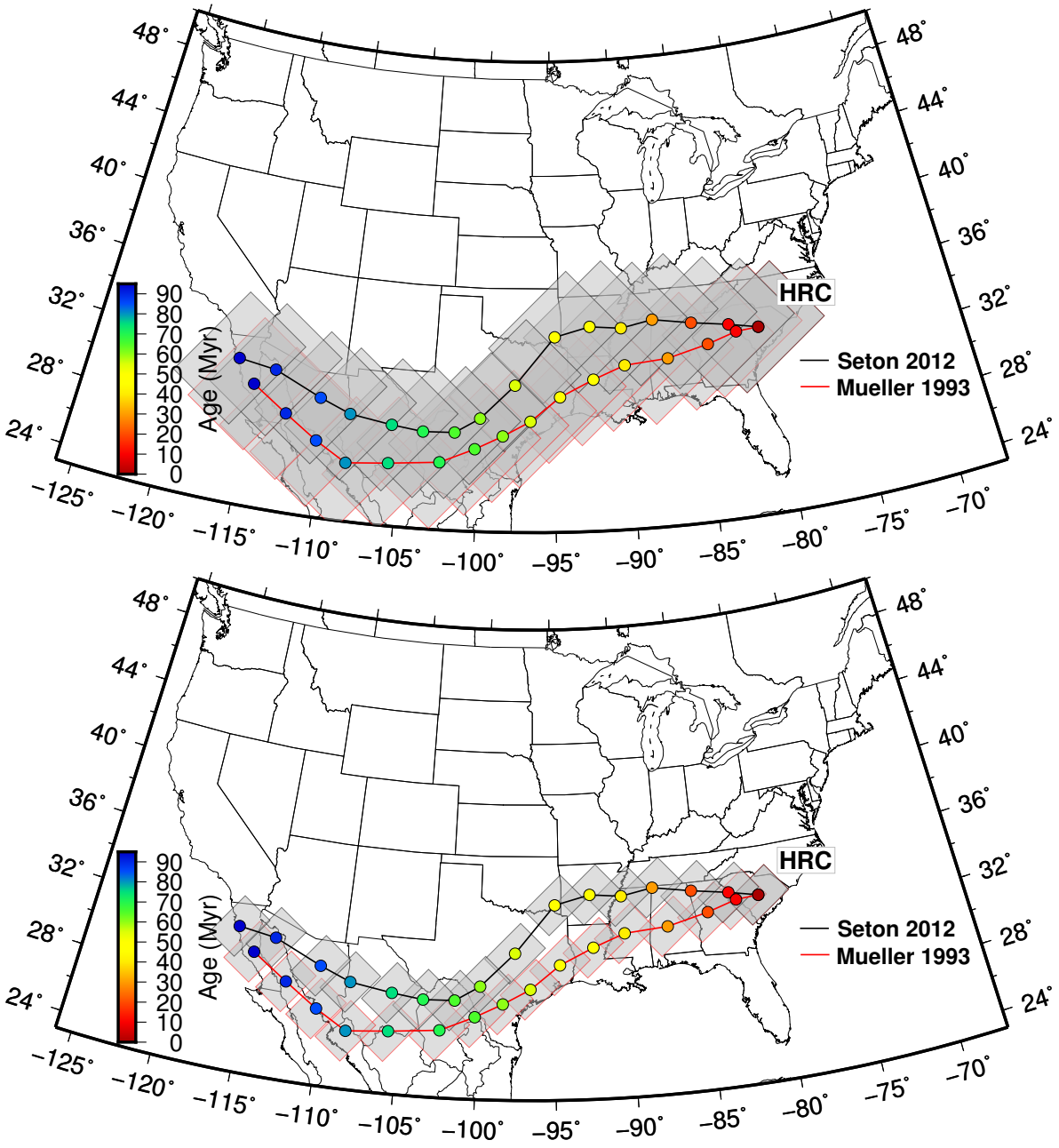

Figure 3.7. Two plate motion tracks of the Hess Rise Conjugate(HRC) with the flat slab and oceanic plateau end member sized boxes on each point to illustrate the possible areal extent of the subducted structure and the portions of the crust it may have influenced as the North American plate moved over it.

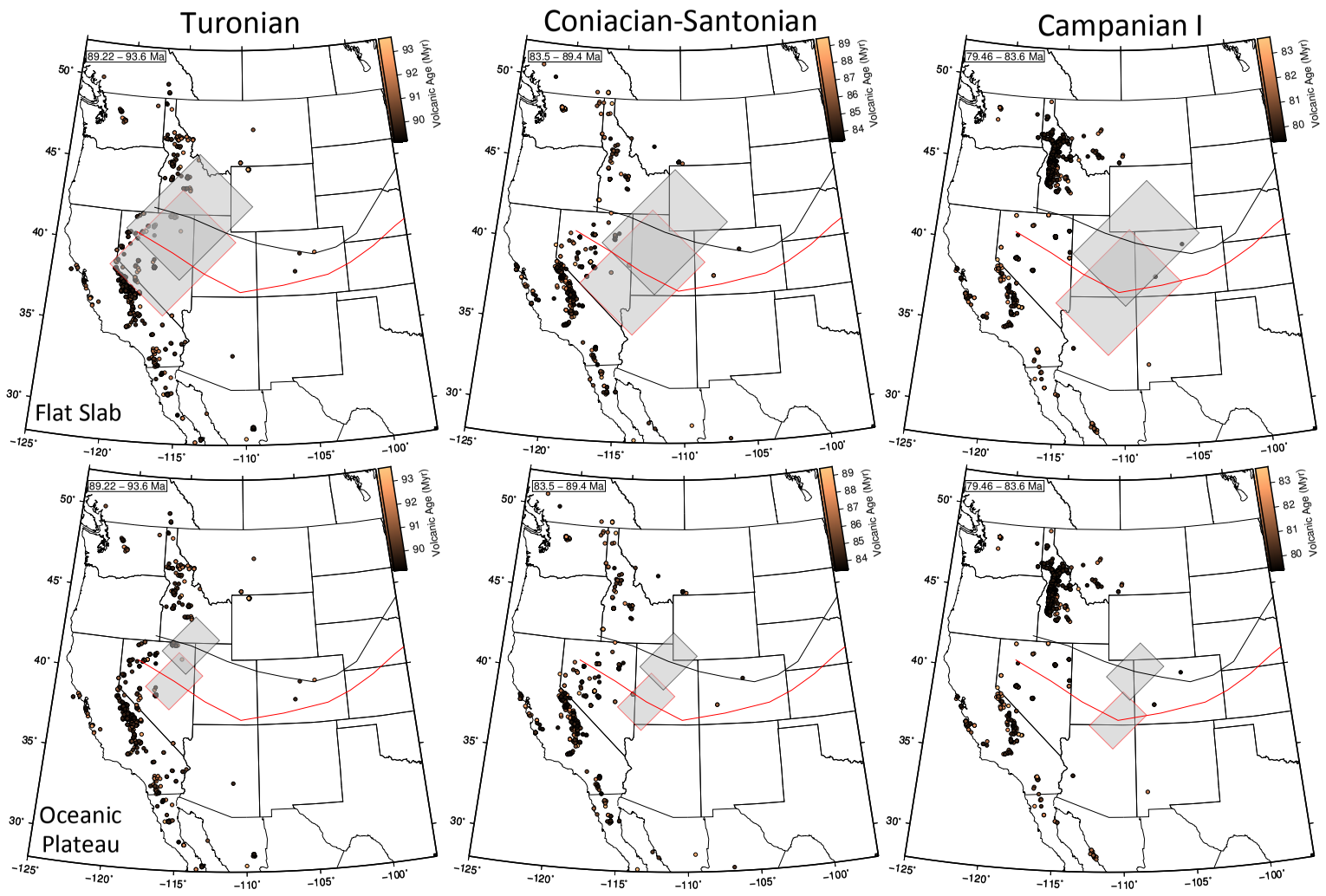

Figure 3.8. Combined volcanics and subducted structure end member locations through time. Red lines and boxes are the path of the subducted structure, tracked with respect to the plate reconstructions of *Dietmar Müller et al.* (1993). Black lines and boxes are the path of the subducted structure, tracked with respect to the plate reconstructions of *Seton et al.* (2012).

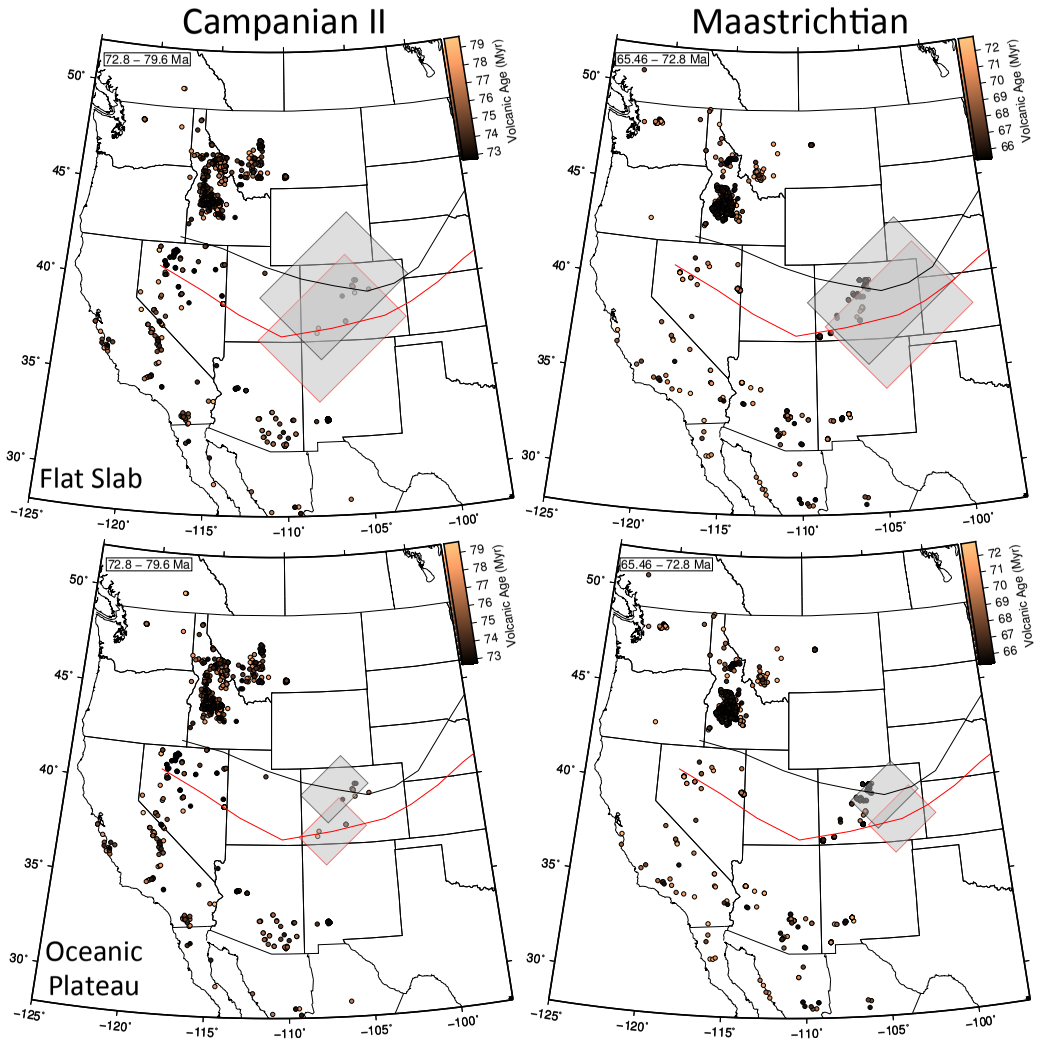

Figure 3.8. Combined volcanics and subducted structure end member locations through time. Red lines and boxes are the path of the subducted structure, tracked with respect to the plate reconstructions of *Dietmar Müller et al.* (1993). Black lines and boxes are the path of the subducted structure, tracked with respect to the plate reconstructions of *Seton et al.* (2012).

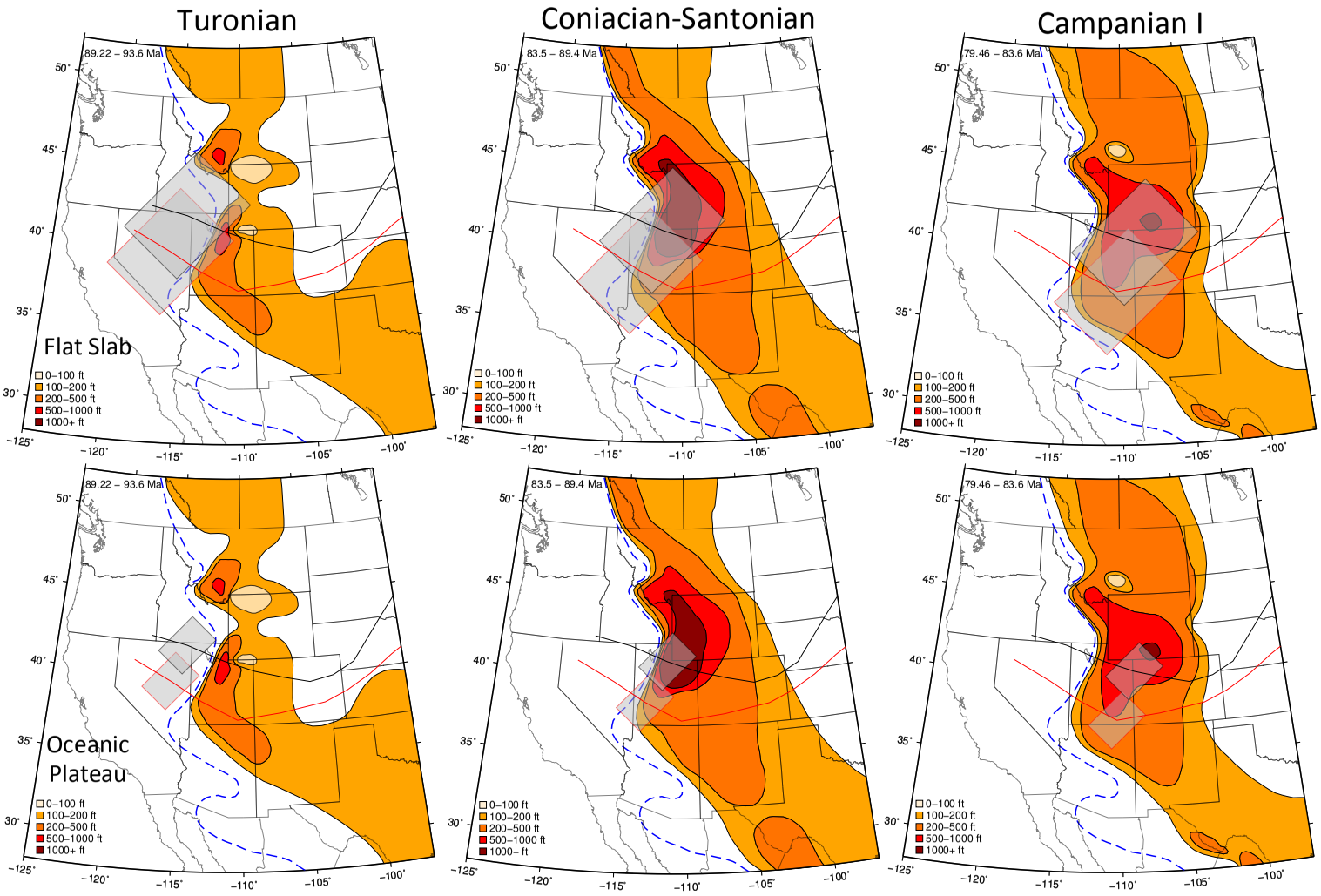

Figure 3.9. Combined sediment isopachs and subducted structure end member locations through time. Red lines and boxes are the path of the subducted structure, tracked with respect to the plate reconstructions of *Dietmar Müller et al.* (1993). Black lines and boxes are the path of the subducted structure, tracked with respect to the plate reconstructions of *Seton et al.* (2012).

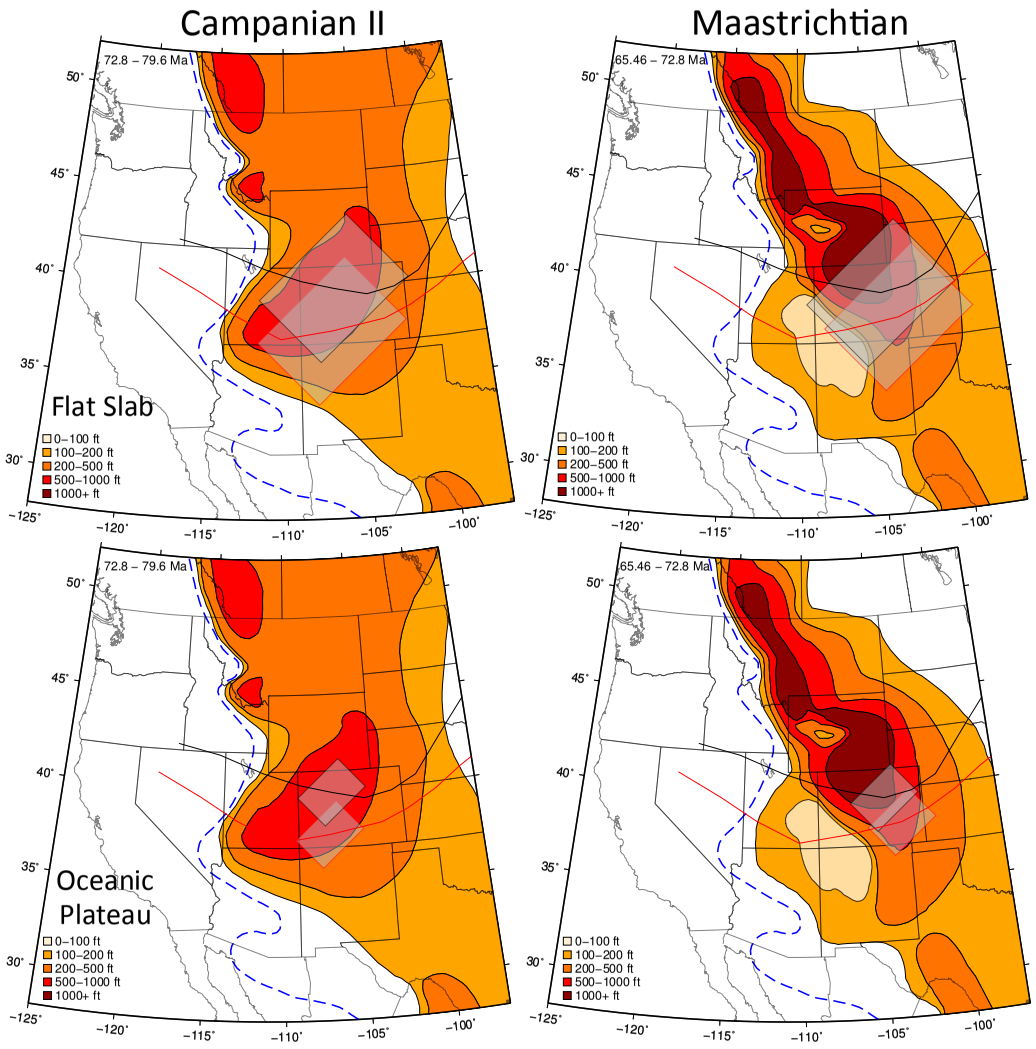

Figure 3.9. Combined sediment isopachs and subducted structure end members through time. Red lines and boxes are the path of the subducted structure, tracked with respect to the plate reconstructions of *Dietmar Müller et al.* (1993). Black lines and boxes are the path of the subducted structure, tracked with respect to the plate reconstructions of *Seton et al.* (2012).

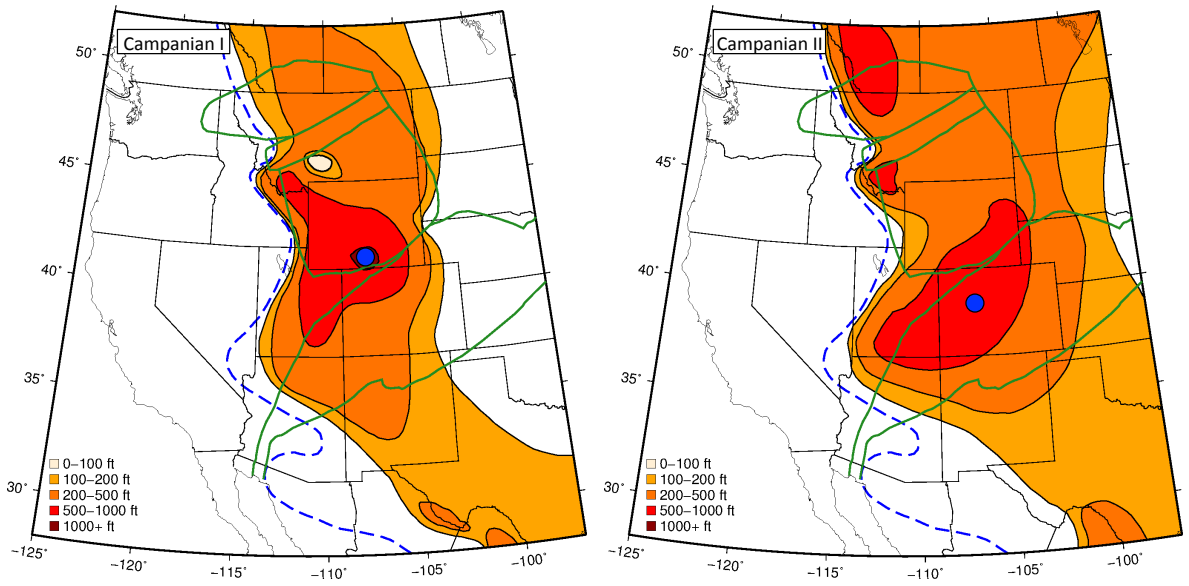

Figure 3.10. Campanian I and Campanian II isopachs from *Roberts and Kirschbaum* (1995) overlain with crustal structures and the location of maximum deposition during the period marked with a blue dot.

locations are shown in Figure 3.11. To compare those locations with the locations of Farallon Slab fragments, we used multiple tomographic models previously aggregated by the IRIS EMC (*IRIS-DMC*, 2011), namely GYPSUM (*Simmons et al.*, 2010), TX2011 (*Grand*, 2002), and S362ANI+M (*Moulik and Ekström*, 2014), to locate high velocity anomalies along the east coast of North America that are interpreted as Farallon slab fragments. These tomographic models were chosen due to their global coverage and differing input data. This ensures that no one type of input data could bias the comparison with our modeled locations. The conservative estimated location of the forward modeled Campanian depocenters along with the previously mentioned tomographic models is shown in Figure 3.12.

3.3. Results

Figure 3.1 shows the relationship between the major crustal structures of the Western US with the pattern of volcanic activity during the Late Cretaceous. A major feature in the volcanic data are two bands of arc volcanism in California and Idaho which were caused by the subduction of the Farallon slab. These two differing volcanic bands are offset along a line that aligns with the GFTZ. Although both arcs are formed by the same mechanism, they have different patterns. The Californian band moves eastward as it ages while the Idahoan band stays located in the same place and overprints itself. This may be due to a flattened portion of the subducting slab or some other mechanism entirely. Other crustal structures do not seem to have a major effect on the locations of volcanism with the exception of the GFTZ. In the western quarter of the that feature there is a small cluster of volcanism of a similar age to the arc volcanism discussed earlier. It is possible that this clustering is caused by the deflection of melt from the descending slab around the competent crust of the MHB and WC Archean fragments.

When the volcanic locations and crustal features are plotted alongside the sediment isopachs in Figures 3.2 and 3.3 a number of patterns appear because volcanism is split out into time intervals rather than plotted all at once. The most obvious is that the dominant location for volcanism switches from the arc in California to Idaho at the beginning of the Campanian Age. At the same time, the pattern of volcanism in California changes from a single line to a more dispersed pattern west of the original arc into Colorado. Figure 3.3 shows that there is no strong relationship between the majority of crustal structures and the sediment isopachs as the basins cut across the crustal boundaries with no deflection or thickness changes. One exception to this is shown in Figure 3.3A and B, where the

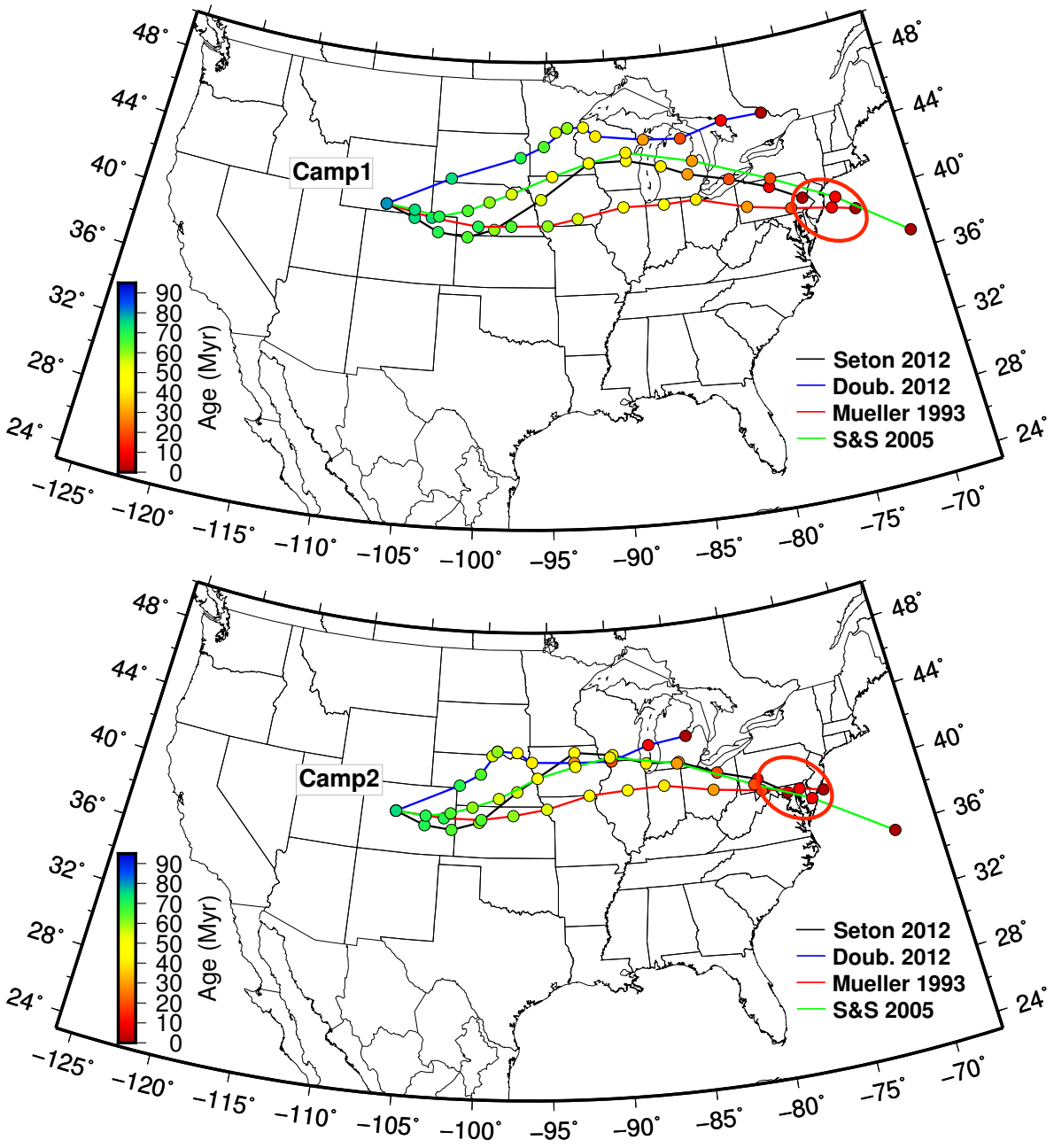

Figure 3.11. The Campanian I and Campanian II maximum deposition locations from Figure 3.10 tracked forward in time to the present day using plate reconstruction models.

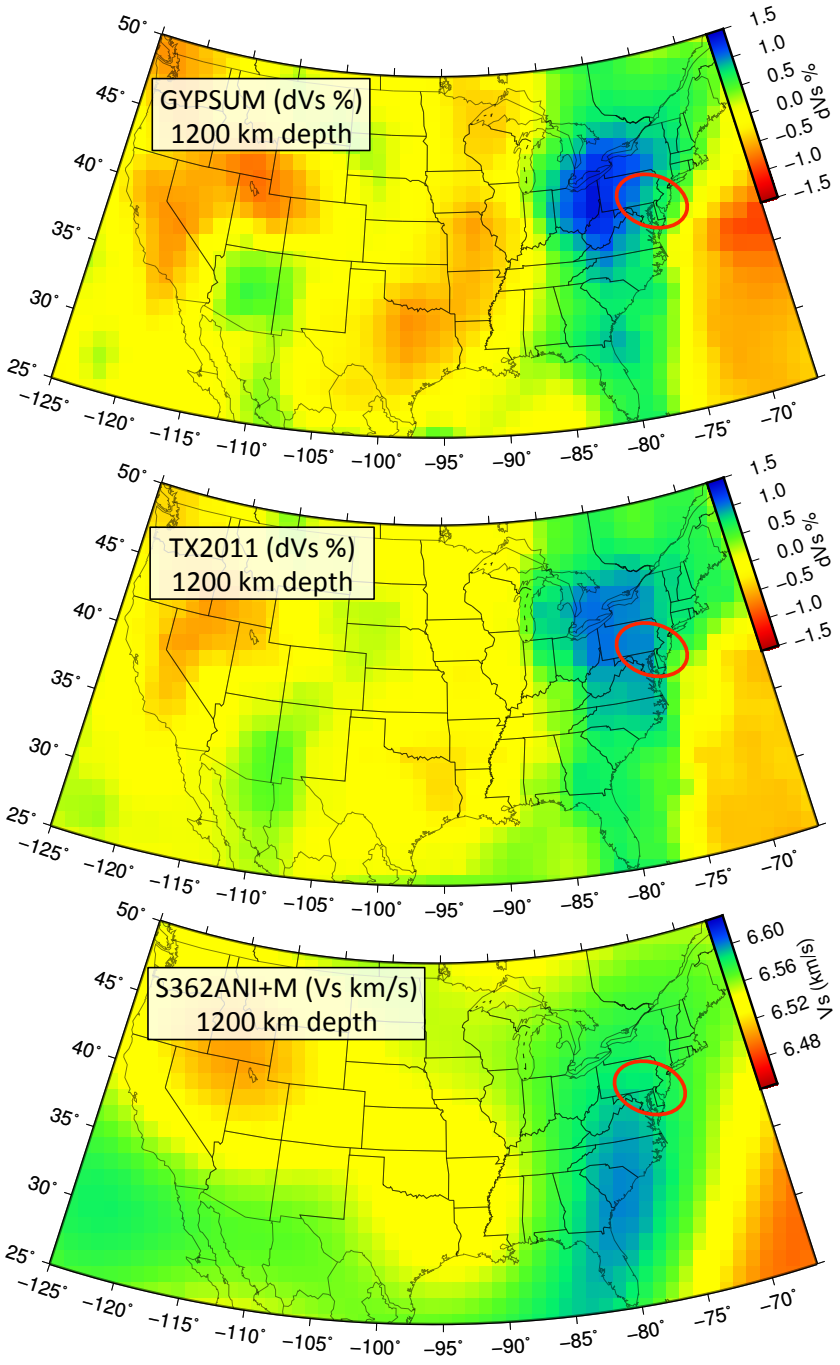

Figure 3.12. Comparison of multiple tomographic models of with the reconstructed location of a slab feature that could have caused the expansion of the WIB.

deepest portion of smaller mini-basins form at the western corners of the Wyoming Craton. As time moves on, the mini-basins coalesce and move westward, seemingly uninfluenced by crustal structures. A second exception is visible in Figure 3.3F, where there is a region of little to no sedimentation in the same location as the eastern portion of the Colorado Plateau. This could be due to the initial uplift of the plateau on its northwestern flank at that time.

The plots of cumulative sedimentation throughout the Late Cretaceous were initially created to map changes in the depocenter through time, but there was much less change than expected. In general, we can see the basin moving southward over time and during the Campanian I the deposition style switches from a traditional foreland basin style with the basins relatively close to the orogenic front to the wider foreland basin style we associate with the WIB (Figure 3.4). With that change the depocenter also moves to the east, further away from the orogenic front.

To investigate both oceanic plateau conjugates, the SRC and HRC were tracked through time to determine if either were plausible sources for crust-slab interactions, resulting in the anomalously wide WIB (Figure 3.5). This modeling showed that after subduction, the center of the SRC traversed roughly the same region as where the WIB occurred while the center of the HRC did not. As the extent of the SRC and HRC was not taken into account, the slab fragment end members were then plotted along with the plate motion tracks of the conjugates (Figure 3.6 and 3.7), resulting in the finding that even with the large flat slab end member, the HRC subducted too far south to have a major impact on the formation of the WIB. With respect to the SRC, either end member seems plausible so they were investigated further.

Figures 3.8 and 3.9 show the results of plotting the slab fragment end members along the plate motion track against the volcanism locations and the sediment isopachs through time. The relationship between the subducting slab and the volcanism does not appear to be a complicated one. As previously mentioned, the pattern of volcanism changes throughout the Late Cretaceous. This seems to be related to the movement of the slab fragment away from the subduction zone as the pattern of volcanism changes when the edge of the slab moves under present day Colorado. From the figures, it is also apparent that the plate reconstruction model of *Seton et al.* (2012) is a better fit to the isopach features than *Dietmar Müller et al.* (1993) due to the slab fragment end members consistently being located over or juxtaposed to the deepest portion of the WIB at each time step.

In Figure 3.10, we see how the depocenter of the WIB moved southward over the Campanian Age. The location of the two blue circles were forward modeled to present day with plate reconstruction software and the models of *Seton et al.* (2012) and *Dietmar Müller et al.* (1993) cluster together at slightly different locations along the east coast of North America (Figure 3.11). When comparing these locations with the velocity structure extracted from the tomographic models GYPSUM (*Simmons et al.*, 2010), TX2011 (*Grand*, 2002), and S362ANI+M (*Moulik and Ekström*, 2014) at a depth of 1200 km, GYPSUM and TX2011 have a high velocity anomaly whose southeastern edge overlaps with the modeled location. S362ANI+M on the other hand, has a high velocity anomaly to the south of the modeled location (Figure 3.12). Due to the uncertainty in plate reconstruction models and the possible discrepancies in the exact location of the slab-crust interaction during the Campanian, it is not surprising that the forward modeled locations

and the locations of the high velocity anomalies do not perfectly align. That being said, it is reasonable to assume that the high velocity anomaly imaged by the tomographic models is a Farallon slab fragment that may have influenced the formation of the WIB.

3.4. Discussion

When viewing the volcanic location data in Figure 3.2d-e we see that the arc magmatism in California weakens and magmatism west of the arc into Colorado increases. This is most likely due to a shallow dip of the subducting Farallon slab. In the case of a shallowly dipping subducted slab, the location where the slab crosses the dehydration zone will move away from the trench, which in turn causes the related surface volcanism to move away from the subduction as well. In the case of our study, this causes the arc volcanism present in California to dissipate as the subducting slab shallows. The arc volcanism is then replaced by dispersed volcanism that reaches as far as Colorado. This flat slab subduction has been considered a possible cause of the Laramide Orogeny for almost 50 years (*Lipman et al.*, 1971; *Snyder et al.*, 1976; *Coney and Reynolds*, 1977). The widening of the WIB in the Campanian through the Maastrichtian seen in the sediment isopach data coincides with the western movement of the volcanism as seen in Figure 3.2. This coincidence aligns with the hypotheses of *Jones et al.* (2011) and *Liu et al.* (2010) that an anomalous fragment of the Farallon plate, be it shallowly subducting or an oceanic plateau, interacted with the overlying crust and pulled it downwards, influencing the formation of the WIB and eventually causing the Laramide Orogeny.

Using plate reconstruction models to track the location of slab fragments through time created another useful data type for our study. When mapping the plate reconstruction

tracks, slab fragment end members, and sediment isopachs, there is a correlation with the widening and deepening of the WIB with the movement of the slab fragment through the region. During the Coniacian-Santonian Ages slab fragments begin to move eastward, crossing the Sevier front and the WIB begins to widen, but the depocenter stays close to the Sevier Front as is expected in a normal foreland basin (*Bird*, 1984). From the Campanian Age onward, when the slab fragments have moved completely past the Sevier Front, the WIB continues to widen and the depocenter migrates to the east departing from the expected geometry of foreland basins. This suggests some manner of crust-slab interaction, but our data does not have the qualities necessary to identify the type and extent. Therefore, we were not able to make any conclusions about which slab fragment end member is the more likely cause of the anomalous WIB or what exact mechanism of crust/slab interaction occurred at the time, but with the combination of these datasets we can conclude that the fragments were in the right place at the right time to interact with the crust and possibly influence the formation of the WIB.

As a part of the widening that happens to the WIB in the late Cretaceous, the depocenter moves east and southward. The eastward movement can be solely attributed to the widening of the basin, but the southward movement is more complicated. There are two other data types that change in a north-south oriented direction in addition to the sediment isopachs. First is the change in volcanic pattern with the majority of the volcanism changing from the southern arc in California to the northern arc in Idaho. The second is the plate reconstruction tracks of the slab fragments. Both tracks have a southeasterly direction through the first half of our time period before turning to the

northeast. While it is possible that these three data types align coincidently, it is unlikely. More likely is that all three are connected in the following way. As the Farallon slab was being subducted causing the arc volcanism in California, the relative motion of the North American plate with respect to the subducted Farallon slab changed to a more southwesterly direction. At this point, the majority of volcanism started transitioning to the Idahoan arc, and the Californian volcanism spread out to the northeast in a flat slab subduction pattern. Along with the flat slab volcanism, the sediment isopachs show the widening of the WIB at the same time. The coincident nature of the isopachs and volcanism with the movement of the slab makes it increasingly likely that the events are related.

Given that the SRC or a larger segment of shallowly subducting Farallon slab discussed earlier may not have been the cause of the unique geometry of the WIB, we investigated other possible mantle features that could have been involved. By forward modeling the location of the WIB depocenters during the Campanian I and Campanian II time periods to present day using plate reconstruction models, we were given rough locations to search for other possible features that could have interacted with the crust beneath the WIB. The three tomographic models used all showed a high velocity anomaly around the forward modeled depocenter locations at a depth of 1200 km. In tomographic images of the mantle, high velocity anomalies are generally considered to be slab fragments as long as the geologic context does not preclude it. We know that the Farallon plate was recently subducted beneath the North American plate so this is a safe assumption for the context of our study. The slab locations in the tomography do not perfectly align with the forward modeled locations of the depocenters, but there are a number of uncertainties that can

explain this. Seismic tomography does not currently have the resolution to create perfect images of structures in the mantle or core; due to this the images shown have a small location error because of the smearing of the signal along the ray paths. A larger location uncertainty comes in the form of the plate reconstruction models. The variability seen in Figure 3.11 clearly illustrates this and only includes four models. The last sources of uncertainty come from our simplistic assumptions. When setting up this workflow we made the assumption that the location of greatest deposition is also the source of the crust-slab interaction. This may not actually be the case. Due to the variable composition and physical properties of the crust, stress and deformation from the slab-crust interaction may be transferred to a location other than the depocenter. With the combination of these uncertainties, it is reasonable to assume that the slab fragments interpreted from the tomographic models are possible sources of crust-slab interaction that may have played a part in the formation of the WIB.

3.5. Conclusions and Further Questions

The WIB has created many unanswered questions about its formation and through various methods we have attempted to answer as many of them as possible. When starting this project, the goal was to combine datasets that would not normally be combined to investigate correlations that might support existing hypotheses on the formation of the WIB. While we were unable to unequivocally prove or disprove any of them, we did find that fragments of the subducted Farallon slab were likely shallowly subducted and would have been in the correct location and the correct time to influence the formation of the WIB.

Combining numerous unique datasets allows for opportunities to analyze problems from different angles as we have done here, but there are a number of ways that our results can be improved upon. The first would be to create new regional isopach maps with improved resolution. The isopachs from *Roberts and Kirschbaum* (1995), while very useful, are now over 20 years old and the amount of data that was available to them at the time was relatively limited. A way to accomplish this would be to use the Macrostrat database (*Peters and Heim*, 2010). Although this tool has the potential to be very powerful, at this time more data needs to be added before it can complete this task. Another area that would add insight to the formation of the WIB is crustal flexural modeling. *Jones et al.* (2011) includes some 2-D models of dynamic topography, but a 3-D model that includes the physical properties of crustal structures would give much more insight than our simple spatial comparison. A third possibility for improvement would be to plot the end member slab locations and volcanism locations at each time step on a palinspastic reconstruction of Western North America for that time step. This would remove location error from the extension of the Basin and Range and other regions in the west that occurred after the WIB was deposited and the North American plate moved over the fragments of subducted slab.

CHAPTER 4

Aspects of operating a broadband seismic field experiment: SPREE

4.1. Introduction

A vital but often overlooked part of a seismic network is the time, effort, and foresight it takes to install and maintain it. While most researchers focus on the data that comes out of the project, without a competent field crew the data acquired would most definitely suffer in both quality and quantity. As little formal documentation exists that covers best practices for seismic experiments, I will attempt to summarize personal field experience in an effort to prevent others from having delays or complications due to common issues myself and others have encountered while in the field. I have personally participated in field work in the United States, Canada, Mexico and Egypt, but only the US and Canada were seismic installations. Within those seismic installations I was a siting team member for the Northern Missouri/Southern Iowa portion of the TA and in Canada I was a siting and installation team leader for the Canadian portion of SPREE. Even though some weren't seismic related, they lent experiences that have been applicable in many field excursions since. Any location that field work is undertaken will have idiosyncrasies but while those may add complexity to the field work they should not prevent successful completion. The simplest phrase that sums up field work is "Everything rarely goes as planned, so be as prepared as reasonably possible." No matter the level of preparedness going into the field, there will almost always be surprises. Being prepared and open to alternatives will greatly increase the chances of successful data acquisition as well as saving money and time.

4.2. Station Siting

Before any equipment can be put in the ground for a seismic network, the locations for each station need to be selected. A necessary first step is to create a general plan for the arrangement of the stations, taking into account the nature of investigation and the overall goals of the project. The network could be in a grid arrangement or in lines bisecting a specific feature, depending on the goals of the project. In the case of SPREE (Superior Rifting EarthScope Experiment) (*van der Lee et al.*, 2011, 2013; *Wolin et al.*, 2015), we installed stations to investigate the 1.1 Ga Mid-continent rift in Minnesota, Wisconsin and Northern Ontario. The US stations were placed in one line along and two lines across the Bouguer gravity anomaly associated with the rift with 13 km station spacing. As the gravity signature varies along the axis of the rift, the cross-lines of the SPREE network were chosen to bisect the lowest and highest gravity anomalies along the rift. The combination of these three lines enabled the investigation of along-rift and across-rift structural variability. Since there was no rift-associated gravity anomaly in Ontario, the Canadian stations were arranged with a station spacing of 75 km to extend the station coverage of the Transportable Array (*Meltzer et al.*, 1999) into Canada (Figure 4.1). The initial or Phase I arrangement of the SPREE network was developed by the Principle Investigators (PIs) based on the geology and geophysics of the area. The locations developed in this phase are a general guide for the final locations that do not take into account aspects such as landowner issues, noise constraints (listed in Figure 4.2), access issues, and cell phone signal (if using telemetered seismic stations). Those issues are the responsibility of the field teams in charge of the Phase II or final station locations.

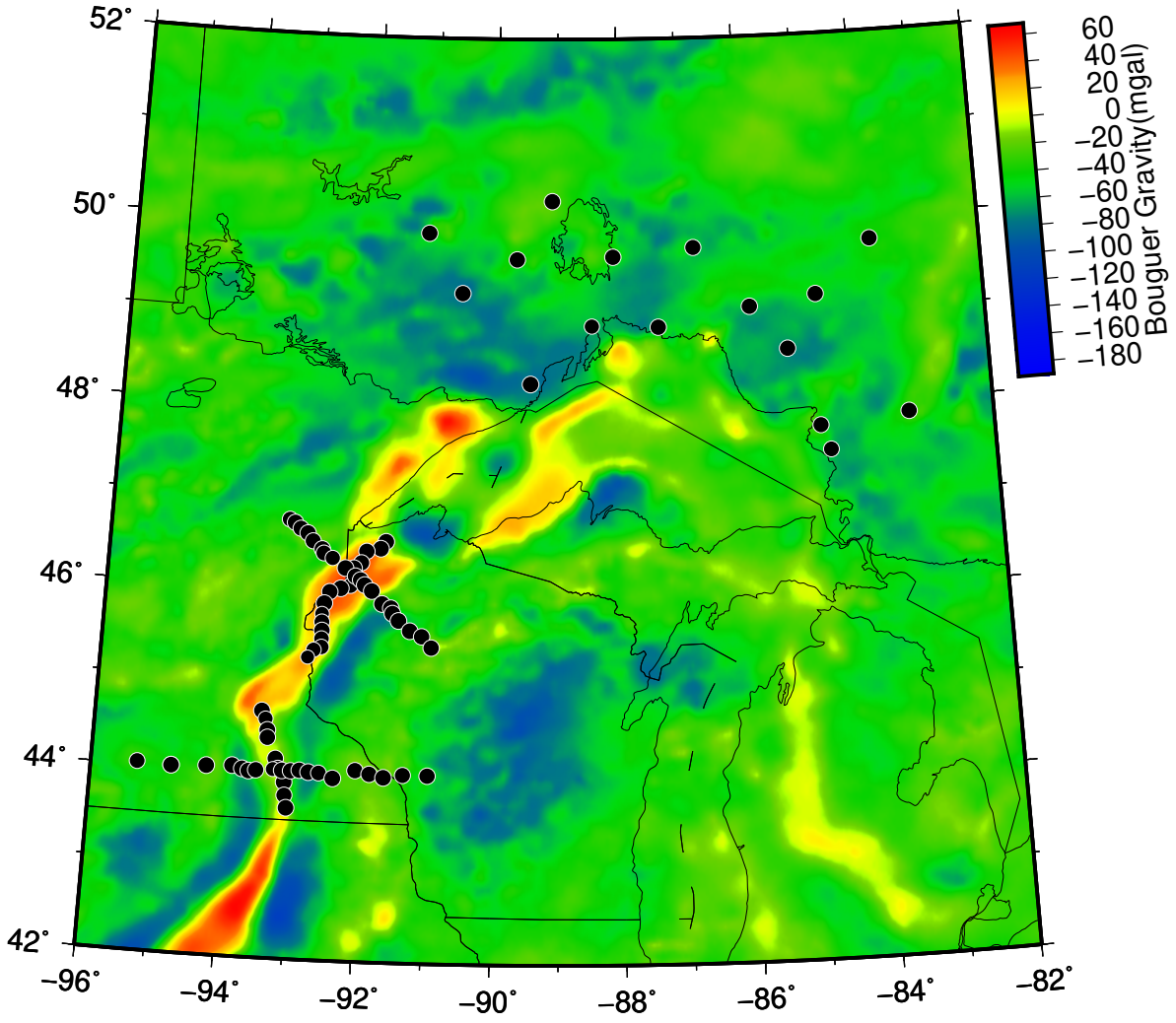

Figure 4.1. Map of the stations (red circles) used in SPREE, shown with the Midcontinent Rift Bouguer gravity anomaly.

The most used method of locating viable Phase II station locations near the initial planned location is to create maps of the station location with an acceptable buffer zone around them of a specific radius. The buffer zone is the area within a maximum acceptable distance from the initial location that the station can be placed. A general rule for acceptable deviations for seismic installations such as the Transportable Array is 75

Noise Source	Preferred Distance		Minimum Distance
Railroads	10 km		3 km
Highways	3 km		1.5 km
Local roads	1 km		500 m
Driveways	200 m		100 m
Occupied buildings	400 m		200 m
Irrigation Pumps	2 km		500 m
Residential water wells	4x depth		2x depth
Objects exposed to wind	2x height		1x height
(trees, old buildings, power poles)			
Rivers with dams or rapids	3 km		1 km
Oil/gas Production	3 km		1 km
Oil/gas pumping stations	3 km		2 km
Construction/industry	3 km		2 km

Figure 4.2. A list of common noise sources and the preferred minimum distance a seismic station should be located from them. From the Siting station criteria for USArray Transportable Array stations.

km, but in densely spaced station arrangements such as the US portion of SPREE, the allowable distance from the initial location is much lower. This can create another limiting factor in the site selection process, although this was not an issue in the Canadian portion of the SPREE network where the station spacing was as large or larger than the TA arrangement. Within the chosen buffer zone, take note of the major roads and other large noise sources (towns, railroads, etc.) that need to be avoided but also can provide access

to areas within the buffer zone. Next pick a number of smaller roads away from large noise sources to begin your search for an acceptable site along those. Depending on the number and quality of roads in the field area, this process can be either quick or rather involved. To shrink the search area and simplify the process, I generally start my drives as far away from the known noise sources as possible and work towards them. This method preferentially selects station locations with lower noise baselines before those with higher noise.

Siting seismic stations for different networks have similarities and differences depending on the goals of the study. For instance, we can compare the siting procedures of the USArray TA Network and the Flex Array SPREE network. Siting for each network has many similarities such as concerns with the same noise sources and their minimum exclusion distances. This is due to the SPREE siting teams adopting the noise source estimation procedures directly from the TA siting training. One large difference in siting methods is due to the construction of the station. TA stations in the contiguous United States employ large 8 ft deep, 3 ft wide vaults that require heavy machinery to build. SPREE stations on the other hand, are much smaller, only 3 ft deep, 1.5 ft wide, and were dug by hand. With this in mind, when siting for TA sites, it was necessary to find locations that had access for the heavy machinery to make it to the site. On the other hand, many SPREE stations were able to be installed in more remote locations after walking the equipment in by hand. Another difference in siting methods is the acceptable deviation from the initial station location. In the case of the TA, there is a hard limit of 75 km from the initial location, and to move the station outside this zone would require an extenuating circumstance such as the initial location being located in the middle of a

large metro area, road, or lake. SPREE had two different acceptable deviations, 10 km for the US SPREE stations and 75-100 km for the Canadian SPREE stations. Because of the dense spacing of the US SPREE stations, much smaller deviations were necessary to preserve the linear pattern of the US portion of the network and so stations did not end up extremely close together. A smaller buffer area can severely limit locations for stations, so in certain circumstances, non-ideal stations were chosen due to the lack of choices. The Canadian stations were allowed 75 km or greater since they were mimicking the TA spacing in the US and some stations required the larger deviations due to their remoteness, the lack of access roads, and a sparsity of private landowners.

Once a possible location is found, comes the part that many people find unappealing, talking to strangers. Since landowners must agree to host a station, it becomes the job of the siting team to convince a complete stranger that putting complex, unfamiliar, equipment in the ground and leaving it there for two or more years is not only a good idea but a great one that they should be excited to help with. Most people that answer the door will be naturally apprehensive and suspicious of unfamiliar people. A way to counter this is to highlight that the field team works with a local or associated university and this is especially the case if students are a part of the field team. People are generally less suspicious and more likely to help someone from a university as opposed to a private company. This should be used to the advantage of the field team. Be friendly, start the conversation with a firm handshake, make a short introduction of the field team, and make sure to never wear sunglasses. The last point is because people will naturally trust people more if they can see their eyes when talking with them. Even when using these tips, there is always the possibility the landowner will decide they are not interested during

the team introduction or explanation of the project. I have had multiple doors closed in my face that illustrated this point. This should not discourage the field team as they should simply move on and find the next possible location.

If the landowner does seem interested in the project, it is not helpful to give an overly technical explanation. This is due to the fact that the majority of the landowners will not understand seismology to the extent of members of the field team. The project and should be explained in simple terms without seeming condescending. At this stage it helps to have a handout explaining the goals of the project, pictures of what an installed station would look like, and the types of data that will be gathered at the station. Multiple copies of these should be available to give to any interested landowners.

The siting phase of a seismic network is also the phase that puts field teams in the most situations with the potential for danger from people. While the majority of people that may be encountered in the field will not be a hazard, it is easy to prepare for those that might. The easiest deterrent is to never go into the field without having a partner. A single person in an area they might not be familiar with is always more of a target than a group. When looking for sites it is also helpful to use the judgement of the team in selecting the homes to approach in search of landowners. The team should always be aware of their surroundings and if anything gives them an uneasy feeling, they should simply move on to the next house. As is always the case, personal safety should be always come before the other goals of the project.

After a landowner agrees to host a station, the work to find a specific location for the site begins. Before looking around the property, it is useful to ask the landowner for suggestions of places they would prefer the station be or where it definitely cannot be

located. Within the landowners available space, a site must be selected that is unobtrusive, far away from known noise sources as possible, and has a clear view of the southern sky (if using solar panels in the Northern Hemisphere). Figure 4.2 is a list of common noise sources from the USArray Transportable Array siting criteria. Also included are the minimum and preferred buffer distances for each noise source to predispose a station towards a low noise level. This is a good guide of noise sources to avoid but by no means a complete list. Once a satisfactory station is found, it should be marked so that it can be found during the installation phase. This is generally done using a wooden stake and fluorescent paint or flagging tape. The siting team, date, GPS location of the site, pictures in each cardinal direction, landowner contact info, possible noise sources, and general directions to the site should all be captured in the siting report. A siting report for one of the Canadian SPREE stations is included in Appendix B.1.

4.3. Field Work Planning and Execution

Generally 6 months to a year after station siting, the installation phase of seismic field work commences. This allows for additional planning time and the delivery of all equipment to field locations. Although the SPREE network was able to complete the installation phase roughly one year after the siting phase, there are a number of circumstances that can make this impossible. A combination of a remote field location, length of field seasons, logistics, governmental paperwork, equipment and field assistant availability, teaching seasons at universities, extreme weather, and demands from other projects can all influence the viability of a timely installation phase. In some instances where field areas are remote, visas are difficult to obtain or a number of other complications occur,

the station siting and installation phases will occur coincident with each other. This is at the discretion of the project PIs but their decision is usually more influenced by the previously mentioned constraints than by personal preference. My experience leans toward separated phases so that is what will be discussed in the paragraphs that follow.

4.3.1. Pre-installation Planning and Work

Depending on the size of the field area and the distribution of station locations, it is useful to have one or more staging areas. These are places where the equipment and other installation supplies can be delivered, organized, and tested prior to installation. For the SPREE installation there were three staging locations, one in Minneapolis due to its central location within the US station footprint and two in Canada on the east and west side of the Canadian portion of the field area. Having two Canadian staging areas was necessary due to the large swath of land covered in the installation process. It was a more effective use of the installation teams' time to split the stations into two groups, coordinated with separate staging areas, instead of wasting multiple days driving from one side of the field area to the other.

After equipment is delivered to the staging areas and organized, the most important thing to accomplish is a huddle test. This is an equipment status test in which all vital equipment is powered on and unlocked to make sure the seismometer, Data Acquisition System (DAS), and GPS are functioning properly. The main goal of the huddle test is to identify any equipment that may have incurred internal damage during shipping and therefore saving the project from installing faulty equipment to the station sites or losing data to equipment failure soon after installation. If any equipment issues are encountered,

the issue is troubleshot or as a last effort the piece of equipment is replaced with a spare. As an added bonus, this test is usually completed in the relative comfort of the staging area without having to cope with the elements out in the field. In projects with telemetered data it can also decrease the need for an extra servicing run to fix/replace faulty equipment immediately after the failure is detected remotely. This test is documented for future reference on Huddle test forms that are very similar to the installation and servicing reports (Appendices B.2 and B.3 respectively).

4.3.2. Installation

Once the Huddle test is finished, the installation phase of the project begins. In the case of SPREE, the first installation was used as a training opportunity for the multiple installation teams involved in the project. Members with the most experience installing seismic stations demonstrated how to install and test a station for functionality as well as answer any questions. Generally installation is done by groups of two or more people. The more people in the installation crew will increase the speed of installation but more than 4 or 5 reduces returns. With that number of people it gets increasingly difficult to get everything done, both due to the limited amount of things that can be done at once and that there simply isn't enough room for everyone in the footprint of the station. The first few stations you install will most likely take longer than expected. There are two reasons for this. The first is that it takes time to find the most efficient method and order to put tother all the individual parts of the station. The second is related to the people in your installation crew. Unless you have a seasoned installation veteran with you directing the work, the first few stations installed by a new team will take a longer period of time

in which everyone slowly identifies their roles in the installation. Once these issues are worked out, each installation will be smoother and more efficient than the last.

4.3.3. Landowner Relationships

Maintaining contact with your landowners is vital to the success of a project. When going on installation and servicing runs, it is a good practice to contact them at least 2-3 weeks in advance, then again the day before your visit. This will allow them time to prepare for your visit rather than showing up unannounced and taking them by surprise. Apart from site visits many landowners enjoy seeing how the project is progressing. One item that is very useful for this is giving them handouts of data recorded at their station. For instance, SPREE would give hosts record sections of larger earthquakes with the station they are hosting highlighted. An example of a record section handout for the Canadian SPREE stations is included as Figure 4.3. Before giving out the handouts to specific landowners, it is helpful to denote which of the seismograms shown were recorded by their station. Another method is giving presentations at local schools. While being appreciated by the teachers and community, it also exposes children to real science being worked on in their own neighborhood. These methods give the landowners and community a sense of ownership of the data being acquired and the interpersonal relationships between the landowners and the field team will benefit as a result.

4.3.4. Route Planning

An aspect of field work that should not be overlooked is route planning. If the field area is large there are a number of aspects that need to be planned for. When driving to field

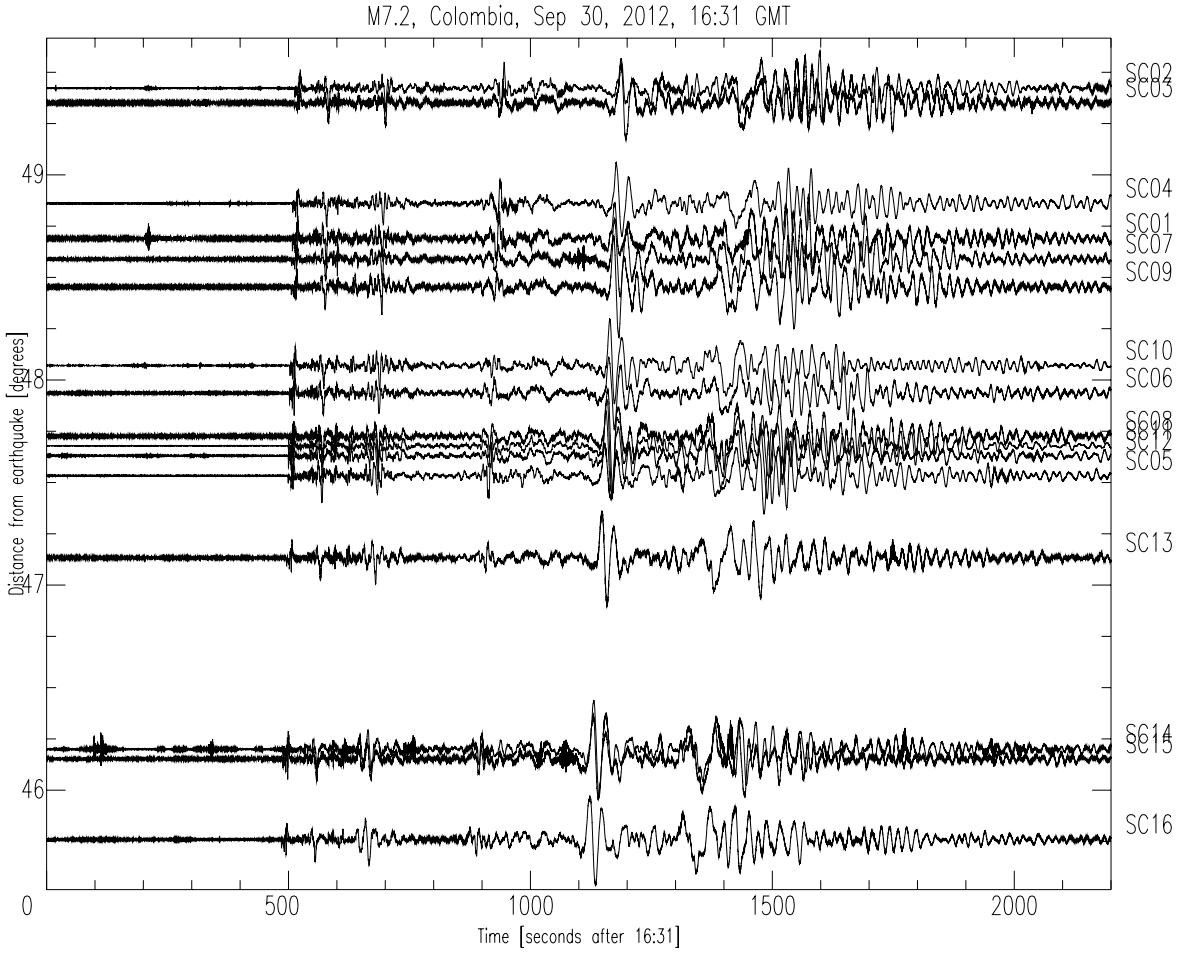

Figure 4.3. An example of a record section handout for the Canadian SPREE stations. The earthquake shown is the 7.2 magnitude event from Colombia, South America on September 30, 2012.

locations the most important thing to be aware of is the availability of fuel for the vehicle. In more remote regions, locations with fuel may be few and far between. If this is the case it is imperative that fuel is obtained before leaving said locations, even if the vehicle is not low on fuel. Another aspect of route planning for field work in remote areas is finding housing. If you do not plan on staying in a tent or your vehicle at the end of each day as some field locations may require, a hotel is the best option. This presents a similar

challenge to the previously stated fuel issue. The chosen route through the field area must take into account the location of fuel and overnight lodging. This might require taking shorter days than is ideal, but it is much preferred to being stranded hours from anyone that may be in a position to help. Yet another factor in route planning is the availability of food and water for the field team. Sometimes there will be towns on the chosen route where these can be purchased, but if this is not the case, they must be brought along. Depending on the distance and time between towns, having a cooler can be beneficial. Once these and other factors have been taken into account, there is the task of planning the most efficient route through your field area. Since budgets are almost always limited, it is beneficial to make field excursions as efficient as reasonably possible. This includes the total cost and total productive time in the field. While efficiency is a valuable goal, it should be achieved while also considering the safety of the field crew and a reasonable amount of comfort for those involved.

4.3.5. Computers in the Field

Traditional geology field work makes use of a field notebook as the sole note taking tool, but due to the use of multiple pieces of electronic equipment in seismic field work, a portable computer is a vital part of any seismologists field tool kit. Many times it is difficult to assess if a station is in working order without first completing a quality control of recent data from the station. This is done by visualizing station health data along with small snippets of data from the seismometer with software on a field laptop. Along with assessing station health a field laptop is also used to download data from the station and to create backups of said data. The data backups are a necessary redundancy in

case the original data is corrupted or damaged in transit. Backups are normally stored on an external solid state storage drive, preferably one that is robust enough to endure field conditions. Including electronics in a field kit adds even more complexity to field work with the foremost aspect being device charging. Similarly to fuel and housing issues discussed as major factors in route planning, charging of devices should also be taken into account. Most field vehicles are not equipped with the capability to charge devices larger than cell phones, so the majority of device charging is done at hotels overnight. One way to alleviate this complication is to purchase a DC to AC power inverter for the vehicle but this may not always be possible. Another issue to be aware of is the robustness of the electronics that are being used. Field work is generally not in a forgiving environment with respect to electronics so if possible it is important to either bring rugged electronics that were specifically designed for field work or take special care to ensure the functionality of said electronics.

4.3.6. Weather Issues

Weather complications are another possibly dangerous facet of field work. While completing the work is important, returning home safe is of the utmost importance. This can be done by always respecting the weather, especially in remote locations. I have personally encountered heat, thunderstorms, snow, and high winds. The majority of risk from these conditions can be mitigated by having the proper equipment (i.e. protective clothing, sunscreen, and 4-wheel drive vehicles). Two other members of the SPREE team were able to service stations in a snow storm but only because they had heavy jackets, snow pants, gloves, boots, a tarp, etc. that protected them and their electronics from the

elements. Even with proper equipment there are a number of situations where the reward is not worth the risk, namely, thunderstorms and large snowstorms. It is possible, albeit uncomfortable to conduct field work in light or sometimes even heavy rain or snow, but when lightning, high winds, and/or intense cold and snow loom, the risks to the field team are very high. You should use your best judgement to decide when the risks have become to high to continue, but in my opinion it is always best to err on the side of caution.

4.3.7. Equipment Failure

Once equipment is installed, another issue can occur, equipment malfunction or damage. Even after conducting a huddle test, it is still possible that some manner of equipment failure over the course of the experiment will happen. This can occur for a number of reasons, most notably environmental conditions, electrical or mechanical issues, and vandalism. Stations can also be effected by insects or mammals, albeit with reduced probability. Many times there is nothing visually amiss with the equipment and malfunction is only noticed when data is quality controlled after being downloaded and weeks or months of data are missing. When this occurs, it is almost certainly due to some type of equipment malfunction. At this point the piece of faulty equipment needs to be identified and corrected. If it is one of the major portions of equipment such as the seismometer, DAS, power inverter, or the GPS unit, simply replace them instead of troubleshooting further, as all of the internal workings of those pieces should not be tampered with except by an expert. Other than replacing faulty units, another aspect to inspect are the connections between each of the major components. Connections coming loose, corroding, or water seeping into the connection could all be a cause of failure.

I have not personally experienced issues relating to insects or mammals but they do occur on occasion. Seeing as the pelican cases that hold all of the electronics except the seismometer are not air tight, it is possible for colonies of insects to inhabit the open space around the electronics. They may even be drawn there by the heat generated by the equipment. Once inside, they can get inside the actual equipment, possibly causing electrical shorts and equipment failure. Mammals on the other hand, can cause a number of other issues. Curious mammals can pry open the pelican cases, exposing the equipment to the elements. Smaller mammals such as rodents apparently have an affinity for the rubberized coating on electrical wires. Once this coating has been punctured, water can get in and short out the system. In some cases these issues are unavoidable but luckily they are an uncommon occurrence.

Occasionally when a site is being approached for servicing, it is obvious that the site was disturbed. The most likely cause of this is vandalism. On separate occasions, I have seen solar panels shot with a rifle and seismometer containers opened and the seismometer disturbed. Other groups have had wires cut and every piece of equipment completely stolen. Even though station sites are selected to be away from high traffic areas, there is always the possibility of unwanted intrusion. At that stage, there are two options, fix issues caused by the disturbance or completely move the site. The latter takes a large amount of extra time unless there is already an alternative site picked out, but in the long run it may be a better option. To avoid this situation altogether, it is beneficial to place stations on private land where landowners are nearby to deter any outside intrusion.

4.3.8. Unforeseen Circumstances

With most endeavors, unforeseen risks and circumstances must be dealt with in the moment. Most of the issues in this category I encountered have been related to field vehicles. I have had a vehicle broken into, a flat tire, and even cracked the transmission case of a vehicle while driving in the field. There is no preparation that can be done to avoid these issues but preparations can be made to reduce down time. A few examples of this are making sure the field vehicle has a spare tire and the equipment necessary to change the tire, checking on cell service in the field area, and creating an itinerary for the trip so contacts not in the field will have rough ideas of the length of time the field team will be out in the field. The last item is simply a good practice in case something happens and the group in the field does not return when expected. Other than these examples, the best thing to do in many of these situations is to stay calm and call for help. Field vehicles that have been rented should be insured, so contacting the rental company office is the best option for most vehicle related issues. They will advise how to proceed. Of course this assumes there is cell service in your field area. If you do not, an expensive option is to carry a satellite phone or GPS tracker with texting capabilities. Barring those, another option is walking to the closest landowners home, if it is close by, or as a last resort, walking to the closest major road and flagging someone down.

A useful skill to deal with unforeseen circumstances is the ability to troubleshoot problems in the field. Initially, this will be a difficult undertaking but over time it will improve. What makes this come easier with respect to seismic field work is a familiarity with the equipment being installed and serviced. In the case of SPREE, the installation teams were shown installation steps and best practices by subject matter experts. These

could then be used in the field by the individual teams. Another important part is the ability to work with the available tools and equipment. Due to the remote nature of many stations, limited replacement parts, and variable equipment needed to fix any problem stations might have, it is not reasonable to bring the proper equipment for every possible problem. This necessitates the need to prioritize equipment for servicing runs. While it is always possible that an uncommon issue may occur, only the equipment for likely failures should be on the equipment list. In my experience, it is advisable to always bring replacements for the DAS, GPS, and solar panel power inverter. A replacement seismometer can also be useful but may not always be available. When arriving at the site, there may be issues that you lack the exact equipment for normal repair. At that point, thinking outside the box to devise a plan with the equipment on hand is necessary. It may not always be possible to fix every issue (some can only be fixed by replacing a very specific part) but an attempt should be made.

4.3.9. Organization and Note Taking

The last general detail of field work planning and execution I wish to stress is the necessity of organization and note taking. Even seemingly insignificant changes with the goal of organization can save a great deal of headaches and stress over time. The degree of organization implemented is up to the team leader, but it is important to find a system that is sufficient for the work being completed. This all starts on siting trips and the documentation taken while on them. It is generally much easier if all documentation equipment is in a backpack in an easy to reach place in the field vehicle. As site installation begins, organization becomes even more important. If multiple stations are being installed

in one trip from the staging area, the field vehicle should be packed in a way that the remaining materials do not need to be taken out and re-packed between each installation. An image of a properly packed field vehicle is shown in Figure 4.4.

When the station servicing phase of the project occurs, a part of the project that many people might overlook is the amount of paperwork that starts to accumulate. Depending on the number of stations you are servicing and the length of the project, the number of reports can increase very quickly. Because of this, it is beneficial to have both digital and analog copies of siting/reconaissance reports (Appendix B.1), installation reports (Appendix B.2), and servicing reports (Appendix B.3), organized in a way they can be easily referenced in the future. Having multiple copies of the reports is a necessity for when one of those versions is lost, destroyed, or stolen. Doing this has prevented me from completely losing all of my previous documentation when my car was broken into as stated previously. These organizational suggestions are merely the system that was most useful to me. There are most certainly other project specific issues that would benefit from organization and have not been discussed here.

4.4. Field Work in Other Countries

Completing field work in other countries adds another layer of complexity to an already complex undertaking. This is especially true if specific/expensive equipment is a necessity for a field excursion as it is for seismic fieldwork. Whether the necessary equipment is large or there are numerous items, it is much easier to have the it shipped over the border by a broker. This significantly simplifies the process since brokers do this on a regular basis for all different types of clients. In the case of my field work in Canada, the details

Figure 4.4. Picture of the author with a van properly packed for seismic field work.

for the broker were handled by the Portable Array Seismic Studies of the Continental Lithosphere (PASSCAL). Even with a broker, delays from moving the equipment through customs are a real possibility. Delays can happen for a number of reasons, be it government holidays, worker strikes, a significant backlog of items moving through customs or other unforeseen circumstances. Efforts to limit the amount of supplies being taken into another country should be made, both for simplicity in entering the country and to give back to the local economy by purchasing readily available items in country. Things like lumber, tarps, and other basic items can most likely be purchased in any country with a hardware store. This is not always the case so some research should be done to ascertain what supplies can be gathered in country before the start of field work.

On shorter trips, such as servicing runs, where extensive equipment is not needed, having your equipment shipped is not advisable. Instead you should bring the small amount of tools you need with you. For my Canadian field work this involved me driving through customs at the Canadian border with a small toolbox and a few replacement parts. After going through customs in this fashion eight different times, I have learned the methods that made getting through customs with equipment much easier. One of the first questions the customs agent will ask is, "What is the purpose of your trip?" A good response is to very quickly explain the experiment in layman's terms making note of the universities you are working with in country. Do not go into great detail. If the agent has further questions about the trip's purpose they will ask. Knowing the specific names of people working on the project from that country and what university affiliation they have is very helpful. They will almost definitely not check these names but saying them with confidence and without hesitation will speed the process along. Another question that

will be asked is “Do you have anything to declare?”. You should then tell them about the equipment you have brought. Make sure to mention that none of the equipment will be left in country temporarily as this would trigger the need for an import tax and ATA Carnet. Another issue I encountered, from US customs, was extra scrutiny due to visas on my passport from countries on the United States high risk list. The visa stamp in question was from Egypt that I had received for field work years prior. This resulted in a 15-20 minute discussion about what the purpose of my trip to Egypt was and what else I had done while there. It finally ended when I mentioned that the trip was funded by the National Science Foundation. As you never know when such encounters might occur, it is helpful to have a succinct reason on hand for visiting any country or it can look suspicious in the eyes of customs agents. Especially if that country considered a high risk destination by the country you are entering or leaving.

Another challenging aspect of doing field work in another country is the possibility of a language barrier. This can become an issue when purchasing equipment for field work, completing field work, or dealing with the previously mentioned unforeseen circumstances. While many other countries also speak English in the larger cities, generally the farther you go from the cities the more people only speak the language native to that region. There are a few ways to deal with this situation. Learning the necessary languages to be successful in that region, working with individuals from universities in that country who speak that language, or as a last resort, hiring a translator. I have seen the first two options used. In Mexico the lead investigator had been working in the region for such a long time that she became fluent in Spanish. It was very apparent that the work it took had paid dividends. In Egypt, we collaborated with numerous Egyptian universities

whose professors and students did fieldwork with us and were a huge help conversing with any people we came across. Even in countries whose main language is English such as Canada, there can be issues in communication. Given that there are local colloquialisms in any language, it is possible that an essential tool could be called by a different name. I have not personally experienced this, but it would complicate field work.

Depending on the country your field work is in, there may be challenges associated with transportation to the field area. While in developed countries it is simplest to drive to the necessary field locations, this is not always possible in every country. This can be due to the lack of personal knowledge of the roads, the quality of the roads, or even due to language barrier issues. When combined, these issues can exponentially complicate the undertaking. In extreme cases it is the most prudent option to hire a driver to mitigate the risks and hassle caused by these issues. It is worth noting that in many countries, the only vehicles available will be manual transmission. As this is not the norm in the United States, it is best to prepare for this inevitability before hand.

4.5. Dependence on Technology

Due to the increased availability of technology in research settings and every day life, it is easy to continue to rely on it in the field. This can result in wasted time, loss of data, and severe frustration for the individuals completing field work. In my experience, technology that was not designed specifically for the field is much more likely to fail while in the field. Even if that equipment is tested before embarking, there is always the possibility of technological complications. One way to mitigate this is to lessen the amount individuals in the field depend on technology to a realistic level.

There are many different ways that this can be accomplished but most of the examples I am familiar with, revolve around not relying on the numerous functions of your cell phone. One extremely simple example is to carry paper maps as a backup for any digital form of navigation you may use to traverse your field area. It is not uncommon for cell phone reception to be intermittent or non-existent in these areas. Another reason cell phones can be unreliable in field situations is battery life. Due to this it is important to have analog versions of any data being stored on any of your devices if there is not a method to keep those devices charged. For example, instead of keeping all contact information on only a laptop or phone it can be extremely useful to have this information on paper as well for reference.

4.6. Noise Estimation at Station Sites

The main criteria in selecting a seismic site are related to the incipient noise sources in the vicinity. A visual inspection and discussions with landowners are usually the best possible method for site selection during siting trips, but it is difficult to assess the quality of the station before it collects any data. One method to determine the quality of stations is to complete a look-back on each site, noting if they have low noise levels in the anthropogenic portion of the frequency spectrum. With this knowledge, sites for future seismic installations can benefit from the experience gained. In the case of the Canadian SPREE stations, this look back can be completed using probability density function (PDF) plots of noise spectra created in the manner of *McNamara and Buland* (2004) and *Wolin et al.* (2015) using data downloaded from each site (Figure 4.6) and the documentation taken during the initial siting trip at the beginning of the project.

Figure 4.5 shows the locations and names of the Canadian portion of the SPREE seismic network and Figure 4.7 notes the noise sources documented during the siting trip for each station. Comparing the noise sources in the Figure 4.7 with the noise spectra in Figure 4.6 confirms which stations were suspected to have larger noise signatures or the lack thereof. Determining the exact characteristics of each noise source in the noise spectra is difficult due to all of the noted noise sources occurring within the cultural noise band (10 - 2Hz) and would therefore overprint each other.

For each of the stations, data from the three broadband channels (BHZ, BHN, and BHE) were further divided into subgroups by season and whether it was day or night when the data was being acquired. Therefore, for each of the channels, spectra were created for summer days, winter days, summer nights, and winter nights. This was done to better understand the noise sources and how they might change throughout the year or 24 hour periods. Before delving into the spectra of each station individually, a few common observations should be noted. In general, the stations are less noisy in the high frequency portion of the seismic spectrum (10 - 2Hz) during the winter and at night by 10-2 dB and 15-5 dB respectively. This diurnal characteristic is due to a reduction in anthropogenic activity during those times relative to the summer and during the day. Another possible source of noise during the day would be the diurnal wind speed changes discussed by *Wolin et al.* (2015). As wind speeds generally peak in the early afternoon then gradually decrease towards evening, it stands to reason that the noise related to wind would do the same. This leads to higher cultural noise during the day than at night. It is worth mentioning that *Wolin et al.* (2015) only found negligible day/night changes in the vertical channel of the US SPREE stations so this may only be a minor effect. The

microseism peak between 2 and 0.1 Hz is much more pronounced in the winter spectra by a range of 5-10 dB. This is due to the increased storm intensity in the Atlantic and Pacific Oceans during the fall and winter months (*McNamara and Buland*, 2004). Lastly, the horizontal channels at most stations have larger power levels during the summer months than they do in the winter months within a range of 5-13 dB. This phenomenon was also noted in the SPREE stations in Minnesota and Wisconsin by *Wolin et al.* (2015) and they determine that this change is due to variable coupling to various atmospheric tides. The shallow seismic vaults used in the installation of the SPREE network make the sensors especially susceptible to this effect.

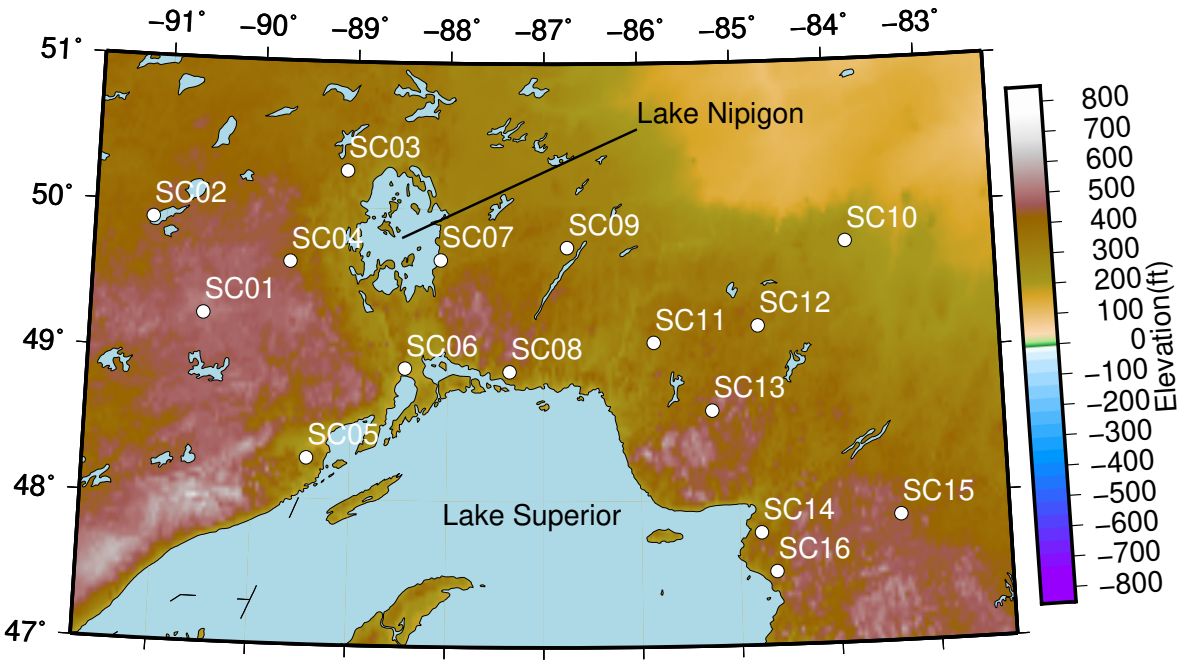

Figure 4.5. Map of the Canadian SPREE stations with station name annotations and elevation.

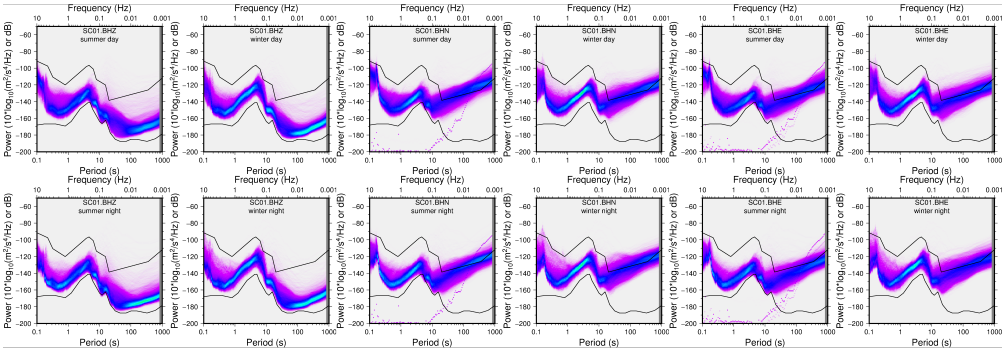

(a) SC01

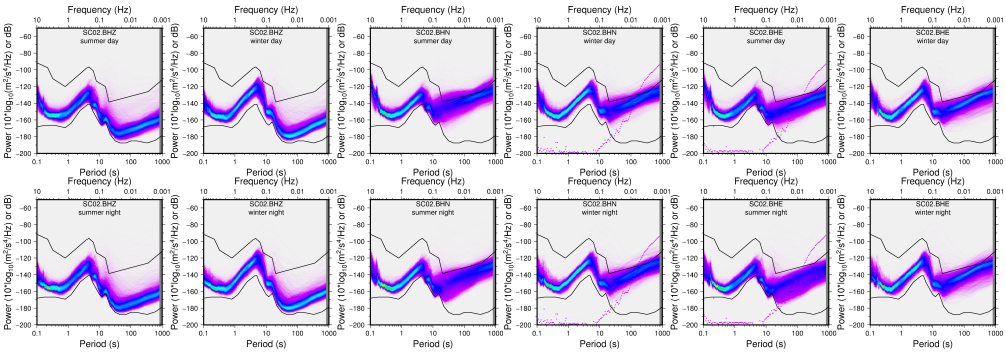

(b) SC02

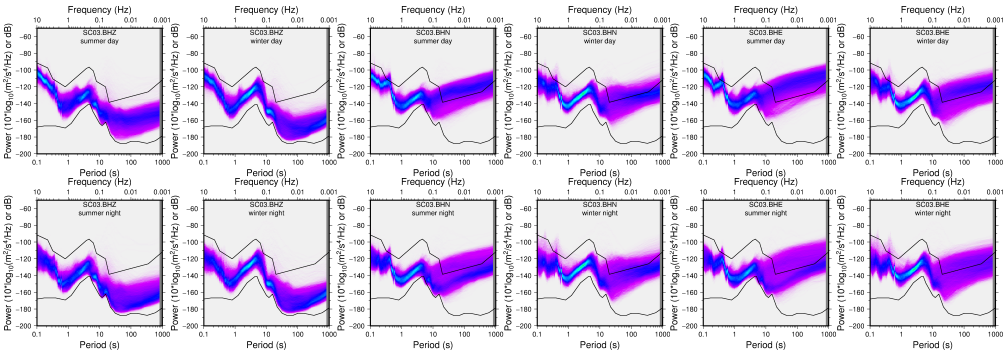

(c) SC03

Figure 4.6. Noise spectra plots of the 16 Canadian SPREE stations. For each of the broadband channels (BHZ, BHN, and BHE), plots shown for summer days and nights and winter days and nights. Cyan color denotes likely noise state while magenta is less likely. Figure created by Emily Wolin.

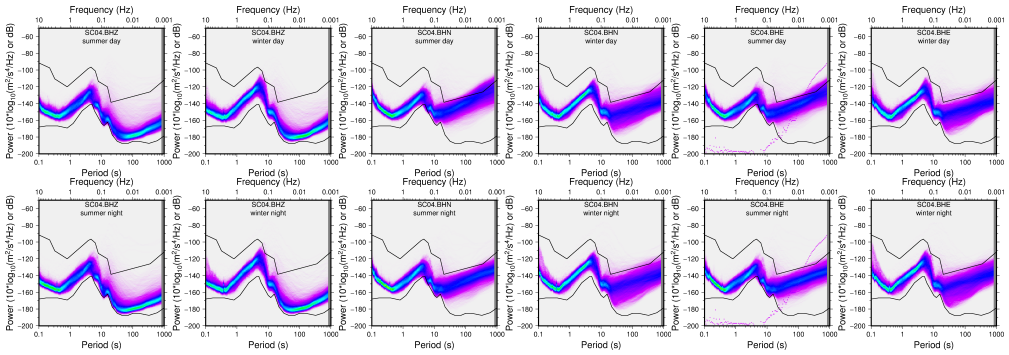

(d) SC04

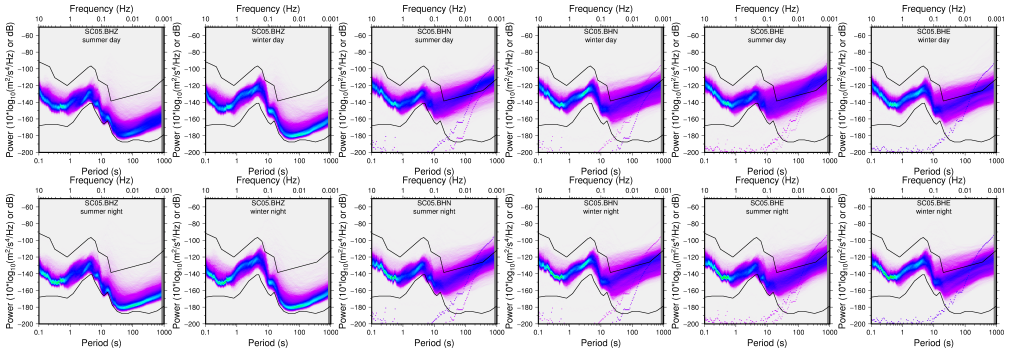

(e) SC05

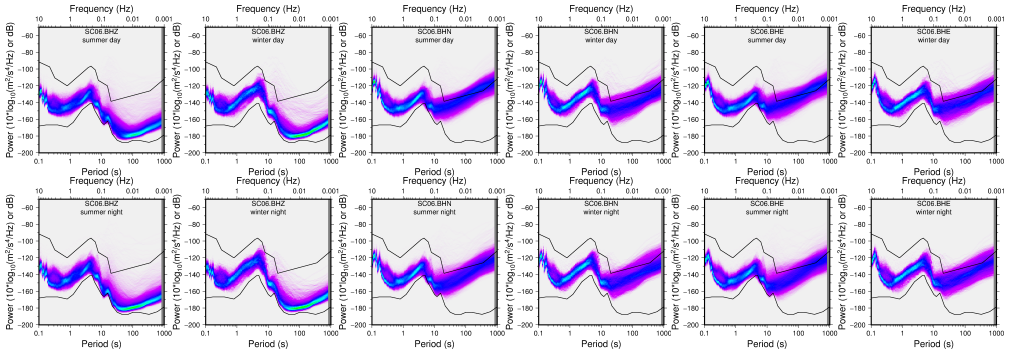

(f) SC06

Figure 4.6. Noise spectra plots of the 16 Canadian SPREE stations. For each of the broadband channels (BHZ, BHN, and BHE), plots shown for summer days and nights and winter days and nights. Cyan color denotes likely noise state while magenta is less likely. Figure created by Emily Wolin.

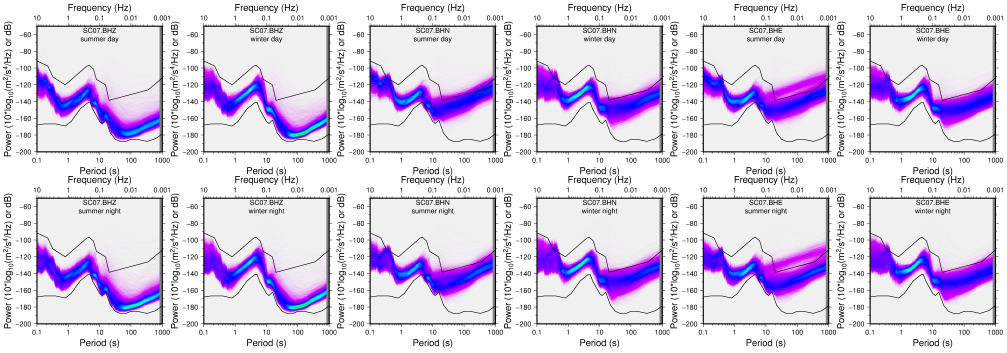

(g) SC07

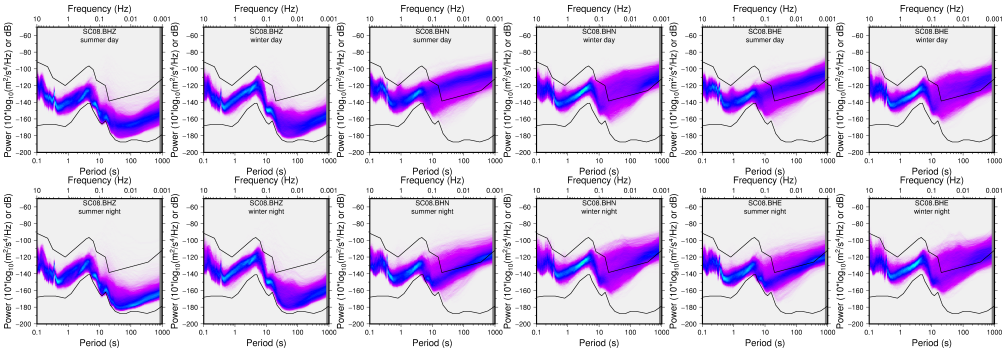

(h) SC08

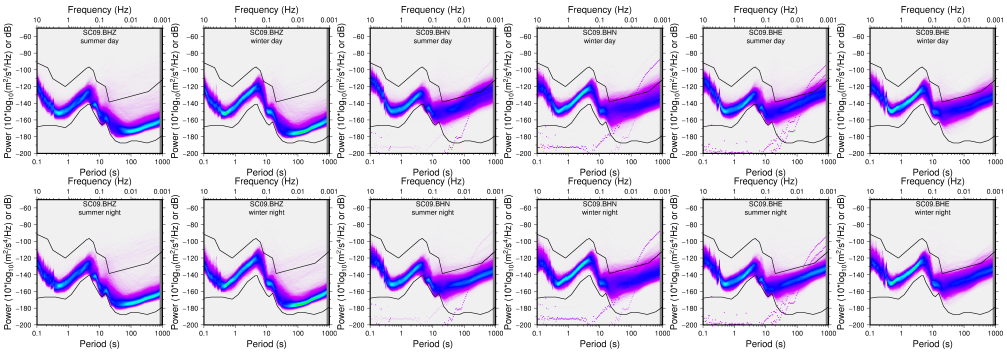

(i) SC09

Figure 4.6. Noise spectra plots of the 16 Canadian SPREE stations. For each of the broadband channels (BHZ, BHN, and BHE), plots shown for summer days and nights and winter days and nights. Cyan color denotes likely noise state while magenta is less likely. Figure created by Emily Wolin.

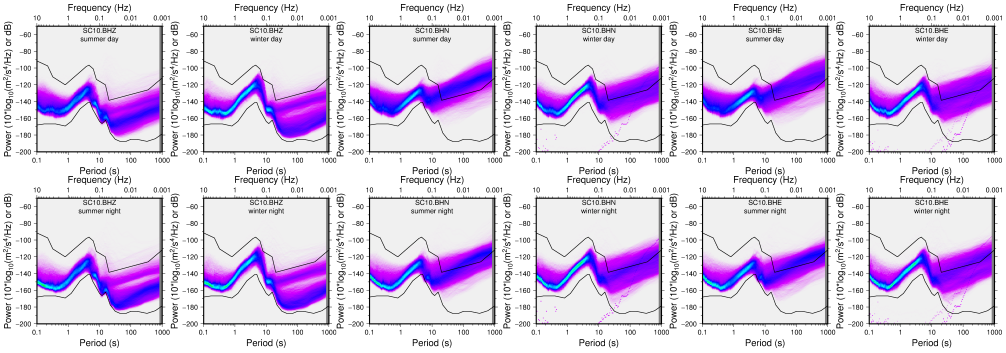

(j) SC10

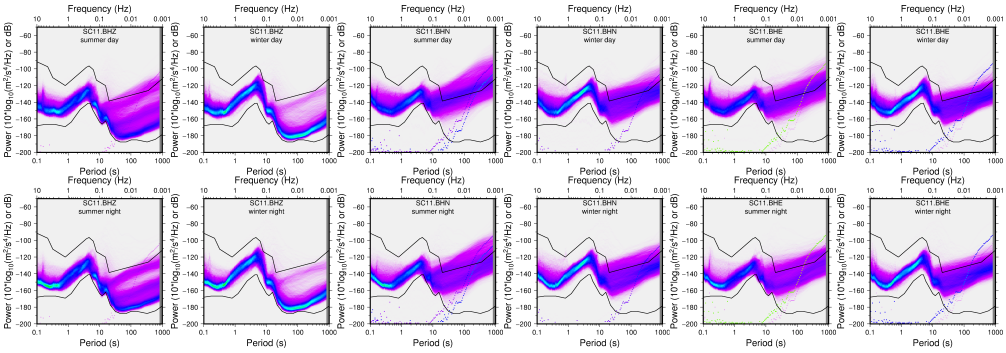

(k) SC11

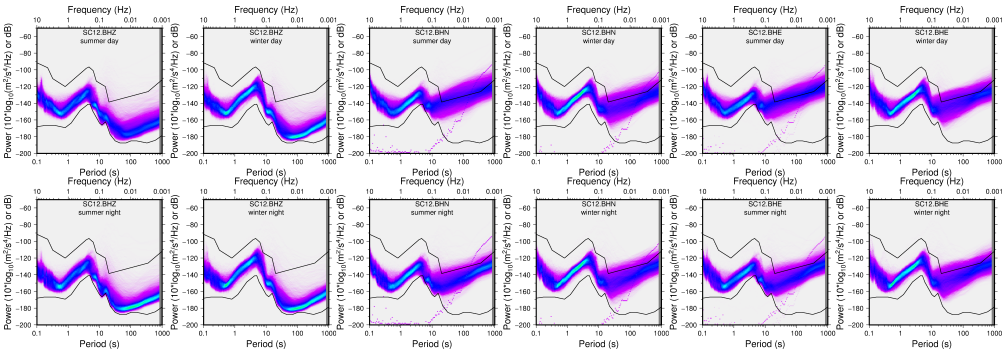

(l) SC12

Figure 4.6. Noise spectra plots of the 16 Canadian SPREE stations. For each of the broadband channels (BHZ, BHN, and BHE), plots shown for summer days and nights and winter days and nights. Cyan color denotes likely noise state while magenta is less likely. Figure created by Emily Wolin.

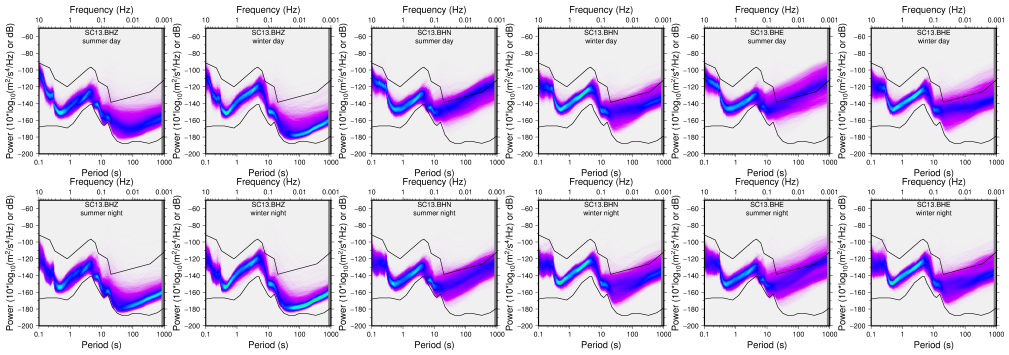

(m) SC13

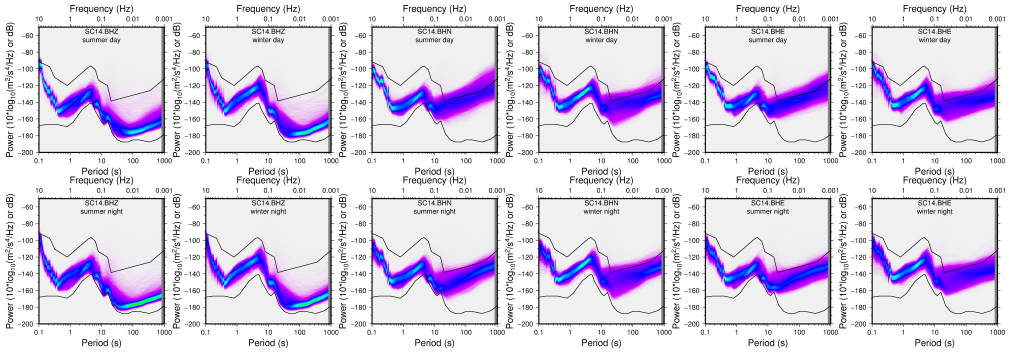

(n) SC14

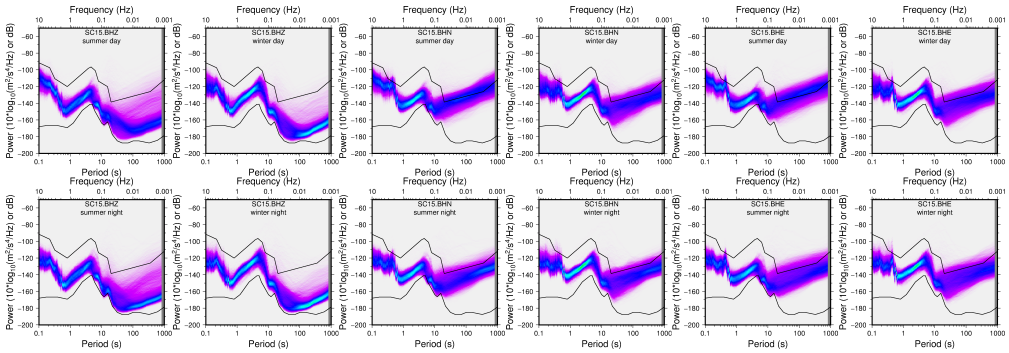

(o) SC15

Figure 4.6. Noise spectra plots of the 16 Canadian SPREE stations. For each of the broadband channels (BHZ, BHN, and BHE), plots shown for summer days and nights and winter days and nights. Cyan color denotes likely noise state while magenta is less likely. Figure created by Emily Wolin.

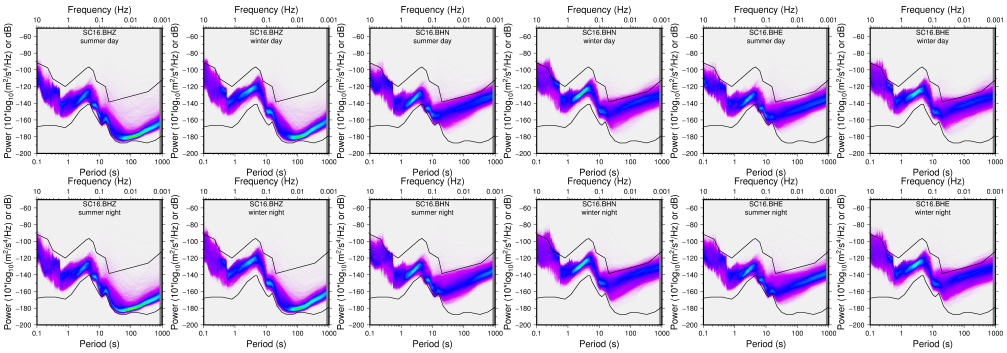

(p) SC16

Figure 4.6. Noise spectra plots of the 16 Canadian SPREE stations. For each of the broadband channels (BHZ, BHN, and BHE), plots shown for summer days and nights and winter days and nights. Cyan color denotes likely noise state while magenta is less likely. Figure created by Emily Wolin.

4.6.1. SC01

Station SC01 had high levels of cultural noise (-100 dB) which is not completely surprising due to the stations location at a summer cabin near a small lake. What was surprising is that this was one of the stations with the most cultural noise. Other stations with similar noise levels were much closer to major highways or small towns while this station was rather remote other than being within a group of 10-15 homes. The amount of noise in the summer was not surprising due to the close proximity to other homes and recreational activity on the lake but even in the winter the cultural noise level only reduces from the summer level by 10 dB. At this time of the year only one house (not the station landowner's) is inhabited and the lake is iced over. A possible source of noise could be

	Noise Sources	Land Use	Other Comments
SC01	Wind, occasional mowing in Summer, Trees (20m to the north), house & machine shed (100m south), 120 ft deep water well (500ft), waves from the lake (30m)	Residential	During winter no one onsite
SC02	Occasional mowing in summer, trees - some will be removed (30m), house (50m to the west), traffic from campers	Residential	
SC03	Wind, occasional mowing in summer, house (30m to the west), waves from the lake (15m)	Residential	
SC04	Wind, larger trees (30m), building (~10m), Driveway (20 m) with local traffic only	Hunting Camp	During winter no one onsite
SC05	Wind, pond (30 m), buildings (100m), Gravel Road (150m), Snow mobiles in winter	Residential	Site in the middle of a field
SC06	Wind, gravel road (50m), house (100 m), Trans Canada Hwy (~1.5km)	Residential	Site in the middle of a field
SC07	Wind, Trees (30m), house (70m), Lake Nipigon (~.5 km), in the owners garden	Lake Camp	On a cliff above lake Nipigon, more traffic on weekends
SC08	Wind, trees (10m), waves from lake (15m), cabin (50m), could hear the train tracks from the other side of the lake	Lake Camp	On a small peninsula out in a lake
SC09	Wind, trees (20m), house (50m), garage (10m), driveway (15m), Trans-Canada Hwy (~2km), occasional mowing in summer	Residential	
SC10	Wind, driveway (20m), road-last house on road (40m), Trans-Canada Hwy (~3km)	Residential	Site in the middle of a field
SC11	Wind, airport road, some helicopters, minimal plane use, airport office (150m)	Airport	
SC12	Wind, planes, parking lot (8m), airport office (10m), occasional mowing in summer	Airport	
SC13	Wind, 1 close tree (15m), gravel road (10-15m), occasional mowing during summer, lake (~150m)	Residential	
SC14	Wind, very close to the Trans-Canada Hwy (20m), trees and brush (20m)	Provincial Park	
SC15	Wind, trees and brush (20m), some local traffic, waves from lake (40m)	Lake Camp	
SC16	Wind, waves from Lake Superior (.75km), trees and brush (25m),	Provincial Park	Behind a closed gate in an unused portion of the park. Best site?

Figure 4.7. Table of the identified noise sources at each of the Canadian SPREE stations.

wind interacting with the trees close by but I would not expect the power level observed at the station to come solely from that source.

4.6.2. SC02

Station SC02 had low levels of cultural noise (-120 dB) which is less than expected due to the station being in close proximity to the landowners home and near a road leading to a boat dock and small campground. The vertical channel PDFs are very close to the low noise model, indicating a good quality station. Not surprisingly, there is less noise during the winter as the campground is closed, the nearby lakes are frozen over, and the homeowners are the only people on site but due to the quality of the site the power level

only decreases by 5 dB. Another feature is the low energy levels of the .1 - 1s period range in the horizontal channels. Along with SC10 the power levels are much lower than most other stations and this may be attributed to the distance of those stations from Lake Superior.

4.6.3. SC03

Station SC03 had high levels of cultural noise (-95 dB) which is as expected due to its close proximity to the landowners home (20 m). The area this station was sited in was severely limited in possible station sites as the only thing in the area is a small town with only one road in or out. The vast majority of people living there are in the town, so we were forced to look for sites on the outskirts of the town where there was still a large amount of cultural noise instead of more remote locations as we did for other stations.

Another feature in the noise PDFs is the blocky characteristic of the high energy levels in the .1 - .5 s period region of the horizontal channels. This differs from the cultural noise signature seen in vertical channels in the 10 - 2 Hz range. This characteristic is likely due to a thicker than average unconsolidated sediment package beneath the station. Most of the Canadian SPREE stations are within 10 feet of bedrock due to glaciation events removing any sediment that was present and depositing it to the south. This station is located in one of the rare places where there is a thicker sediment package and the seismic spectra reflects this. The ratio between the amplitudes of the horizontal and vertical channels (HVSR) will create a peak at a frequency that is related to the thickness of the unconsolidated material above competent bedrock (*Ibs-von Seht and Wohlenberg*, 1999). In the case of this station, it occurs at 2 Hz. Due to the thickness of the sediment at this

location, it is one of the few stations where the frequency of the HVSR does not occur within the cultural frequency band and can therefore be easily observed.

Differing from most other stations, the long period region of the vertical channel has a dB range of 35 while most other stations have a range of 20 dB, denoting a highly variable noise state at those periods. Lastly, this station also has only small changes in the noise signature between summer and winter, which is very likely due to the close proximity of the landowners home and that she lives there year round.

4.6.4. SC04

Station SC04 has extremely low cultural noise levels (-140 dB) and thus is the quietest station in the Canadian portion of the SPREE network. It was noted in the reconnaissance report for this station that it would likely be the quietest station in the network due to its remoteness. The noise levels measured seem to align with this hypothesis. In the 10 - 2 Hz range, there is an unusual signature that small portion of the energy in the winter day and night plots have a larger energy level than is present in the summer plots. This is odd given the remote location of the station and due to the fact that no one is on site during the winter months at the hunting camp the station is located at. None of the other Canadian SPREE stations observe a signature similar to this.

4.6.5. SC05

Station SC05 has low levels of cultural noise (-120 dB). This stations location in a more populated agricultural region makes the lower noise level surprising. An odd feature occurs at the 1 -10 s period range in the summer plots of the vertical channel where

the signal widens and instead of one linear noise state, there seems to be two competing noise states with a more sinuous nature. This feature does not have a day versus night component and is observed in a few other stations but is most pronounced here, in SC08, and SC14.

4.6.6. SC06

Station SC06 had low levels of cultural noise (-120 dB). This was unexpected due to the station being relatively close to the Trans-Canada highway and the gravel road leading to the landowners driveway is within 50m of the station. A notable feature in the PDFs is that between the periods of 1 - 10s, there is not one most likely noise state in the summer plots. This signature is weaker than other stations, but still noticeable.

4.6.7. SC07

Station SC07 had high levels of cultural noise (-100 dB). Similar to the horizontal channels of SC03, there are high energy levels in the .1 - .5s period range. An aspect of the PDFs that goes against the general observations discussed earlier is that the range and height of energy levels in this station are higher during the winter than in the summer. This is counterintuitive since there is usually less cultural activity during the winter but it is likely due to wind noise from winter storms coming off of Lake Nipigon, as the station is located on a cliff overlooking the lake.

4.6.8. SC08

Station SC08 had moderate levels of cultural noise (-110 dB). In the long period region of the vertical channel, the signal is relatively wide, denoting a highly variable noise state at those periods. As is seen in a number of other stations, there is an increased energy level from .1 - .5s period in the horizontal channels. The 1 - 10s period of the summer vertical channel plots have the characteristic of two competing noise states as seen in SC05 and SC14. The most notable feature in this stations PDFs is the energy levels of the horizontal channels in the long period range. In fact they are higher than any of the other stations. It is not clear why this is the case.

4.6.9. SC09

Station SC09 had moderate levels of cultural noise (-110 dB). This station has no other notable features like those discussed for other stations and is a generally quiet station other than the cultural noise range.

4.6.10. SC10

Station SC10 had minor levels of cultural noise (-130 dB). One notable feature in the station's PDFs are found in the long period region of the vertical channel. At that location, there are two distinct noise states. This aspect is most apparent on winter nights but is still visible at any time of the year. Another feature is the low energy levels of the .1 - 1s period range in the horizontal channels. Along with SC02 they are much lower than most other stations and could be attributed to the fact that these stations are the farthest from Lake Superior.

4.6.11. SC11

Station SC11 had low levels of cultural noise (-120 dB). Interestingly, he highest energy level in the cultural noise range did not occur at the smallest period of .1s at this station. Instead it occurred at .2s. Similar to SC10 in the long period region of the vertical channel, there are numerous noise states visible in the PDFs. Differing from SC10 there are 3 different states instead of 2 and they are more prominent during the summer rather than the winter. Between the periods of 1 - 10s, there is not one most likely noise state in the vertical channel summer plots. This signature is weaker than in SC05, SC08, and SC14, but still noticeable.

4.6.12. SC12

Station SC12 had moderate levels of cultural noise (-120 dB). Like SC11, the highest energy level in the cultural noise range did not occur at the smallest period of .1s. Instead it occurred at .2s. It is unclear why this is the case. Between the periods of 1 - 10s, there is not one most likely noise state in the vertical channel summer plots. This signature is weaker than in SC05, SC08, SC14 and even SC11, but still noticeable when specifically looking for it. Other than those characteristics, this station is a rather quiet with only minor changes from summer to winter.

4.6.13. SC13

Station SC13 had high levels of cultural noise (-95 dB). This is not surprising as the station is within 10-15 meters from a gravel road that the landowners neighbors use to access their property. As is seen in a number of other stations, there is a blocky increased

energy level from .1 - .5s period in the horizontal channels. Between the periods of 1 - 10s, there is not one most likely noise state in the vertical channel summer plots. This signature is weaker than in SC05, SC08, and SC14, but similar to SC11 in strength. In the long period region of the vertical channel the noise is increasingly variable during the summer months and decreases during the winter and at night.

4.6.14. SC14

Station SC14 had extremely high levels of cultural noise (-85 dB), the highest levels in the stations discussed. This was not surprising due to being in close proximity to the Trans-Canada Highway (20m) and being located on the edge of Lake Superior Provincial Park's maintenance lot. In the .1 - .5s period range in the horizontal channels there are increased energy levels but the PDF's don't take on the blocky nature seen in other stations where these energy levels were also seen. This could be due to high cultural noise overprinting the signal of the "blocky" noise. The 1 - 10s period of the summer vertical channel plots have a distinct characteristic of two competing noise states as seen in SC05 and SC08.

4.6.15. SC15

Station SC15 had high levels of cultural noise (-95 dB). As is seen in a number of other stations, there is an increased energy level from .1 - .5s period in the horizontal channels. There is a slight hint of a secondary noise state in the long period region of the vertical channel. It is much smaller than what was seen in SC10 and SC11 but is present. This

feature does not appear in the winter PDFs as it did in the other stations, possibly due to the minor nature of the signal.

4.6.16. SC16

Station SC16 had high levels of cultural noise (-100 dB). This was surprising due to the fact that the station was located in a rarely accessed portion of Lake Superior Provincial Park behind a locked gate. As is seen in a number of other stations, there is an increased energy level from .1 - .5s period in the horizontal channels. There is a hint of two separate noise states in the 1 - 10s period of the vertical channel summer plots but it seems to be partially obscured by the noisiness of the station. This station is an outlier when compared to the other stations in terms of summer vs winter cultural noise levels and the horizontal long period power levels. It is actually louder during the winter months than the summer and has the exact same power level in the horizontal in the winter and summer seasons. It is possible that these two characteristics could be due to the station being situated in a bay filled with unconsolidated sand. While other stations may have been in sand, the amount of sand at this location is much greater than all other stations.

4.7. Discussion of Interesting Noise Features

As seen in the description of each station's PDFs, there were a number of common features noted. Namely, increased energy levels with a blocky pattern in the .1 - .5s period range of the horizontal channels, the presence of multiple noise states in the long period region of the vertical channel, and the highest power level within the cultural noise portion of the plot. While it is difficult to determine the exact source of many of these features,

it is possible to determine if there is a spatial aspect to the noise. We accomplish this by indicating which of the stations has been noted to have each feature in their PDFs on a map. The stations with blocky noise in the .1 - .5s period range in the horizontal channels are shown in Figure 4.8, stations with multiple noise states in the long period interval of the vertical channel in Figure 4.9, stations with two noise states in the 1 -10s period interval during the summer in the vertical channel in Figure 4.10, and the cultural noise levels of all stations are shown in Figure 4.11.

From those plots, we can see that the blocky noise signature seems to only occur at stations in a linear path from the northeast to the southwest. An initial hypothesis was that this feature was related to wave action on the larger lakes due to many of these stations being located on close proximity to them, but if that were the case, stations SC02 and SC06 would also have this feature. It is still unclear what the source of this feature is, so further investigation is needed. No patterns emerge from plotting the stations where multiple noise states are seen in the long period interval of the vertical channel. Even if you included stations SC12 and SC13 which have a wider spread in the long period portion of their vertical channel PDFs but no obvious separate noise state, the only pattern that emerges would be a general grouping of stations in the eastern half of the map. It is possible that the source of the higher energy noise states could be from teleseismic earthquakes but if this were the case, there would need to be a reason that only some stations have this feature while others do not. Differences in soil type and depth to bedrock are possible explanations for this issue.

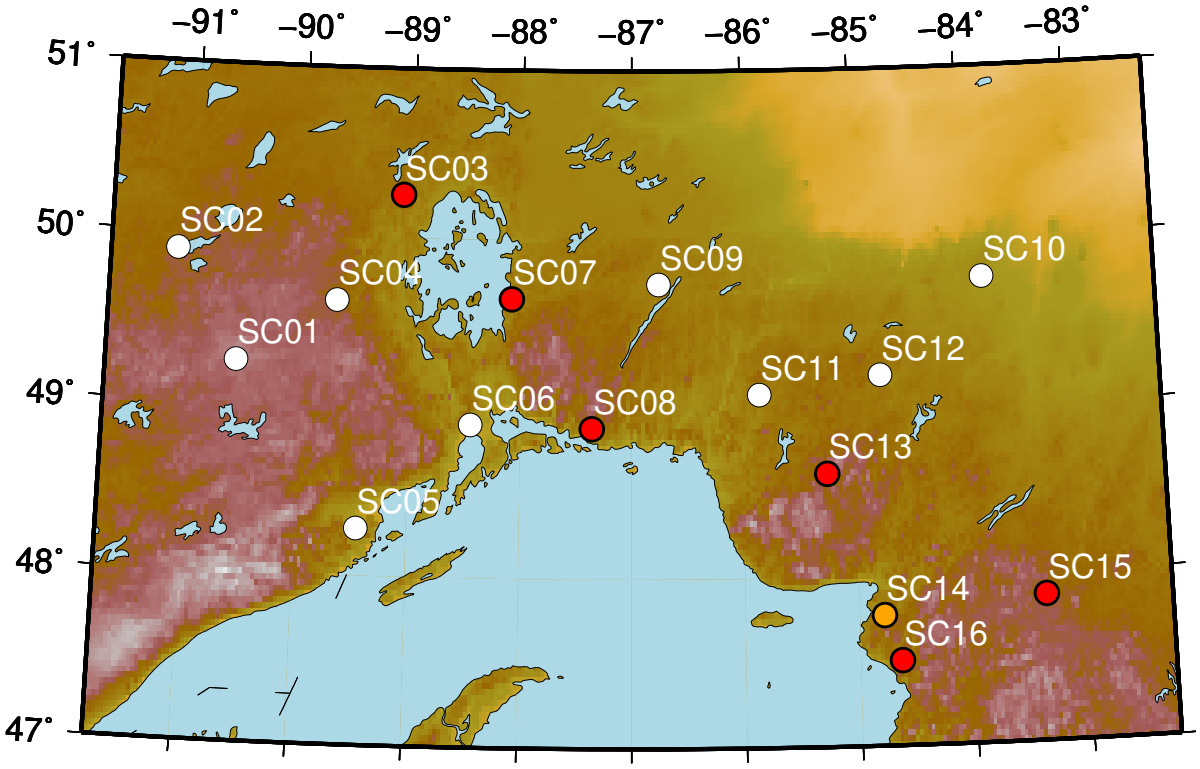

Figure 4.8. Map of the Canadian SPREE stations that have a blocky increased noise level in the .1 to .5s period interval on the horizontal channel plots. Stations are annotated with their name and those that have this noise feature are colored in red. Station SC14 is colored in orange due to the fact that it may have this feature but overprinted by noise from the nearby highway.

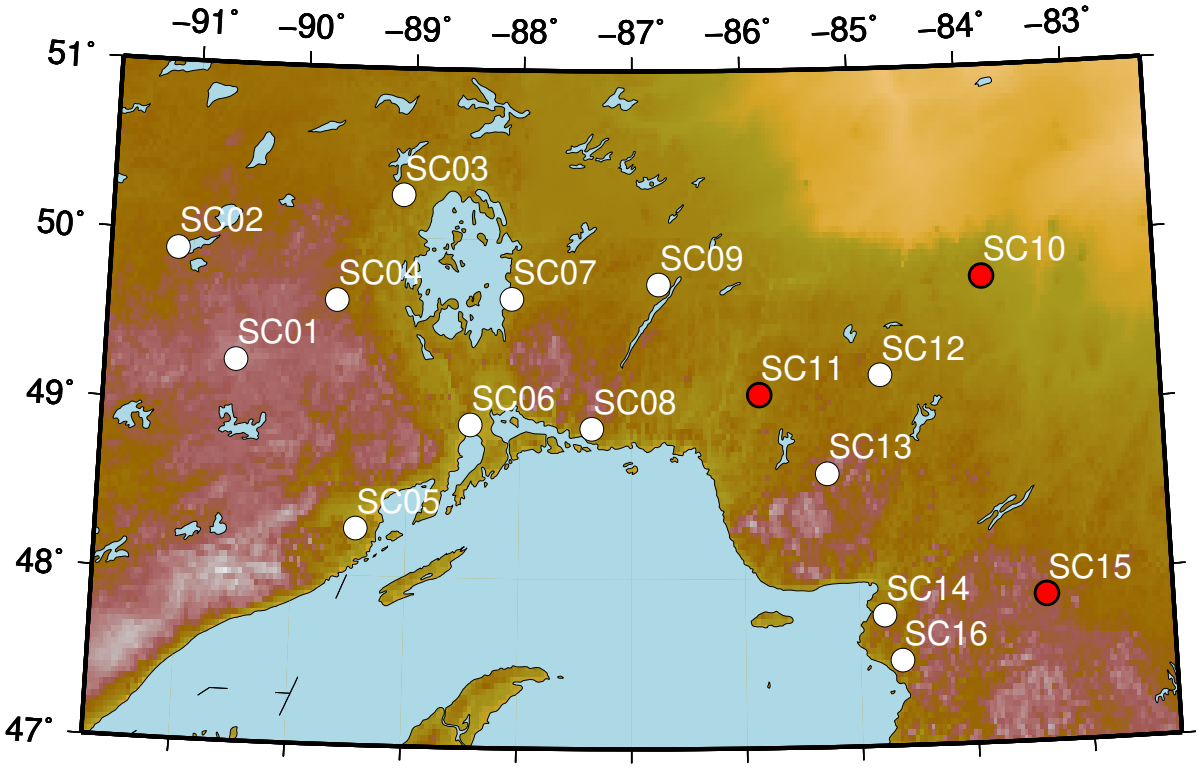

Figure 4.9. Map of the Canadian SPREE stations that have multiple noise states in the long period interval (0.03-0.001 Hz, 33-1000s) on the vertical channel. Stations are annotated with their name and the stations that have this noise feature are colored red.

4.7.1. Lake Superior Microseisms

One figure that does seem to have a pattern is Figure 4.10. In this plot, the stations closest to Lake Superior all have the noise characteristic of having two distinct noise states in the 1 - 10s period interval in the vertical channel but only during the summer. When looking back at the descriptions of noise characteristics for each station we see that stations SC07 and SC12 have a weaker manifestation of this characteristic. The other stations in the Canadian portion of the SPREE, likely have this same signature but the strength of the

signal is low enough that it does not stand out above the rest of the signal in the seismic spectrum. With this feature occurring at a frequency less than 2 hertz, the source of the noise is unlikely to have a cultural source. If we assume the source of the noise was Lake Superior, it stands to reason that as the energy moves away from the source it will attenuate, therefore creating a weaker signal at SC07 and SC12, the stations that are farthest from the lake but still have this feature in their noise spectrum. *Anthony et al.* (2018) states that Lake Superior microseisms occur with a peak between 0.7 and 1.65 seconds which is within the range of where we observe this characteristic. I believe that the feature that we observe is a bit more complicated than purely a microseismic peak. When comparing the summer and winter PDF plots, a shoulder on the main microseismic peak occurs within the frequency range of Lake Superior microseisms that looks very similar to one of the noise states seen in the vertical channel summer PDF plots. The other noise state has a power level closer to the low noise level model so it is reasonable to assume that this noise state is from a relatively quiet time period. Due to the images in Figure 4.6 being a summation of 6 month periods that are roughly winter and summer, the signature we observe is likely an overprint between a Lake Superior microseism noise state and a quiet noise state. The winter plots for the stations in question show a clear secondary peak or shoulder on the main microseismic peak at 1 Hz that fit the description of Lake Superior microseisms by *Anthony et al.* (2018) that are due to storms happening more frequently during the winter. If the time periods used to create the summer/winter plots were instead separated into when there were storms on Lake Superior and when they were not, it would likely separate these two noise states.

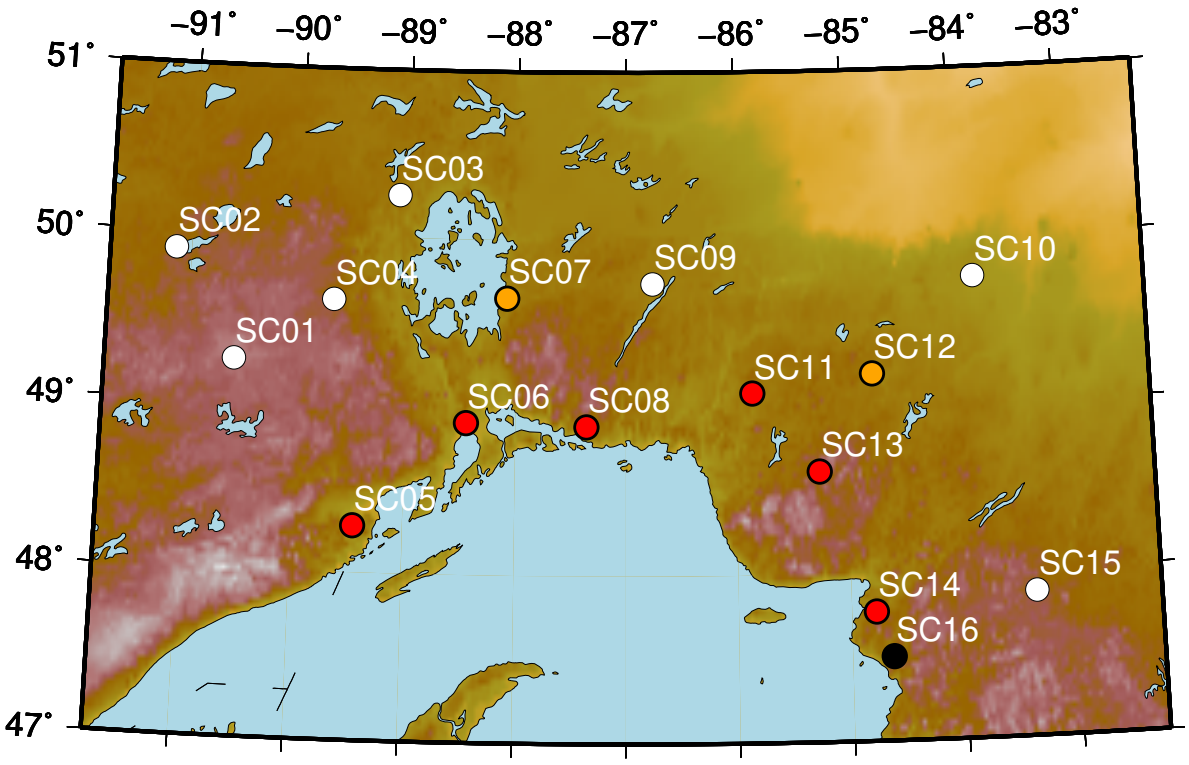

Figure 4.10. Map of the Canadian SPREE stations that have multiple noise states in the 1 - 10s period (1 - 0.1 Hz) range during the summer on the vertical channel. Stations are annotated with their name and the stations that have this noise feature are colored red. Station SC16 is colored in orange due to the fact that it may have this feature but overprinted by noise.

4.7.2. Cultural Noise

Figure 4.11 shows that there is no significant pattern in the levels of cultural noise at each station. This is most likely due to cultural noise being locally generated and each of the stations having different cultural noise sources being recorded. Another possibility is that simply measuring the highest peak of the noise levels in the cultural band is not the best estimation of the noise content within that region of the PDFs. As a comparison, the

cultural noise levels from 8 TA stations in northern Minnesota, Wisconsin, and Michigan were measured in the same manner to compare with the SPREE station measurements. The measurements all lay within the dB range of -110 to -125. This is a significantly smaller range than the values measured for the Canadian SPREE stations and could be due to the more robust station construction of the TA network, including positioning the seismometers more than double the depth of their SPREE counterparts, effectively insulating them from a portion of the cultural noise. Even though the dB ranges of the two networks to overlap, it is not a fair comparison because of the large discrepancy in the range of power levels. Due to the large amount of scatter seen in the cultural noise levels in the SPREE network, a similar exercise was not completed for other noise bands measured at each station.

4.8. Conclusions

Seismic fieldwork is a complex but necessary facet of a large portion of seismic research and without it the amount of data and resolving power that seismologists work with would be severely limited. Field work begins with finding a site that fits the proper criteria relating to adjacent cultural noise sources and obtaining landowner permission to install the station. In situations where site locations are limited, it is sometimes necessary to to select a station that is not ideal. Each non-ideal location will have different noise sources and it falls on the siting team to weigh the options and select a station that will have the lowest noise level.

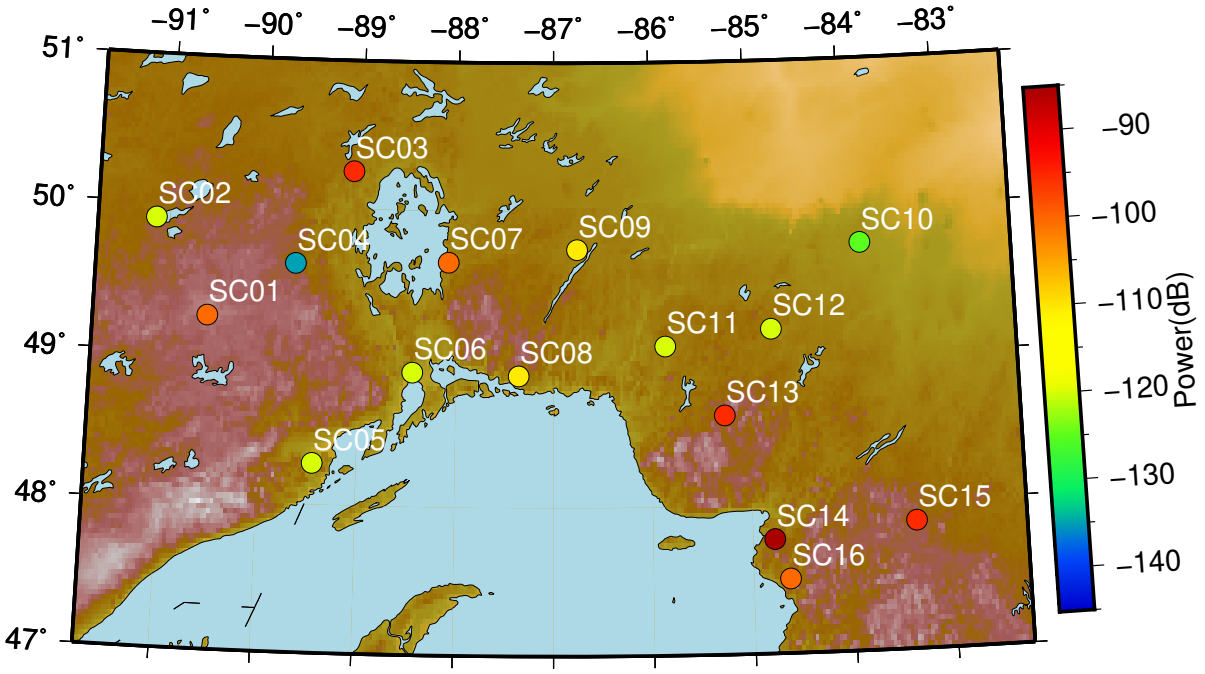

Figure 4.11. Map of the cultural noise levels at each of the Canadian SPREE stations with station name annotations. Values are the highest Power (dB) measured within the cultural noise band (10-4 Hz, 0.1-0.25 s) of the noise spectra in the summer day plot.

Even though the station may not end up being perfect, almost any station is better than not having one at all. When going into the field to install these stations, there are a number of issues to take into account when planning the route to them. Vehicle fuel, nightly lodging, and the ability to charge electronics as well as selecting an efficient path should effect the final route. While an efficient route is important, the safety and comfort of the field team should also be kept in mind. A related subject of equal or greater importance is organization during field work. There are many moving pieces in any project that requires field work but seismic field work is especially so due to the large amount of electronics being brought into the field and the numerous trips to site, install, and service the stations. Every one of the trips to the field and the documentation that

they create benefit from some form of organization. What form that takes is dependent on the project and the persons undertaking it.

After a seismic project has concluded, it is beneficial to complete a look-back on the quality of the stations using the noise spectra of the data over the project timeframe. This informs project members on the efficacy of station siting and can improve future station siting trips. At the same time the look-back is completed, an investigation into the patterns in the noise spectra for each of the stations can be completed. In the case of the Canadian SPREE stations, this led to observations of diurnal, vertical channel, noise level changes in the cultural frequency range due to anthropogenic noise and/or daily wind speed changes, summer/winter differences in the long period range of the horizontal channels related to atmospheric tides, and the observation of microseisms originating from Lake Superior. The latter was clearly present during the winter months in stations close to the lake but during the summer the signal was more nuanced. Due to the lower frequency of storms over the lake during summer, the Lake Superior microseism noise state was overprinting with a noise state relating to more tranquil periods of time on the lake.

References

Allen, P., and J. Allen (1990), Basin Analysis–Principles and Applications., 1990, *British Petroleum Company pic., London*.

Anderson, R., and R. McKay (1997), *Clastic rocks associated with the Midcontinent Rift System in Iowa*, 1989, US Geological Survey.

Anthony, R. E., A. T. Ringler, and D. C. Wilson (2018), The widespread influence of Great Lakes microseisms across the midwestern United States revealed by the 2014 polar vortex, *Geophysical Research Letters*, *45*(8), 3436–3444.

Bastow, I., A. Nyblade, G. Stuart, T. Rooney, and M. Benoit (2008), Upper mantle seismic structure beneath the Ethiopian hot spot: Rifting at the edge of the African low-velocity anomaly, *Geochemistry, Geophysics, Geosystems*, *9*(12), Q12022.

Bedle, H., and S. van der Lee (2009), S velocity variations beneath North America, *Journal of Geophysical Research: Solid Earth*, *114*(B7), B07308.

Behrendt, J. C., D. Hutchinson, M. Lee, C. Thornber, A. Trehu, W. Cannon, and A. Green (1990), GLIMPCE seismic reflection evidence of deep-crustal and upper-mantle intrusions and magmatic underplating associated with the Midcontinent Rift system of North America, *Tectonophysics*, *173*(1-4), 595–615.

Bird, P. (1984), Laramide crustal thickening event in the Rocky Mountain foreland and Great Plains, *Tectonics*, *3*(7), 741–758.

Bleeker, W. (2003), The late Archean record: a puzzle in ca. 35 pieces, *Lithos*, *71*(2), 99–134.

Bowring, S. A., and K. E. Karlstrom (1990), Growth, stabilization, and reactivation of Proterozoic lithosphere in the southwestern United States, *Geology*, *18*(12), 1203–1206.

Boyden, J. A., R. D. Müller, M. Gurnis, T. H. Torsvik, J. A. Clark, M. Turner, H. Ivey-Law, R. J. Watson, and J. S. Cannon (2011), Next-generation plate-tectonic reconstructions using GPlates, *Geoinformatics: cyberinfrastructure for the solid earth sciences*, pp. 95–114.

Brace, W., and D. Kohlstedt (1980), Limits on lithospheric stress imposed by laboratory experiments, *Journal of Geophysical Research: Solid Earth (1978–2012)*, *85*(B11), 6248–6252.

Brown, L., L. Jensen, J. Oliver, S. Kaufman, and D. Steiner (1982), Rift structure beneath the Michigan Basin from COCORP profiling, *Geology*, *10*(12), 645–649.

Buiter, S. J., and T. H. Torsvik (2014), A review of Wilson Cycle plate margins: A role for mantle plumes in continental break-up along sutures?, *Gondwana Research*, *26*(2), 627–653.

Bunge, H.-P., and S. P. Grand (2000), Mesozoic plate-motion history below the northeast Pacific Ocean from seismic images of the subducted Farallon slab, *Nature*, *405*(6784), 337–340.

Burdick, S., et al. (2014), Model Update January 2013: Upper Mantle Heterogeneity beneath North America from Travel-Time Tomography with Global and USArray Transportable Array Data, *Seismological Research Letters*, *85*(1), 77–81.

Butler, R., et al. (2004), The Global Seismographic Network surpasses its design goal, *Eos, Transactions American Geophysical Union*, *85*(23), 225–229.

Cannon, W., et al. (1989), The North American Midcontinent rift beneath Lake Superior from GLIMPCE seismic reflection profiling, *Tectonics*, *8*(2), 305–332.

Cannon, W. F. (1992), The Midcontinent rift in the Lake Superior region with emphasis on its geodynamic evolution, *Tectonophysics*, *213*(1-2), 41–48.

Cannon, W. F. (1994), Closing of the Midcontinent rift - A far-field effect of Grenvillian compression, *Geology*, *22*(2), 155–158.

Cannon, W. F., M. W. Lee, W. Hinze, K. J. Schulz, and A. G. Green (1991), Deep crustal structure of the Precambrian basement beneath northern Lake Michigan, midcontinent North America, *Geology*, *19*(3), 207–210.

Chandler, V., T. Boerboom, and M. Jirsa (2007), Penokean tectonics along a promontory-embayment margin in east-central Minnesota, *Precambrian Research*, *157*(1), 26–49.

Chase, C. G., and T. H. Gilmer (1973), Precambrian plate tectonics: the midcontinent gravity high, *Earth and Planetary Science Letters*, *21*(1), 70–78.

Coney, P. J., and S. J. Reynolds (1977), Cordilleran Benioff zones, *Nature*, *270*, 403–406.

Darbyshire, F. A., D. W. Eaton, A. W. Frederiksen, and L. Ertolahti (2007), New insights into the lithosphere beneath the Superior Province from Rayleigh wave dispersion and receiver function analysis, *Geophysical Journal International*, *169*(3), 1043–1068.

DeCelles, P. G. (1994), Late Cretaceous-Paleocene synorogenic sedimentation and kinematic history of the Sevier thrust belt, northeast Utah and southwest Wyoming, *Geological Society of America Bulletin*, *106*(1), 32–56.

DeCelles, P. G. (2004), Late Jurassic to Eocene evolution of the Cordilleran thrust belt and foreland basin system, western Usa, *American Journal of Science*, *304*(2), 105–168.

DeConto, R. M., et al. (1999), Alternative global Cretaceous paleogeography, *Evol. Cretac. Ocean.-Clim. Syst*, *332*, 1–435.

Dietmar Müller, R., J.-Y. Royer, and L. A. Lawver (1993), Revised plate motions relative to the hotspots from combined Atlantic and Indian ocean hotspot tracks, *Geology*, *21*, 275.

Doubrovine, P. V., B. Steinberger, and T. H. Torsvik (2012), Absolute plate motions in a reference frame defined by moving hot spots in the Pacific, Atlantic, and Indian oceans, *Journal of Geophysical Research: Solid Earth*, *117*(B9).

Eaton, D., et al. (2005), Investigating Canada's lithosphere and earthquake hazards with portable arrays, *Eos, Transactions American Geophysical Union*, *86*(17), 169–173.

Engebretson, D. C., A. Cox, and R. G. Gordon (1985), Relative motions between oceanic and continental plates in the Pacific basin, *Geological Society of America Special Papers*, *206*, 1–60.

English, J. M., and S. T. Johnston (2004), The Laramide orogeny: what were the driving forces?, *International Geology Review*, *46*(9), 833–838.

Foster, A. E., F. Darbyshire, and A. Schaeffer (2017), A Surface Wave's View of the Mid-Continent Rift, in *AGU Fall Meeting Abstracts*.

Frederiksen, A., S.-K. Miong, F. Darbyshire, D. Eaton, S. Rondenay, and S. Sol (2007), Lithospheric variations across the Superior Province, Ontario, Canada: Evidence from tomography and shear wave splitting, *Journal of Geophysical Research: Solid Earth*, *112*(B7), B07318.

Frederiksen, A., T. Bollmann, F. Darbyshire, and S. van der Lee (2013a), Modification of continental lithosphere by tectonic processes: A tomographic image of central North America, *Journal of Geophysical Research: Solid Earth*, *118*(3), 1051–1066.

Frederiksen, A., I. Deniset, O. Ola, and D. Toni (2013b), Lithospheric fabric variations in central North America: Influence of rifting and Archean tectonic styles, *Geophysical Research Letters*, *40*(17), 4583–4587.

French, S., K. Fischer, E. Syracuse, and M. Wysession (2009), Crustal structure beneath the Florida-to-Edmonton broadband seismometer array, *Geophysical Research Letters*, *36*(8).

Goes, S., and S. van der Lee (2002), Thermal structure of the North American uppermost mantle inferred from seismic tomography, *Journal of Geophysical Research: Solid Earth*, *107*(B3), ETG–2.

Goodge, J. W., and J. D. Vervoort (2006), Origin of Mesoproterozoic A-type granites in Laurentia: Hf isotope evidence, *Earth and Planetary Science Letters*, *243*(3), 711–731.

Grand, S. P. (1994), Mantle shear structure beneath the Americas and surrounding oceans, *Journal of Geophysical Research: Solid Earth*, *99*(B6), 11591–11621.

Grand, S. P. (2002), Mantle shear–wave tomography and the fate of subducted slabs, *Philosophical Transactions of the Royal Society of London. Series A: Mathematical, Physical and Engineering Sciences*, *360*(1800), 2475–2491.

Green, A. G., et al. (1989), A "Glimpce" of the Deep Crust Beneath the Great Lakes, *Properties and Processes of Earth's Lower Crust*, *51*, 65–80.

Hinze, W. J., D. J. Allen, A. J. Fox, D. Sunwood, T. Woelk, and A. G. Green (1992), Geophysical investigations and crustal structure of the North American Midcontinent

Rift system, *Tectonophysics*, *213*(1), 17–32.

Hoffman, P. F. (1988), United Plates of America, the birth of a craton: Early Proterozoic assembly and growth of Laurentia, *Annual Review of Earth and Planetary Sciences*, *16*, 543–603.

Hollings, P., A. Richardson, R. A. Creaser, and J. M. Franklin (2007), Radiogenic isotope characteristics of the Mesoproterozoic intrusive rocks of the Nipigon Embayment, northwestern Ontario, *Canadian Journal of Earth Sciences*, *44*(8), 1111–1129.

Hollings, P., M. Smyk, L. M. Heaman, and H. Halls (2010), The geochemistry, geochronology and paleomagnetism of dikes and sills associated with the Mesoproterozoic Midcontinent Rift near Thunder Bay, Ontario, Canada, *Precambrian Research*, *183*(3), 553–571.

Hollings, P., M. Smyk, and B. Cousens (2012), The radiogenic isotope characteristics of dikes and sills associated with the Mesoproterozoic Midcontinent Rift near Thunder Bay, Ontario, Canada, *Precambrian Research*, *214*, 269–279.

Holm, D., et al. (2007), Reinterpretation of Paleoproterozoic accretionary boundaries of the north-central United States based on a new aeromagnetic-geologic compilation, *Precambrian Research*, *157*(1–4), 71 – 79.

Holm, D. K., W. R. Van Schmus, L. C. MacNeill, T. J. Boerboom, D. Schweitzer, and D. Schneider (2005), U-Pb zircon geochronology of Paleoproterozoic plutons from the northern midcontinent, USA: Evidence for subduction flip and continued convergence after geon 18 Penokean orogenesis, *Geological Society of America Bulletin*, *117*(3-4), 259–275.

Houston, R. S., A. Snoke, J. Steidtmann, and S. Roberts (1993), Late Archean and early Proterozoic geology of southeastern Wyoming, *Geology of Wyoming: Geological Survey of Wyoming Memoir*, *5*, 78–116.

Ibs-von Seht, M., and J. Wohlenberg (1999), Microtremor measurements used to map thickness of soft sediments, *Bulletin of the Seismological Society of America*, *89*(1), 250–259.

IRIS-DMC (2011), Data services products: EMC, a repository of Earth models.

Jones, C. H., G. L. Farmer, B. Sageman, and S. Zhong (2011), Hydrodynamic mechanism for the Laramide orogeny, *Geosphere*, *7*(1), 183–201.

Karlstrom, K. E., and E. D. Humphreys (1998), Persistent influence of Proterozoic accretionary boundaries in the tectonic evolution of southwestern North America Interaction of cratonic grain and mantle modification events, *Rocky Mountain Geology*, *33*(2), 161–179.

Kay, I., S. Sol, J.-M. Kendall, C. Thomson, D. White, I. Asudeh, B. Roberts, and D. Francis (1999), Shear wave splitting observations in the Archean craton of Western Superior, *Geophysical Research Letters*, *26*(17), 2669–2672.

Kennett, B., and E. Engdahl (1991), Traveltimes for global earthquake location and phase identification, *Geophysical Journal International*, *105*(2), 429–465.

Klasner, J., W. Cannon, and W. Van Schmus (1982), 4: The pre-Keweenawan tectonic history of southern Canadian Shield and its influence on formation of the Midcontinent Rift, *Geological Society of America Memoirs*, *156*, 27–46.

Lipman, P. W., H. J. Prostka, and R. L. Christiansen (1971), Evolving subduction zones in the western United States, as interpreted from igneous rocks, *Science*, *174*(4011),

821–825.

Liu, L. (2015), The ups and downs of North America: Evaluating the role of mantle dynamic topography since the mesozoic, *Reviews of Geophysics*, *53*(3), 1022–1049.

Liu, L., M. Gurnis, M. Seton, J. Saleeby, R. D. Müller, and J. M. Jackson (2010), The role of oceanic plateau subduction in the Laramide orogeny, *Nature Geoscience*, *3*(5), 353–357.

Livaccari, R. F., K. Burke, and A. Şengör (1981), Was the Laramide orogeny related to subduction of an oceanic plateau?, *Nature*, *289*(5795), 276.

Lou, X., and S. van der Lee (2014), Observed and predicted North American teleseismic delay times, *Earth and Planetary Science Letters*, *402*, 6–15.

Lou, X., S. van der Lee, and S. Lloyd (2013), AIMBAT: a python/matplotlib tool for measuring teleseismic arrival times, *Seismological Research Letters*, *84*(1), 85–93.

Masse, R. P., J. R. Filson, and A. Murphy (1989), United States National seismograph network, *Tectonophysics*, *167*(2-4), 133–138.

McNamara, D. E., and R. P. Buland (2004), Ambient noise levels in the continental United States, *Bulletin of the seismological society of America*, *94*(4), 1517–1527.

Meltzer, A., et al. (1999), The USArray initiative, *Geological Society of America TODAY*, *9*, 8–10.

Miller, J., S. Nicholson, R. Easton, E. Ripley, and J. Feinberg (2013), Geology and mineral deposits of the 1.1 Ga Midcontinent Rift in the Lake Superior region–an overview, *Field guide to the copper-nickel-platinum group element deposits of the Lake Superior Region. Edited by Miller, J. Precambrian Research Center Guidebook*, pp. 13–01.

Moidaki, M., S. S. Gao, K. H. Liu, and E. Atekwana (2013), Crustal thickness and Moho sharpness beneath the Midcontinent rift from receiver functions, *Research in Geophysics*, *3*(1), 1–7.

Moulik, P., and G. Ekström (2014), An anisotropic shear velocity model of the Earth's mantle using normal modes, body waves, surface waves and long-period waveforms, *Geophysical Journal International*, *199*(3), 1713–1738.

Mueller, P. A., J. L. Wooden, D. W. Mogk, A. P. Nutman, and I. Williams (1996), Extended history of a 3.5 ga trondhjemitic gneiss, Wyoming Province, USA: evidence from UPb systematics in zircon, *Precambrian Research*, *78*(1-3), 41–52.

Mueller, P. A., A. L. Heatherington, D. M. Kelly, J. L. Wooden, and D. W. Mogk (2002), Paleoproterozoic crust within the Great Falls tectonic zone: Implications for the assembly of southern Laurentia, *Geology*, *30*(2), 127–130.

Nakanishi, M., W. W. Sager, and A. Klaus (1999), Magnetic lineations within Shatsky Rise, northwest Pacific Ocean: Implications for hot spot-triple junction interaction and oceanic plateau formation, *Journal of Geophysical Research: Solid Earth*, *104*(B4), 7539–7556.

Nations, J. D. (1989), Cretaceous history of northeastern and east-central Arizona, *Geology of Arizona: Arizona Geological Society Digest*, pp. 435–446.

North, R., and P. Basham (1993), Modernization of the Canadian National Seismograph Network, *Seismological Research Letters*, *64*, 41.

Ojakangas, R., G. Morey, and J. Green (2001), The Mesoproterozoic midcontinent rift system, Lake Superior region, USA, *Sedimentary Geology*, *141*, 421–442.

Ojakangas, R. W., and A. B. Dickas (2002), The 1.1-Ga Midcontinent Rift System, central North America: sedimentology of two deep boreholes, Lake Superior region, *Sedimentary Geology*, *147*(1), 13–36.

Ola, O., et al. (2016), Anisotropic zonation in the lithosphere of Central North America: Influence of a strong cratonic lithosphere on the Mid-Continent Rift, *Tectonophysics*, *683*, 367–381.

Owens, T. J., H. P. Crotwell, C. Groves, and P. Oliver-Paul (2004), SOD: Standing order for data, *Seismological Research Letters*, *75*(4), 515–520.

Park, Y., and A. A. Nyblade (2006), P-wave tomography reveals a westward dipping low velocity zone beneath the Kenya Rift, *Geophysical Research Letters*, *33*(7), L07311.

Parker, R. L. (1994), *Geophysical inverse theory*, Princeton University Press.

Peters, S. E., and N. A. Heim (2010), The geological completeness of paleontological sampling in North America, *Paleobiology*, *36*(1), 61–79.

Pollitz, F. F., and W. D. Mooney (2014), Seismic structure of the Central US crust and shallow upper mantle: Uniqueness of the Reelfoot Rift, *Earth and Planetary Science Letters*, *402*, 157–166.

Roberts, L. N. R., and M. A. Kirschbaum (1995), Paleogeography of the Late Cretaceous of the Western Interior of middle North America-coal distribution and sediment accumulation, *United States Geological Survey, Professional Paper*, *1561*.

Sager, W. W., J. Zhang, J. Korenaga, T. Sano, A. A. Koppers, M. Widdowson, and J. J. Mahoney (2013), An immense shield volcano within the Shatsky Rise oceanic plateau, northwest Pacific Ocean, *Nature Geoscience*, *6*(11), 976–981.

Saleeby, J. (2003), Segmentation of the Laramide slab—Evidence from the southern Sierra Nevada region, *Geological Society of America Bulletin*, *115*(6), 655–668.

Schettino, A., and C. R. Scotese (2005), Apparent polar wander paths for the major continents (200 ma to the present day): a palaeomagnetic reference frame for global plate tectonic reconstructions, *Geophysical Journal International*, *163*(2), 727–759.

Schmandt, B., and F.-C. Lin (2014), P and S wave tomography of the mantle beneath the United States, *Geophysical Research Letters*, *41*(18), 6342–6349.

Schneider, D., M. Bickford, W. Cannon, K. Schulz, and M. Hamilton (2002), Age of volcanic rocks and syndepositional iron formations, Marquette Range Supergroup: implications for the tectonic setting of Paleoproterozoic iron formations of the Lake Superior region, *Canadian Journal of Earth Sciences*, *39*(6), 999–1012.

Schulz, K. J., and W. F. Cannon (2007), The Penokean orogeny in the Lake Superior region, *Precambrian Research*, *157*(1), 4–25.

Seton, M., et al. (2012), Global continental and ocean basin reconstructions since 200Ma, *Earth-Science Reviews*, *113*(3), 212–270.

Shaw, C. A., and K. E. Karlstrom (1999), The Yavapai-Mazatzal crustal boundary in the southern Rocky Mountains, *Rocky Mountain Geology*, *34*(1), 37–52.

Shen, W., M. H. Ritzwoller, and V. Schulte-Pelkum (2013), Crustal and uppermost mantle structure in the central US encompassing the Midcontinent Rift, *Journal of Geophysical Research: Solid Earth*, *118*(8), 4325–4344.

Sigloch, K., and M. G. Mihalynuk (2013), Intra-oceanic subduction shaped the assembly of Cordilleran North America, *Nature*, *496*(7443), 50–56.

Silver, P. G., and S. Kaneshima (1993), Constraints on mantle anisotropy beneath Precambrian North America from a transportable teleseismic experiment, *Geophysical Research Letters*, *20*(12), 1127–1130.

Simmons, N. A., A. M. Forte, L. Boschi, and S. P. Grand (2010), GyPSuM: A joint tomographic model of mantle density and seismic wave speeds, *Journal of Geophysical Research: Solid Earth*, *115*(B12).

Sims, P., K. Card, G. Morey, and Z. Peterman (1980), The Great Lakes tectonic zone—A major crustal structure in central North America, *Geological Society of America Bulletin*, *91*(12), 690–698.

Sims, P., W. V. Schmus, K. Schulz, and Z. Peterman (1989), Tectono-stratigraphic evolution of the Early Proterozoic Wisconsin magmatic terranes of the Penokean Orogen, *Canadian Journal of Earth Sciences*, *26*(10), 2145–2158.

Snyder, W., W. Dickinson, and M. Silberman (1976), Tectonic implications of space-time patterns of Cenozoic magmatism in the western United States, *Earth and Planetary Science Letters*, *32*(1), 91–106.

Spencer, J. E., and P. J. Patchett (1997), Sr isotope evidence for a lacustrine origin for the upper Miocene to Pliocene Bouse Formation, lower Colorado River trough, and implications for timing of Colorado Plateau uplift, *Geological Society of America Bulletin*, *109*(6), 767–778.

Tanner, J. G., et al. (1988), Gravity anomaly map of North America, *The Leading Edge*, *7*(11), 15–18.

Turcotte, D. L., and G. Schubert (2014), *Geodynamics*, Cambridge University Press.

van der Lee, S., and A. Frederiksen (2005), Surface wave tomography applied to the North American upper mantle, in *Seismic Earth: Array Analysis of Broadband Seismograms*, *Geophysical Monograph Series*, vol. 157, edited by A. Levander and G. Nolet, pp. 67–80.

van der Lee, S., and G. Nolet (1997), Seismic image of the subducted trailing fragments of the Farallon plate, *Nature*, *386*(6622), 266–269.

van der Lee, S., and D. A. Wiens (2006), Seismological constraints on Earth's deep water cycle, *Geophysical Monograph-American Geophysical Union*, *168*, 13–27.

van der Lee, S., D. A. Wiens, J. Revenaugh, A. Frederiksen, and F. Darbyshire (2011), Superior Province Rifting Earthscope Experiment. International Federation of Digital Seismograph Networks. Dataset/Seismic Network, doi:10.7914/SN/XI-2011.

van der Lee, S., E. Wolin, T. Bollmann, and K. Tekverk (2013), Crust and mantle structure of a closed rift system from the Superior Province Rifting Earthscope Experiment (SPREE), in *AGU Fall Meeting Abstracts*, vol. 1, p. 01.

Van Schmus, W. (1992), Tectonic setting of the Midcontinent Rift system, *Tectonophysics*, *213*(1-2), 1–15.

Van Schmus, W., and W. Hinze (1985), The midcontinent rift system, *Annual Review of Earth and Planetary Sciences*, *13*, 345–383.

Van Schmus, W., M. Bickford, and A. Turek (1996), Proterozoic geology of the east-central Midcontinent basement, *Special Papers-Geological Society of America*, pp. 7–32.

VanDecar, J., and R. Crosson (1990), Determination of teleseismic relative phase arrival times using multi-channel cross-correlation and least squares, *Bulletin of the Seismological Society of America*, *80*(1), 150–169.

VanDecar, J. C. (1991), Upper-mantle structure of the Cascadia subduction zone from non-linear teleseismic travel-time inversion, Ph.D. thesis, University of Washington, Seattle.

Walker, J. D., T. D. Bowers, R. A. Black, A. F. Glazner, G. L. Farmer, and R. W. Carlson (2006), A geochemical database for western North American volcanic and intrusive rocks (NAVDAT), *Geological Society of America Special Papers*, *397*, 61–71.

Wessel, P., W. H. Smith, R. Scharroo, J. Luis, and F. Wobbe (2013), Generic mapping tools: improved version released, *Eos, Transactions American Geophysical Union*, *94*(45), 409–410.

Whitmeyer, S. J., and K. E. Karlstrom (2007), Tectonic model for the Proterozoic growth of North America, *Geosphere*, *3*(4), 220–259.

Windley, B. F. (1993), Proterozoic anorogenic magmatism and its orogenic connections Fermor Lecture 1991, *Journal of the Geological Society*, *150*(1), 39–50.

Wolin, E., S. van der Lee, T. A. Bollmann, D. A. Wiens, J. Revenaugh, F. A. Darbyshire, A. W. Frederiksen, S. Stein, and M. E. Wysession (2015), Seasonal and Diurnal Variations in Long-Period Noise at SPREE Stations: The Influence of Soil Characteristics on Shallow Stations' Performance, *Bulletin of the Seismological Society of America*, *105*(5), 2433–2452.

Yang, B., G. D. Egbert, A. Kelbert, and N. M. Meqbel (2015), Three-dimensional electrical resistivity of the north-central USA from EarthScope long period magnetotelluric data, *Earth and Planetary Science Letters*, *422*, 87–93.

Yonkee, W., J. P. Evans, and P. DeCelles (1992), Mesozoic tectonics of the northern Wasatch Range, Utah.

Zhang, H., et al. (2016), Distinct crustal structure of the North American Midcontinent Rift from P wave receiver functions, *Journal of Geophysical Research: Solid Earth*, *121*(11), 8136–8153.

APPENDIX A

Supplementary Figures from *P* Wave Teleseismic Traveltime Tomography of the North American Midcontinent

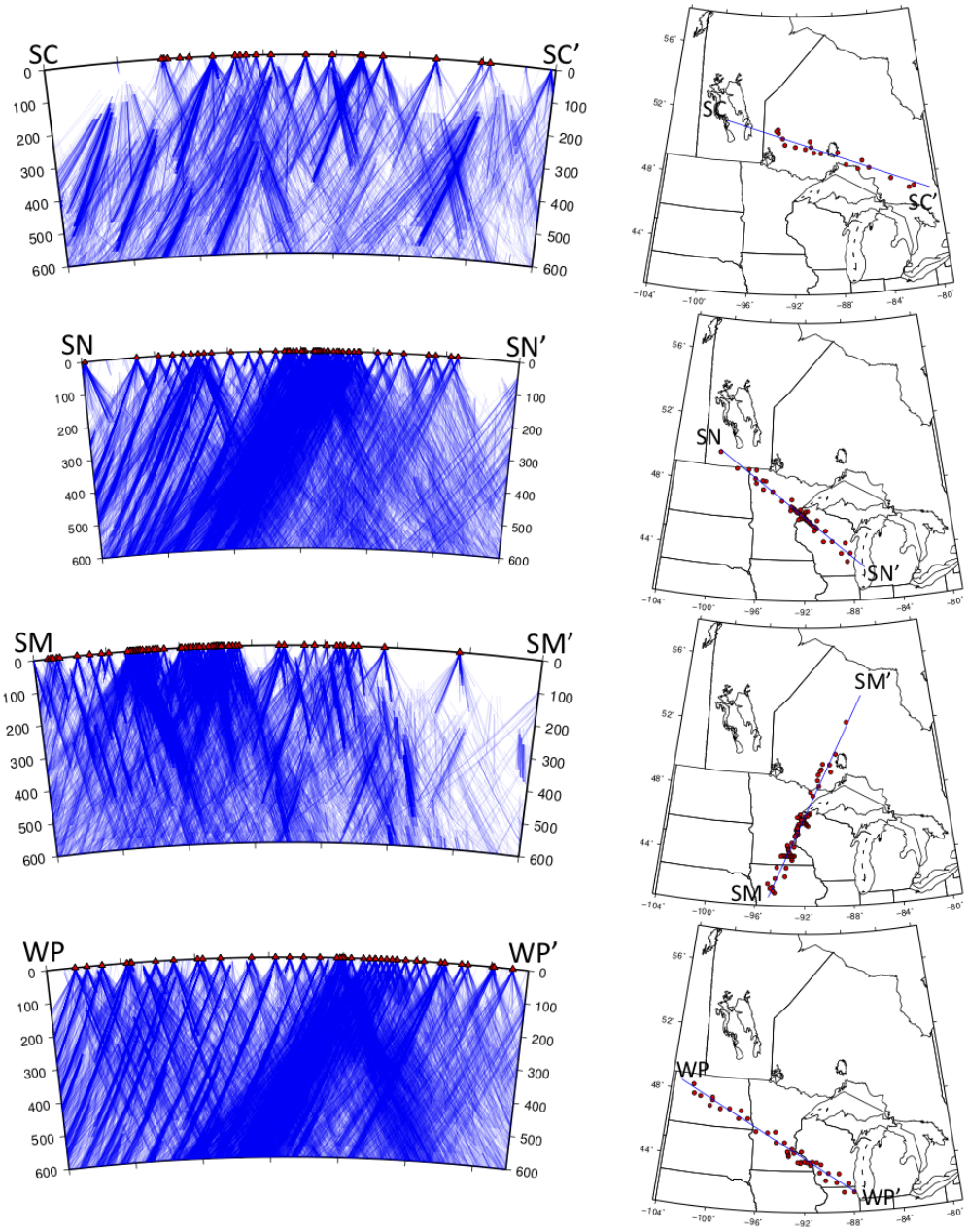

Figure A.1. Ray-path coverage of cross-sections shown in Figure 2.7. Rays within 25 km of the cross-section lines are projected onto the line. In some instances, only portions of rays were within the 25km region surrounding the cross-section line. These rays appear to cut off in the cross-sections. Stations projected onto the line are shown in the map sections to the right as well as the cross-section lines.

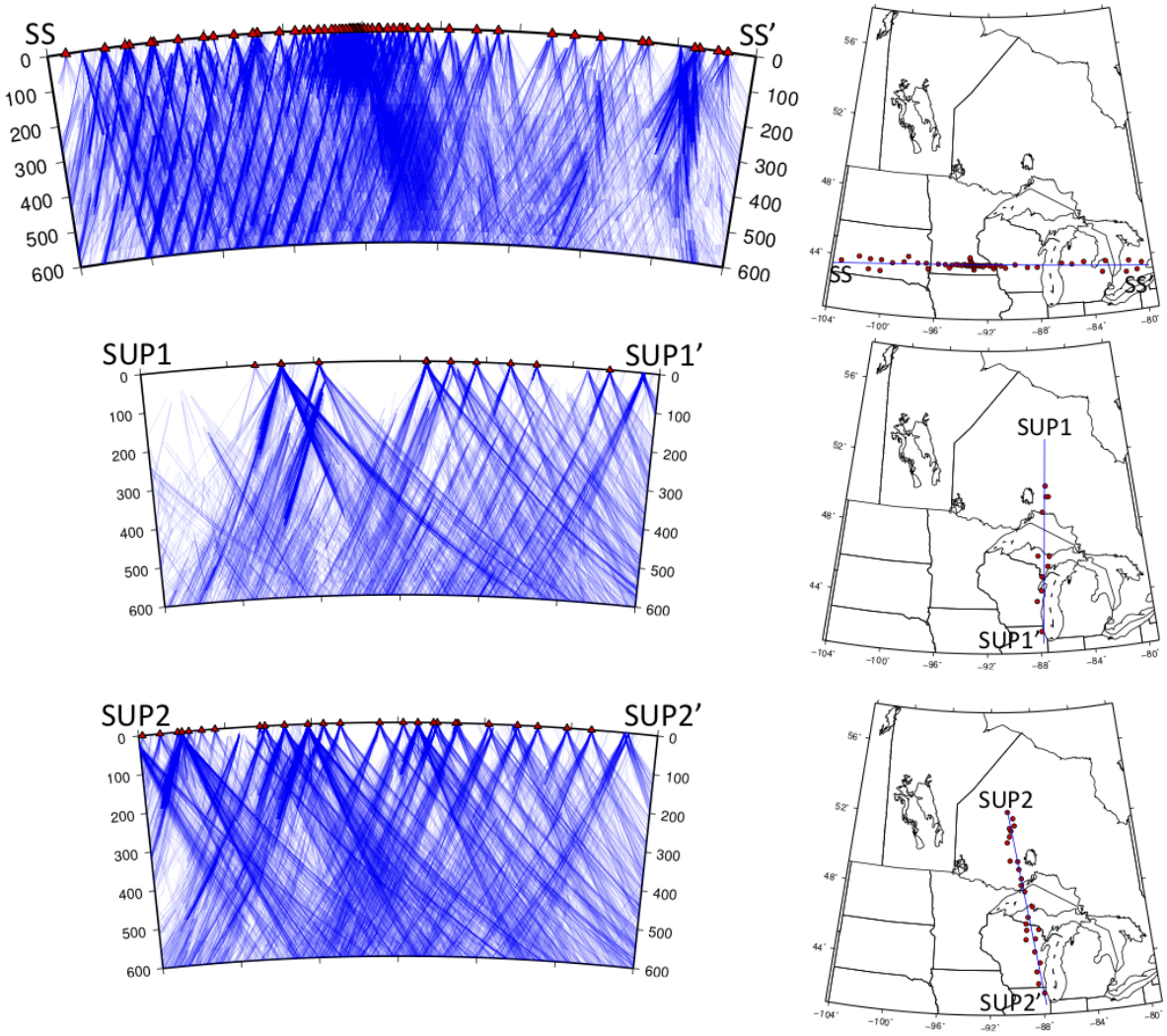

Figure A.2. Additional ray path coverage of cross-sections. The SS cross-section is shown in Figure 2.7. Rays within 25 km of the cross-section lines are projected onto the line. In some instances, only portions of rays were within the 25km region surrounding the cross-section line. These rays appear to cut off in the cross-sections. Stations projected onto the line are shown in the map sections to the right as well as the cross-section lines.

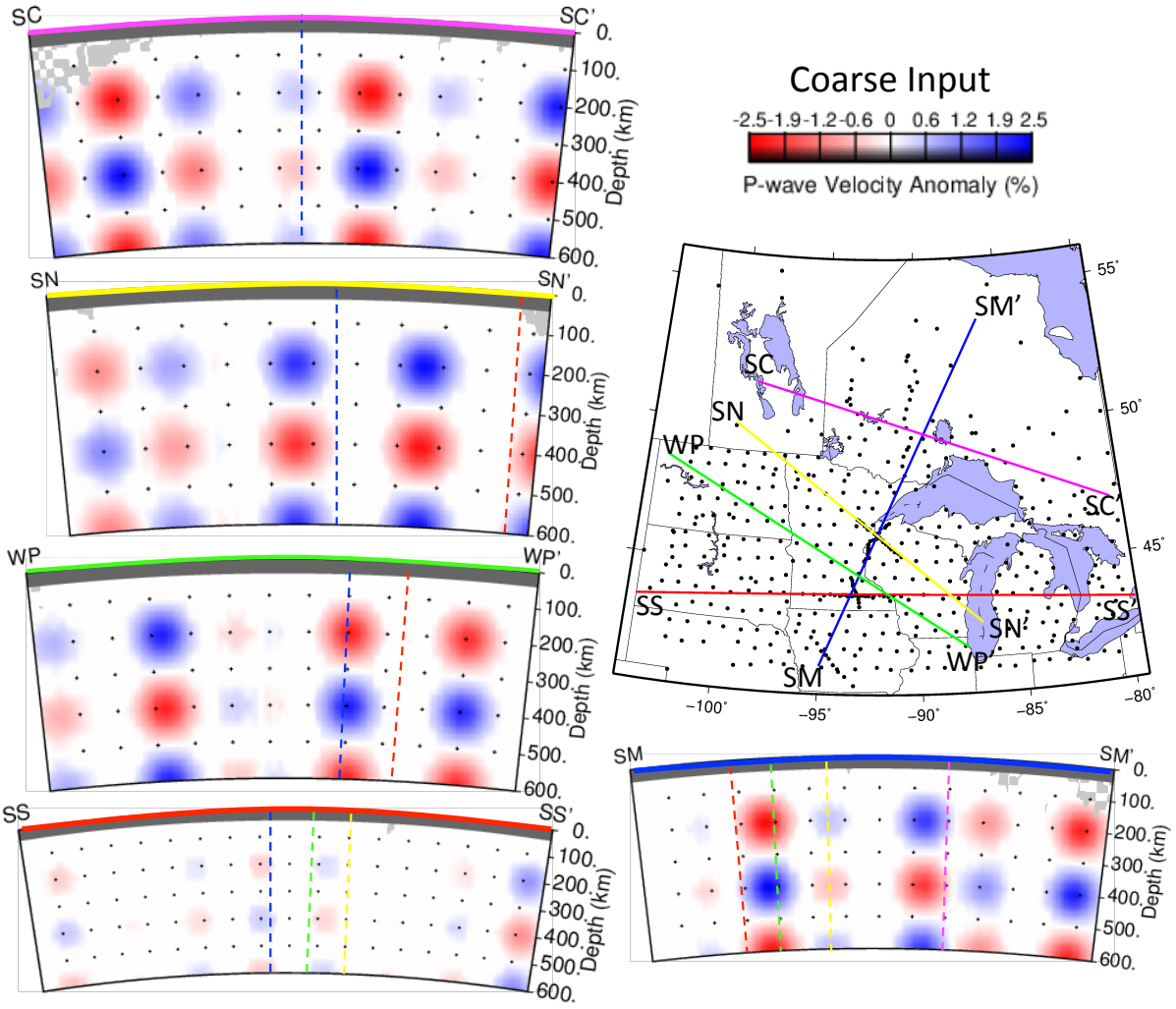

Figure A.3. Vertical slices through the coarse checkerboard input model on the same lines as Figure 2.7.

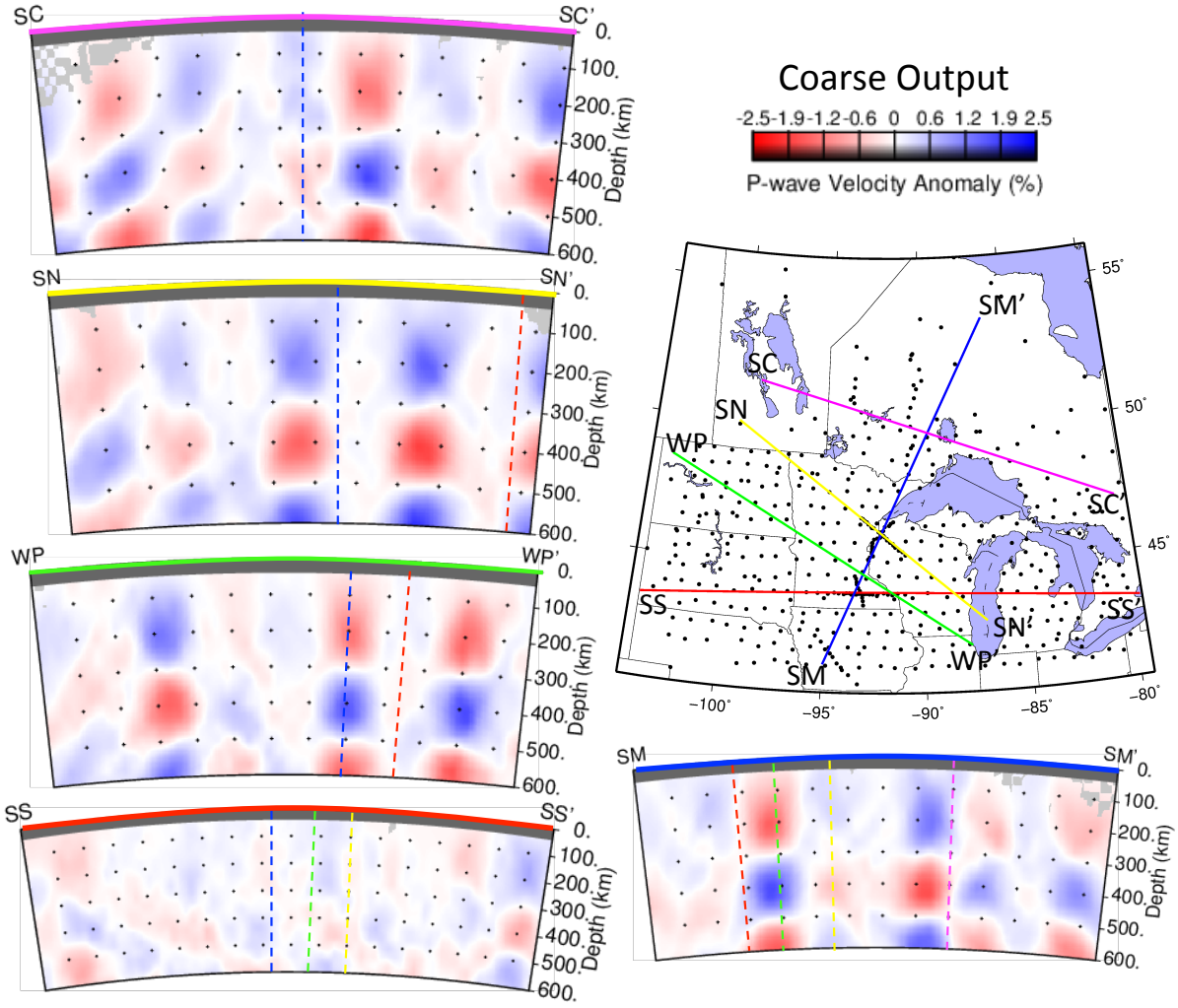

Figure A.4. Vertical slices through the coarse checkerboard output model on the same lines as Figure 2.7.

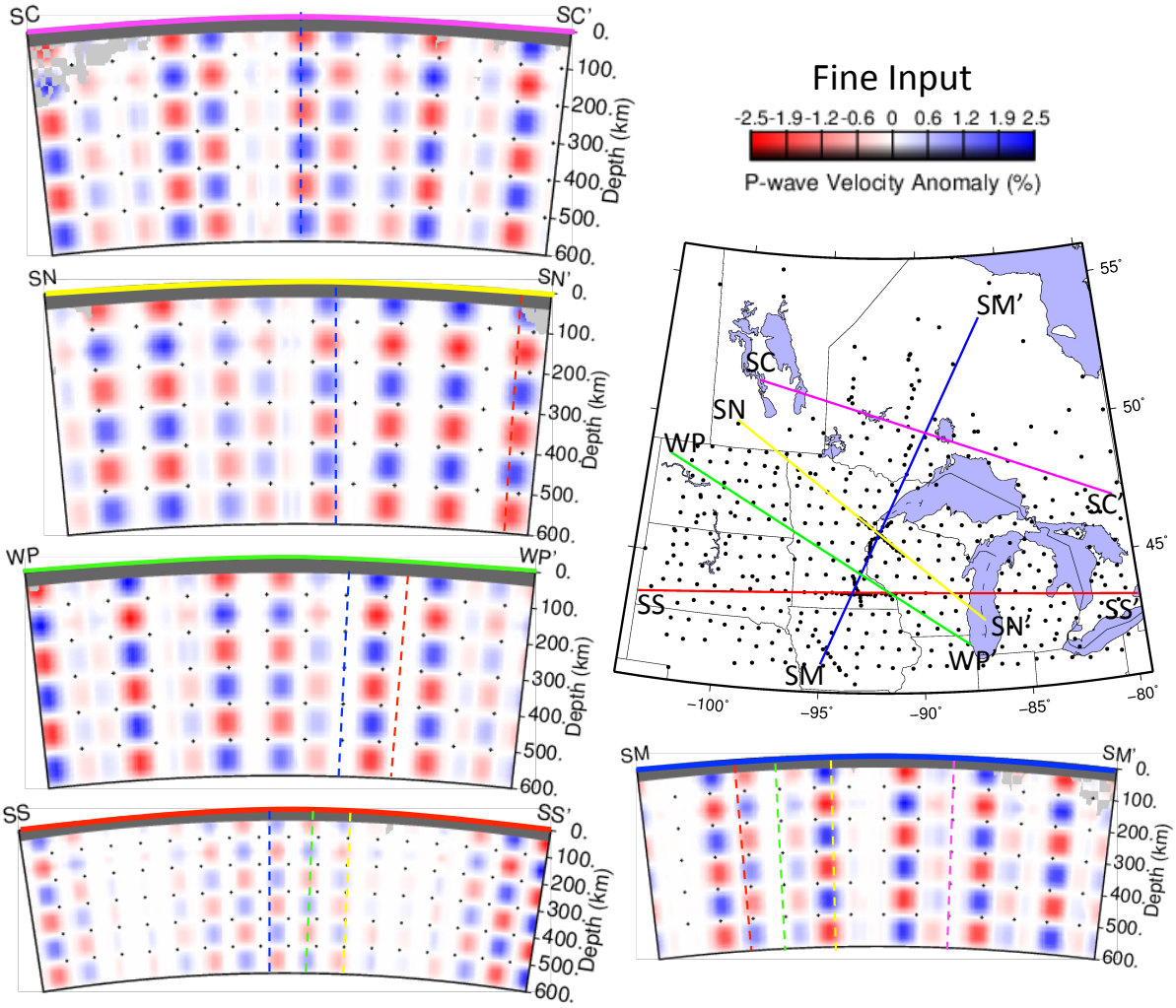

Figure A.5. Vertical slices through the fine checkerboard input model on the same lines as Figure 2.7.

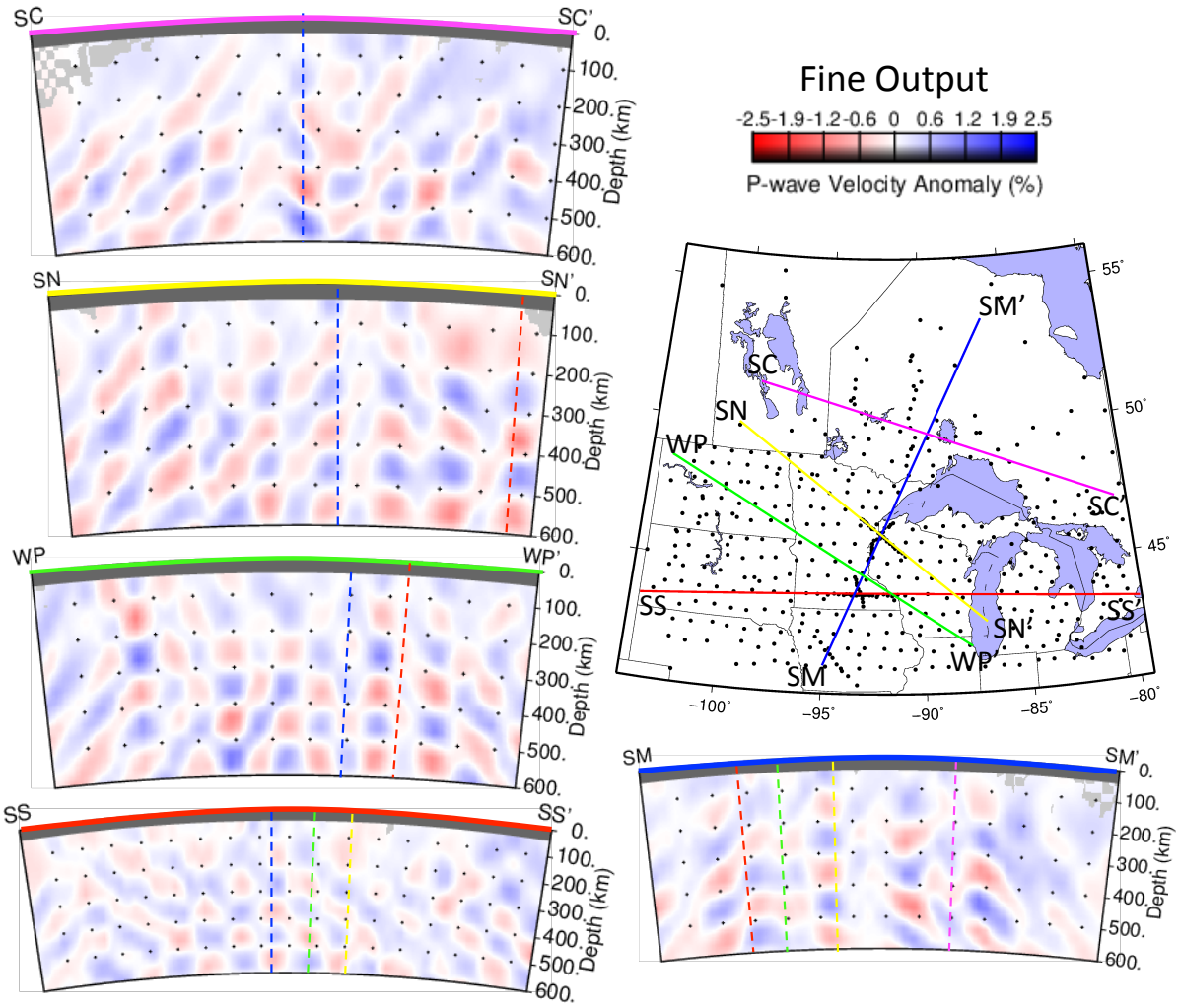

Figure A.6. Vertical slices through the fine checkerboard output model on the same lines as Figure 2.7.

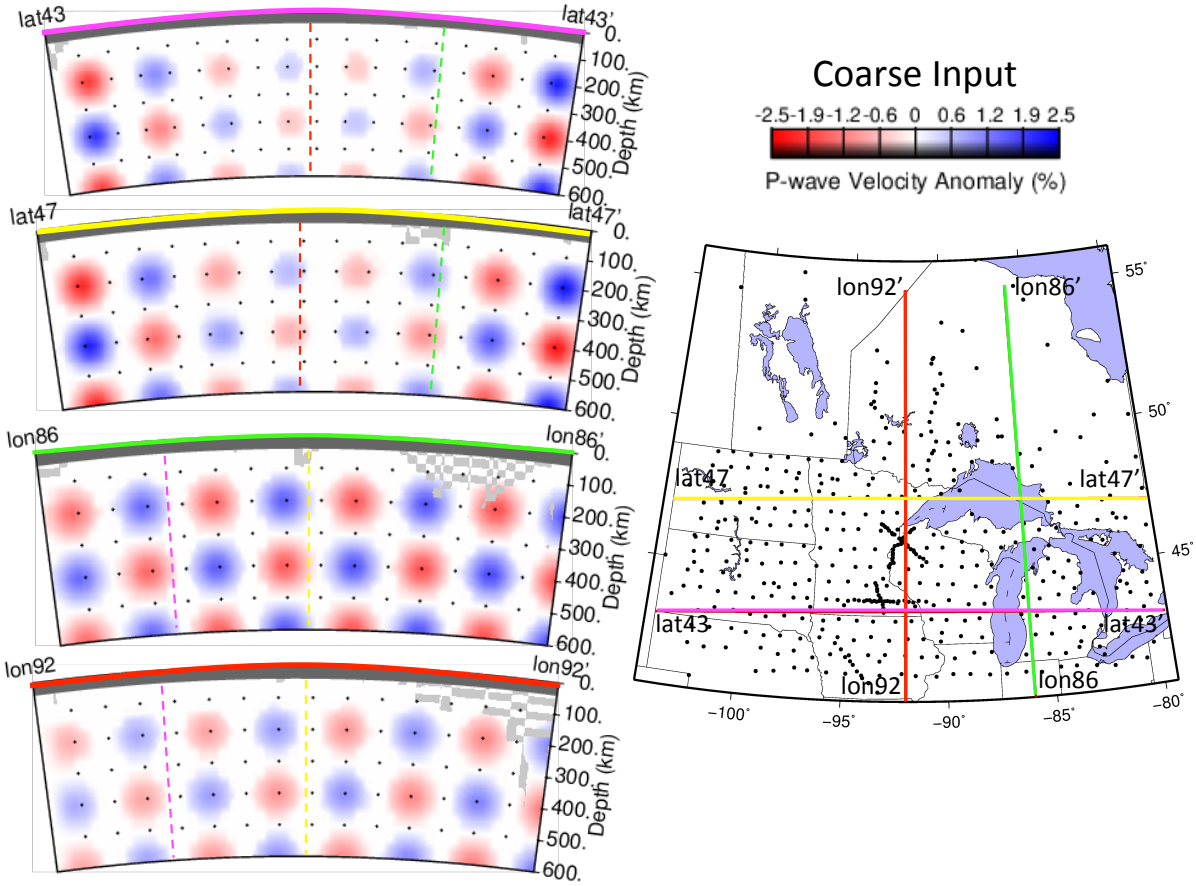

Figure A.7. Vertical slices through the coarse checkerboard input model on S-N and W-E lines.

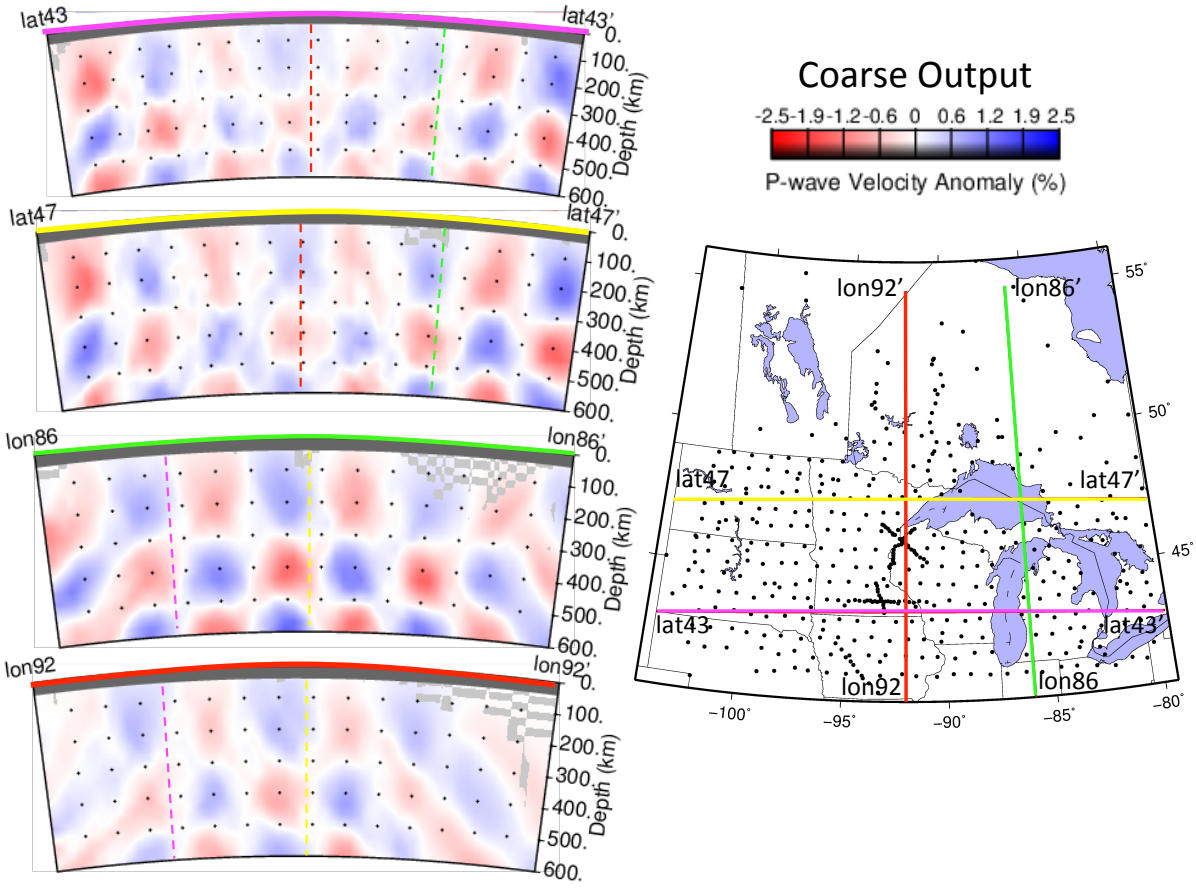

Figure A.8. Vertical slices through the coarse checkerboard output model on S-N and W-E lines.

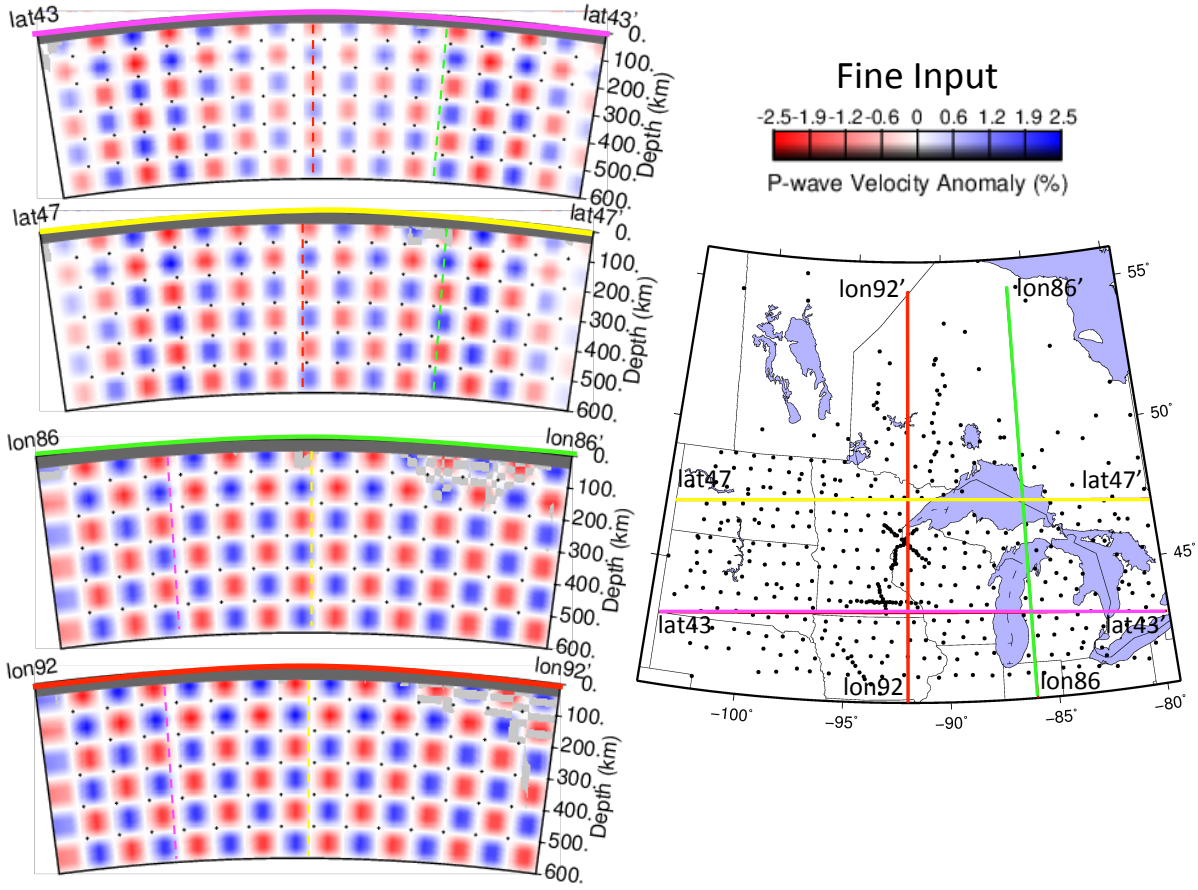

Figure A.9. Vertical slices through the fine checkerboard input model on S-N and W-E lines.

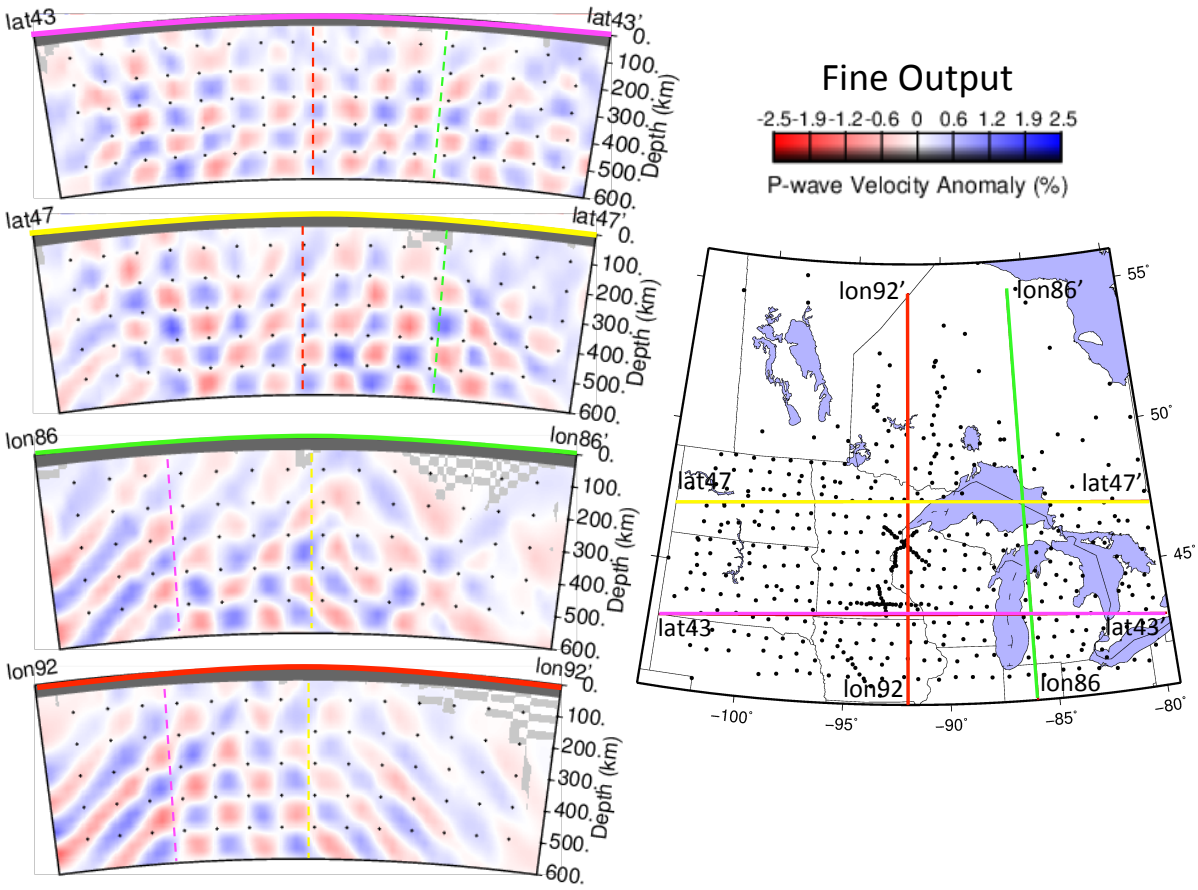

Figure A.10. Vertical slices through the fine checkerboard output model on S-N and W-E lines.

APPENDIX B

Seismic Fieldwork Documentation

B.1. Reconaissance Report

Reconnaissance Report

SPREE Project

Site: SC01 - Graham **Coordinates: N12 34.567, W89 01.23**
Reported by: T. Bollmann, M. Merino **Elevation: N/A**
Visitors: T. Bollmann, M. Merino, T. Zaporozan Time Zone: Central
Date of Initial Recon: August 17, 2010 **Construction: Summer 2011**

Landowner:

Name:	Landowners 1 & 2
MAIL Address:	Street Number City, ONT POT 1NO
Phone:	1-234-567-8901
Cell:	N/A
Email:	landowner@yahoo.com
SITE Address:	Same as landowner's address.

Contact:

Landowner, Mr. or Mrs. Landowner

Driving Directions: (Pictures only at confusing intersections)

From the TOWN, ONT OPP office, drive X.Xmi/X.XXkm on Provincial Hwy XX
Turn Right(N) on NAME Rd. and drive X.XXmi/XX.Xkm
Turn Left (N) right before the XX km marker and drive .Xkm to the landowners house on the right

TO LANDOWNER'S RESIDENCE:
Landowner's residence is XX m north of the turn in and it is a log cabin

Land Use:

Yard that sits next to the lake

Noise: (List all possible noise)

Wind.
Occasional mowing in summer.
Trees
420 m to the north.
House and machine shed 100 m to the south
120ft. deep well 500 feet away
Waves from lake

Issues:

- Landowner required to be notified prior to construction/installation. All personnel must notify contact for permission to enter site area for any work in the future.
- Earthscope/SPREE, at end of occupying site, will remove equipment and the area will be returned to the same condition it was found.
- Location of owner's residence: Onsite
- Water is available on site near the machine shed just west of the landowner's residence (check with landowner first to see where water can be obtained).
- Drive-up access to site: 2WD to grass lane year-round; 2WD to gate if dry.
- Site is secure on private property.
- No bedrock within 1 meter.
- Water table below 1.5 meter.
- Fencing if required around solar mast to protect from Animals
- Lodging/restaurants available in: Ignance, ONT.
- Building materials available in: Thunder Bay, ONT

Landowner (contact): Helpful

Initial Construction Plan:

The Station design would be the FA design with Patrick's improvements unless problems are encountered (i.e. bedrock too shallow)

Tank Vault Design A. The station consists of a 18-inch diameter plastic pipe vertically embedded into the ground to a depth of 2-3 feet (the "vault"), with a concrete base (0.5 cu yd) poured into the bottom. Within 5-6 feet of the vault, a frame is installed on which is mounted solar panel(s). The vault encloses only the sensor. The vault is completely covered with a mound of dirt making it unobtrusive. The data logger and other electrical equipment are housed in a separate enclosure that is connected to the vault using a hose. The data logger enclosure is partially buried and the rest is covered by a tarp.

The location for the site should be away from road traffic (1 km), vehicle parking (200 m), irrigation pumps (1-3 km) or windy hilltops. We try to locate the station so that it bottoms onto competent rock so we often select hillsides or ridge saddles. In agricultural land, irrigation pumps are the main concern.

There are no hazardous materials used in the station on in construction. The environmental impacts are limited to a day or two of dust caused by digging the hole, and some increased noise during construction. If clearance is needed for threatened/endangered species or cultural artifacts, we hire specialists to perform this work. Either the complete site or just the solar panel mast can be fenced to protect livestock and the equipment.

It usually takes one day to dig the hole, install the vault and lid, and backfill around the vault so there is no unattended open hole. The installation of the sensors and communication equipment occurs on the same day.

MAPS:

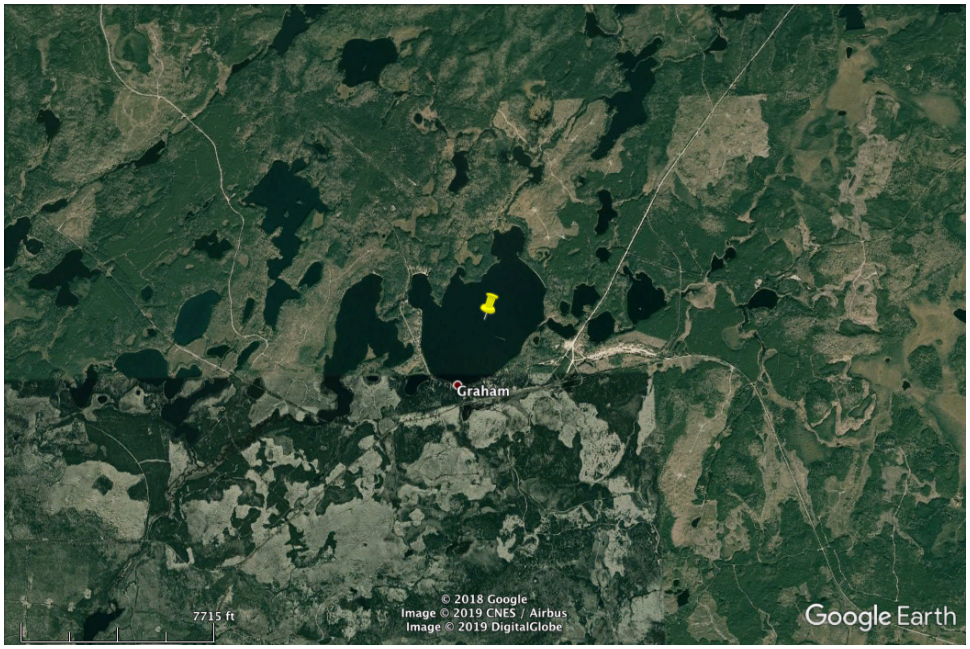
Graham
7715 ft
© 2018 Google
Image © 2019 CNES / Airbus
Image © 2019 DigitalGlobe
Google Earth

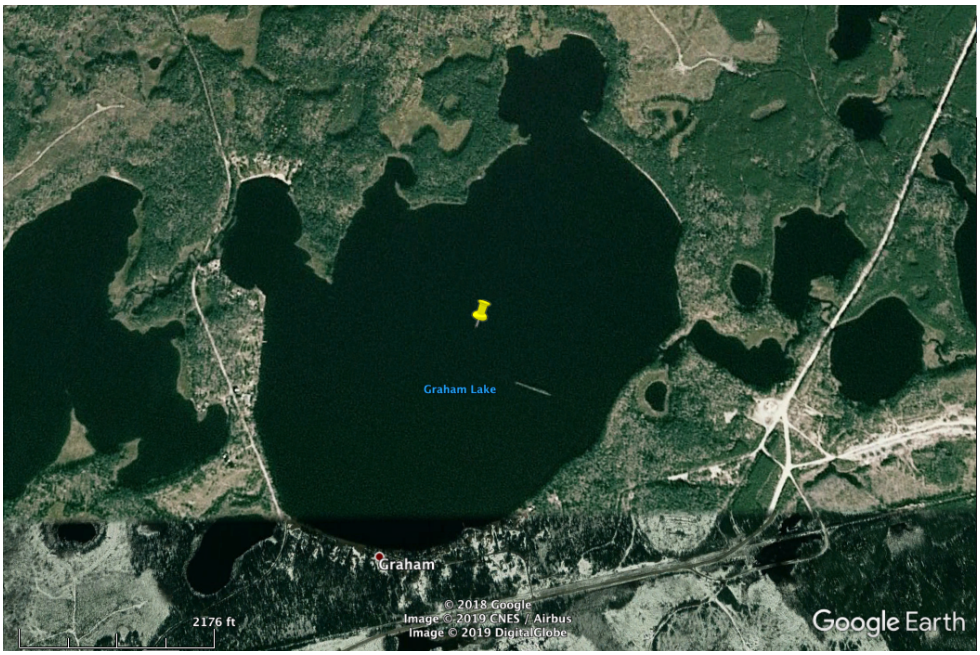
Graham Lake
Graham
2176 ft
© 2018 Google
Image © 2019 CNES / Airbus
Image © 2019 DigitalGlobe
Google Earth

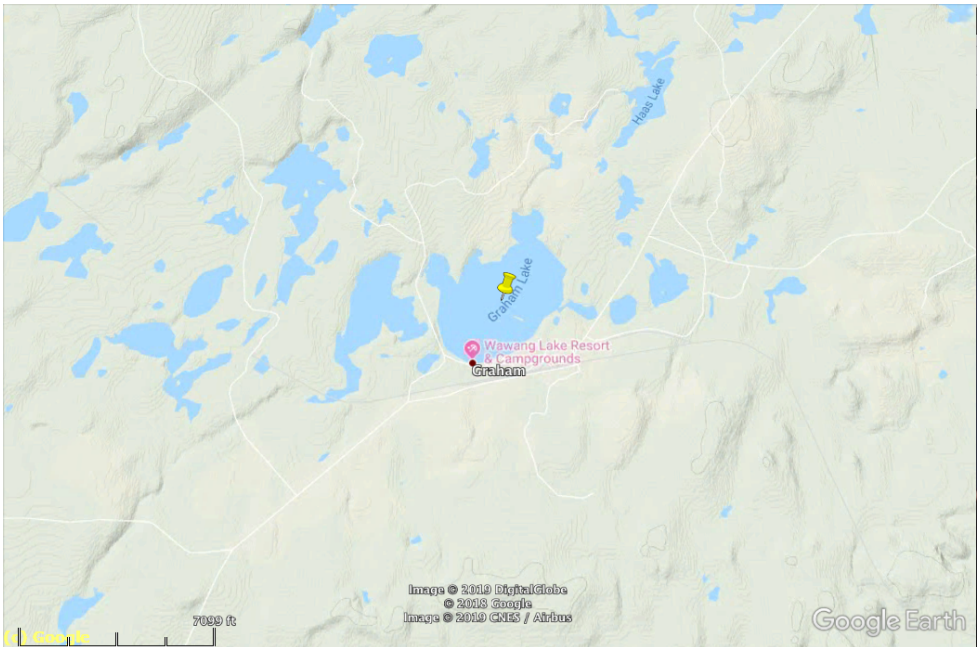
Haas Lake
Graham Lake
Wawang Lake Resort
& Campgrounds
Graham
Image © 2019 DigitalGlobe
© 2018 Google
Image © 2019 CNES / Airbus
7099 ft
Google Earth


Graham Lake
Graham Lake
Wawang Lake Resort
& Campgrounds
Graham
Image © 2019 DigitalGlobe
© 2018 Google
Image © 2019 CNES / Airbus
1364 ft
Google Earth

DIRECTIONAL PHOTOS:

Looking North

Looking East

Looking South

Looking West

ADDITIONAL PHOTOS:

Typical FlexArray Site. After instruments are installed, the vault is covered with excess dirt for thermal protection and to protect from wind noise while the data logger enclosure is covered with a tarp.

B.2. Installation Report

12.3456

SPREE LOG SHEET **INSTALLATION** **Station:** SC03

Date: 06-01-2011 **Julian:** 152,2011 **Time, GMT:** 16:59:12 **Local:** 12:59:12
Field Team: Trevor, Mulu, Allen
GPS Location of Site: lat: N12.3456 **lon:** W123.4567 **elev(m):** 340
CONTACT/LANDOWNER: Landowner #3

EQUIPMENT
SENSOR TYPE: CMG-3T **SENSOR S/N:** T34823
DAS S/N: 98ED **CLOCK S/N:** 3222
FLASH DISK 1 S/N: 5107 **SIZE:** 2GB
FLASH DISK 2 S/N: 5106 **SIZE:** 2GB

LOCATION OF HARDIG CASES In Landowners shed

CHECK POWER SYSTEM (check while PV and battery NOT connected)
PV1: voltage: 21.38 current: [illegible] PV2: voltage: 21.4 current: —
Bat 1: voltage: 12.887 chg. state: full Bat 2: voltage: 12.87 chg. state: Full
Were power checks done with batteries and solar panels disconnected? Yes

INSTALL GURALP Declination used: 4° W

MASS POSITION OFFSETS (NOTE: re-center if mass position offsets are more than 1.5 V)

	voltage (after finish of re-centering)	Attempts
VERT	-0.1	1
N-S	-0.9	1
E-W	40.4	1

INSTALL DAS
1: MODIFY RT130 PARAMETERS AND SEND TO DAS
Work with Config -> load-> "spree-config"
Edit station name and sensor serial # **->Send to DAS**
2. CLEAR RAM (Control -> RAM -> Clear)
3. RESET SYSTEM (Control > Reset)

4. FORMAT FLASH DISK (Control -> Format Disk -> Disk 1: ☑ Disk 2: ☑

5. MONITOR: (Control -> Monitor -> stream 2 ->
ch 1: Midpt: 26455 Range: 83176 tap test: (OK) / NO
ch 2: Midpt: -57449 Range: 430652 tap test: (OK) / NO
ch 3: Midpt: -388147 Range: 178636 tap test: (OK) / NO

6. CHECK CLOCK STATUS (Contol -> Status -> GPS) (clock MUST lock BEFORE starting acquisition)
sec since LL: days: 00 :hr: 00 :min: 00 :sec: 00

7. WRITE .CFG FILE TO DISK (Control>Status>DAS LP/WP-> WRITE) .....☑ YES ☐ NO

8. START ACQUISITION: (Control -> Status -> Start Acq)
start time: days: 152 :hr: 17 :min: 01 :sec: 09

9. VERIFY RAM INCREASING (Control -> Status -> Update): .....☑ YES ☐ NO

10. FORCE RAM DUMP to DISK (Control -> Ram -> Dump)
verify RAM ***DECREASES*** and disk ***INCREASES*** (Control -> Status -> Update) .....☑ YES ☐ NO

Station: SC03

11. BEFORE LEAVING SITE, RECHECK THE FOLLOWING TO ENSURE OPERATION

DAS STATUS (Control -> Status)

Acq: Start (ON)/OFF

Events: 3 RAM: 16 of 4352 (Kb)

Disk 1 0.156 of 1950 Mb Disk 2 0 of 1950 Mb

Temp: 12.5°C Power: input: 13.3 bkup chg: 3.3

ch: 123 DS: CC

Make sure that all plugs and connections have been replaced - esp. SERIAL PORT

RECORD DIRECTIONS TO SITE AND ANY OTHER COMMENTS AND NOTES :

B.3. Servicing Report

SPREE LOG SHEET **SERVICE** **Station:** SC04

Date: 06-06-2011 **Julian:** 157-2011 **Time, GMT:** 19:38 **Local:** 3:35
Field Team: Trevor, Alex
STATION STATUS
Site Condition: Great

DAS S/N: 98DD **CLOCK S/N:** 2841

DAS STATUS (Control -> Status)
Acq: Start (ON)/OFF
Events: 15 3 RAM: 1991 of 4352 (Kb)
Disk 1 0.031 of 3944mb Disk 2 65 of 1950 mb
Temp: 16.9°C Power: input: 14.2 bkup chg: 0.3
ch: 123 DS: CC

CLOCK STATUS (Contol -> Status -> GPS)
sec since LL: days: 00 :hr: 00 :min: 40 :sec: 00
phase diff: +00,000,001

SENSOR STATUS: Sensor Type: CMG-3T **Sensor S/N:** T34928
CENTER MASS POSITION OFFSETS

	Initial	Final	Attempts
Vertical	+4.9	-0.7	1
N-S	+1.7	-0.7	1
E-W	+8.2	-0.8	1

NOTE: re-center if mass position offsets are more than 1.5 V

MONITOR SENSOR: (Control -> Monitor -> stream 2 ->)
ch 1: Midpt: -16473 Range: 27139 tap test: (OK) / NO
ch 2: Midpt: -87240 Range: 96177 tap test: (OK) / NO
ch 3: Midpt: 50271 Range: 14934 tap test: (OK) / NO

1. Calibrate Sensor (Control -> Aux. Control -> Test 1-3) YES ✓ NO
2. Stop Acquisition (Control -> Status -> Stop Acq)
3. Disk Status (Control -> Status -> Update)
Disk 1 0.031 of 3944 Disk 2 67 of 1950
4. Check power system: (check while PV and battery NOT connected)
PV1: voltage: 20.30 current: ok PV2: voltage: 20.20 current: ok
Bat 1: voltage: 13.676 chg. state: unplugged Bat 2: voltage: 13.655 chg. state: unplugged
Were power checks done with batteries and solar panels disconnected? Yes

5. Get RT130 parameters from the DAS (Work with Config -> load -> from DAS) **and check parameters**

6. Record compact flash serial numbers *before swap*
Disk#1 S/N: 4495 SIZE: 2 Gb Disk #2 S/N: 2064 SIZE: 4 Gb

7. SWAP COMPACT FLASH CARDS AND RECORD NEW SERIAL NUMBERS *after the swap*
Disk#1 S/N: 4499 SIZE: 0 Gb Disk#2 S/N: 2064 SIZE: 4 Gb

8. CLEAR RAM (Control -> RAM -> Clear)

9. RESET SYSTEM (Control -> Reset)

10. FORMAT FLASH DISK (Control -> Format Disk -> Disk 1: ☑ Disk 2: ☑

Station: SC04

11. WRITE .CFG FILE TO DISK (Control>Status>DAS LP/WP-> WRITE) .....☑ YES ☐ NO

12. CHECK CLOCK STATUS (Contol -> Status -> GPS) (clock MUST lock BEFORE starting acquisition)
sec since LL: days: 00 :hr: 06 :min: 00 :sec: 00

13. START ACQUISITION: (Control -> Status -> Start Acq)
start time: days:_____:hr:_____:min:_____:sec:_____

14. VERIFY RAM INCREASING (Control -> Status -> Update): .....☑ YES ☐ NO

15. FORCE RAM DUMP to DISK (Control -> Ram -> Dump)
verify RAM ***DECREASES*** and disk ***INCREASES*** (Control -> Status -> Update) .....☑ YES ☐ NO

16. BEFORE LEAVING SITE, RECHECK THE FOLLOWING TO ENSURE OPERATION
DAS STATUS (Control -> Status)
Acq: Start (ON)/OFF
Events: 3 RAM: 13 of 4352 (Kb)
Disk 1 0.031 of 3944MB Disk 2 0.156 of 1950 MB
Temp: 18.9°C Power: input: 14.1 bkup chg: 0.3
ch: 123 DS: CC
Make sure that all plugs and connections have been replaced - esp. SERIAL PORT

RECORD OTHER COMMENTS AND NOTES: